Cell Mechanics in Physiology: A Force Based Approach

by
Vinay Swaminathan

A dissertation submitted to the faculty of the University of North Carolina at Chapel Hill in partial fulfillment of the requirements for the degree of Doctor of Philosophy in the Department of Physics and Astronomy.

Chapel Hill
2011

Approved by:

Richard Superfine, Advisor

Sorin Mitran, Reader

Keith Burridge, Reader

Klaus Hahn, Reader

GC Blobe, Reader

ABSTRACT
VINAY SWAMINATHAN: Cell Mechanics in Physiology: A Force Based Approach.
(Under the direction of Richard Superfine.)

All biological systems rely on complex interactions with their external and internal environments where the key factors are force sensing and force generation. These systems are highly dynamic, and recent studies have shown that it is the control and maintenance of these interactions that are essential for normal functioning. Appreciation of these roles has led to a revolution in instrumentation and techniques to study and model mechanical interaction at all length and time scales in biology. The work presented here is one such effort, utilizing a magnetics based force system to study and understand the mechanisms of cell mechanics and their role in mucuciliary clearance in the lung and in cancer cell invasion and metastasis.

I first introduce the instrumentation and describe basic rheological concepts that govern the study of cell mechanics. I then report on the application of this system to study the force generation and dynamics of airway cilia. The bulk of the work is focussed on the role of cytoskeleton mechanics in cancer. I present our results which show the remarkable relationship between the cell's mechanical properties and its metastatic potential. Finally, I report on a novel pathway which is responsible for force mediated sensing in cells and show that this pathway is deregulated in cancer. These results have strong implications on the potential of stiffness and force sensing pathways as novel cancer therapeutic targets.

"I have been trying to think of the earth as a kind of organism, but it is no go. I cannot think of it this way. It is too big, too complex, with too many working parts lacking visible connections. The other night, driving through a hilly, wooded part of southern New England, I wondered about this. If not like an organism, what is it like? Then, satisfactorily for that moment, it came to me: it is most like a single cell "

- *The Lives of a Cell*, by Lewis Thomas

Dedicated to Karthikeyan Gopalakrishnan.

ACKNOWLEDGMENTS

Nanos gigantium humeris insidentes. None of what lies ahead would ever have been possible without the giants on whose shoulder I have stood on. And Rich has been not only been the giant but also the guiding light for all that I have accomplished and will accomplish in the future. Thank you for everything. I thank my thesis committee-Keith, Klaus, Gerry and Sorin for not only agreeing to be on it but more importantly, being great teachers, collaborators and role models for me. I thank Sean Washburn for giving me the opportunity to be a part of this great school. Michael Falvo, has been a great teacher and even greater friend(there is no other person in academia quite like you). I know what I know about basic biology because of Tim O'Brien. None of the 3DFM work would have been possible without Leandra, Russ, David and especially without Jeremy and Jay. The cilia work was done under the direction of David Hill. Finally, I want to thank Christophe Guilluy for basically making a cell biologist out of me. You have played a very important part in my education.

My work deals with the effect of external environment on cell processes. I thank my friends at NSRG, Ricky, Jeremy, Jerome, Lamar, Kris, Nathan, Brianna, Rachel, Luke, Cory, Shields for making our lab the best environment to be a part of.

Finally, I want to thank Rohit for being a friend, unlike any other. Karthik, this dissertation is dedicated to you, because you have been like a parent to me. Family plays a very important role in ones life and it is even more so when your family is your biggest collaborator. Thank you Mythreye for not making fun when I asked the stupidest of biology questions. We have our paper!!. My mother has always ignored

Contents

List of Figures

List of Abbreviations

CSK   Cytoskeleton

3DFM   Three dimensional force microscope

MHTS   Magnetic high throughput system

ECM   Extra cellular matrix

CISMM   Computer integrated systems for microscopy and manipulation

CF   Cystic fibrosis

GEFs   Guanine exchange factors

GAPs   GTPase activating proteins

LARG   Leukemia associated Rho GEF

MSD   Mean square displacement

GSER   Generalized stokes einstein relationship

PDMS   Polydimethyl siloxane

AFM   Atomic force microscope

FRET   Fluorescence resonance energy transfer

IDA   Inner dynein arm

ODA   Outer dynein arm

CBF   Ciliary beat frequency

CBA   Ciliary beat amplitude

TGF   Transforming growth factor

EMT   Epithelial to mesenchymal transition

ATP   Adenosine triphosphate

GTP   Guanosine triphosphate

MLC   Myosin light chain

List of Symbols

D   Diffusion coefficient

T   Temperature

a   Bead radius

η Viscosity

$\Delta r^2(t)$ Mean square displacement

α Power law exponent

k_B Boltzman constant

J   Compliance

m   Magnetic dipole moment

μ_0 Permeability of free space

μ_r Relative permeability

∇B Magnetic field gradient

G,k   Elastic shear modulus

γ Shear rate

v   Velocity

Chapter 1

Introduction

"Much excellent research has been done with a test tube and a Bunsen burner, but certain problems cannot be successfully attacked without the aid of intricate apparatus. It is the latter type of research, in so far as it applies to the studies on the physical properties of the protoplasm with which this report deals"'

- William Seifriz, (1888-1955)
"Methods of research on the physical properties of the
protoplasm, Plant Physiol 12:99-116"

The advancement of human civilization has been very strongly intertwined with the study of materials and their properties. Infact, materials of choice in a given era have defined the ages with phrases such as the Stone age, Bronze age and Steel age. The characterization of these materials especially on basis of their mechanical properties have driven these choices which is why mechanics of materials is probably the oldest forms of engineering and applied sciences. Cell, the most basic building block of life is probably the most complex form of a material. It is of course then of utmost surprise, that such an important material system has been mechanically one of the least understood systems that we know of. Partly of course this has been due to the complexity of all cell related subsystems as explained in the preface of the "Molecular Biology of the Cell" book, which says that the structure of the universe is better understood than

the workings of a living cell and that while we can tell the age of the sun and predict when it will die, we cannot explain how it is that a human being may live for eighty years, and a mouse only for two. We live now in an age where we finally have the tools and techniques to really understand the true mechanical properties of the cytoplasm and understand how important of a role these properties play in normal functioning of our lives. Having said that, none of the present progress would be possible without the foundation laid by the great scientists of the past who spent all their life seeking the same answers that we seek now, but facing challenges far greater that those of instrumentation and tools.

The 19th century witnessed the great debate between the "Vitalists" and the "Mechanists" about the structure, function and the purpose of the protoplasm. The vitalists believed that vital forces emanated directly from the "Will of Omnipotent and Omnipresent creator and physical forces were a result of vital forces(Carpenter, 1850). The vital force was the equivalent of gravitation for Newton: a central, yet unexplained fact which could be used to give systematic consistency to observable phenomena. In 1850, Carpenter wrote "the degree to which the phenomena of Life are dependent on physical agencies has been the subject of inquiry and speculation among scientific investigators of almost every school. That many actions taking place in the living body are conformable to the laws of mechanics, has been hastily assumed as justifying the conclusion that all its actions are mechanical..". One of the finest works of literature in all the annals of science, is D'Arcy Wentworth Thompson's *On Growth and Form (1917)* in which Thompson writes "..though they resemble known physical phenomena, their nature is still subject of much dubiety and discussion, and neither the forms produced nor the forces at work can yet be satisfactorily and simply explained."

Fighting critiques, skeptics and disbelievers like Thompson and Carpenter, the Mechanists believed that all processes with the cell could be explained by physical or chemical mechanics(Osterhout, 1914)(Seifriz, 1939). The knowledge of living forms for experimental biologists like Georg Klebs could only be achieved through knowledge of their conditions. Wilhelm Roux, in the late 1800's proposed "developmental mechanics" to account for origin and maintenance of organism through a causal morphology that would reduce them to a "movement of parts" and more importantly prove that biology and physics were completely one with each other. The true pioneers of this field were great thinkers, philosophers and perhaps some of the greatest scientists like Antony van Leeuwenhoek and Alexander Stuart in the 18th century and James Paget, William Seifriz and LV Heilbrunn in the 19th and 20th century.

We sit today, in front of our microscopes, claiming to understand parts of cell rheology, mechanics, signaling, structure, cytoskeleton with sophisticated tools like atomic force microscopes, laser tweezers, magnetic tweezers, nano fabrication technologies, high temporal and spatial resolution optics. One remarkable scientist's work is just as sophisticated, insightful and ground breaking as studies today with one main difference. LV Heilbrunn (1892- 1959), the general physiologist, conducted measurements of passive rheology and magnetic manipulations as early as in the 1920's. Heilbrunn's research interests ranged widely, but with a central theme of protoplasmic structure and action. While he is most well known for his study on calcium release theory of stimulation and response and application of this theory on cell division, his two seminal papers on the viscosity of the protoplasm are truly inspirational and ground breaking for all cellular mechanists and biophysicists such as myself(Heilbrunn, 1926; Heilbrunn, 1927). His desire to truly quantify the physics of the cell is underscored by the introduction of his 1926 paper in which he writes, *The early students of protoplasm described*

it as a viscous fluid, and they were content with such a description. But the modern biologist, concerned as he is with the physical behavior of the living material, needs to know approximately how viscous it is. Using approaches from colloidal chemistry, his observations of cell granules to estimate viscosity based on modified stoke's law is essentially passive rheology as we apply it today. His discussion on the effect of size of granules, the mesh size of the protoplasm, damage to the cell and the influence of temperatures are constraints and variables in today's measurements. His venture into active measurements involved injecting iron particles into bacteria and observing how fast they were attracted to an electromagnet. This is the fundamental principal of magnetic tweezers like the one described here in my work.

I will like to end this very brief perusal of the history of cell mechanics and philosophy of science with Heilbrunn's quote in 1927 about the future of cell mechanics and the limitations of his times. *It is much simpler to argue about the physical properties of the cytoplasm than actually measure them. But the physical study is by no means impossible. The biologist may never be able to make the measurements with the precision which the physicist is able to employ in his study of easily accessible inanimate objects. On the other hand measurements can be made and they are being made.*

1.1 The mechanics of the cell

A cell as a system behaves exactly as our body as system behaves. We rely on our musculoskeletal system for structure, support, stability and rely on it for movement. In exactly the same manner, the cell relies on its cytoskeleton for support, stability, structure and its movement. It is now easy to see why the mechanics of the cytoskeleton just like the mechanics of our bones and muscles is a crucial element for normal functioning. However, there is one fundamental difference between the cytoskeleton and musculoskelton. The cytoskeleton is not a fixed structure whose function can be

understood in isolation. It is a highly dynamic and adaptive structure whose component polymers and regulatory proteins are in constant flux.

The mechanical characteristics of the cell mainly comes from three main cytoskeletal polymers: actin filaments, microtubules and a group of polymers known as intermediate filaments(IF). These polymers are arranged in networks that resist deformation in response to externally applied forces. Actin and microtubules generate directed forces by the action of polymerization and depolymerization and interaction with molecular motors that drive cell motion and dictate cell shape and organization of cellular components. Though actin filaments are much less rigid than microtubules, the high concentration of cross linkers binding to actin promotes the assembly of highly organized, stiff structures including isotropic networks, bundled network and branched network. Unlike microtubules, actin filaments do not switch between discrete states of polymerization and non polymerization; instead, they elongate steadily in presence of monomers. For the purpose of my dissertation, the actin network is the most relevant cytoskeletal component. However, it will be scientifically ignorant to claim that the properties we measure or the phenomena that we show is completely isolated from other components of the cytoskeleton. Structures formed from microtubules, actin filaments or IF interact with each other and other cellular structures either non specifically(steric and entanglement interactions) or specifically (through proteins that link one filament type to another; Chapter 5 and Chapter 6. The cytoskeleton structure and contribution will be dealt in detail later in this document.

Before we move on to the importance of cell mechanics in signaling, it is important to appreciate that the mechanical properties of the cell are more than just signal transducers. Many disease are characterized by alteration in cell stiffness and the manifestation of these are physical as opposed to biochemical. An example of the alteration

in mechanical properties of cell leading to disease is in Malaria. Red blood cells which transport oxygen to various parts of the human body by deforming their way through blood vessels and capillaries. Unfortunately, these cells are also coveted by the protozoan *Plasmodium falciparum*, a single cell parasite. These parasites cause extensive molecular and structural changes in the red blood cells which in the end stiffen the cell membrane. At the schizont stage, the infected red cell is found to exhibit a viscoelastic solid behavior which is in contrast to the liquid like behavior demonstrated by healthy and early stage infected red blood cell. This stiffening in the red blood cell results in the impairment of blood flow ultimately leading to coma and death(Suresh, 2007a).

1.2   Mechanotransduction: Cells need to touch

In 1960, cell and developmental biologist Paul A Weiss said *lest our necessary and highly successful preoccupation with cell fragments and fractions obscure the fact that the cell is not just an inert playground for a few almighty mastermind molecules, but is a system, a hierarchically ordered system, of mutually interdependent species of molecules, molecular grouping, and supramolecular entities; and that life, through cell life, depends on the order of their interactions*(Fletcher and Mullins, 2010). Let's start with our body. Our arms and legs are composed of several organs (bones, muscles e etc.). These organs themselves are constructed by combining various tissues (vascular endothelium, nerve, connective tissue) which, in turn are composed of groups of living cells held together by the extracellular matrix (ECM) comprised of a network of collagens, glycoproteins, and proteoglycans. Each cell contains a surface membrane, intracellular organelles, a nucleus, and a filamentous cytoskeleton. Each of these subcellular components is, in turn composed of clusters of different molecules. Thus, our bodies are complex hierarchical structures and mechanical deformation of whole tissues results in coordinated struc-

tural rearrangement on many different size scales. At the protein level, these changes effect binding and conformation of different proteins and thus lead to different protein level functions. Mechanotransduction describes this phenomena of the translation of mechanical signals through external or internal physical cues into biochemical signals. Whether in direct contact with neighboring cells or with dense meshwork of polymers known as the extracellular matrix (ECM), cells receive external signals that guide complex behaviors.

Disease	Primary cells/tissues affected	References
Deafness	Hair cells in the inner ear	(Vollrath et al., 2007)
Arteriosclerosis	Endothelial and smooth muscle cells	(García-Cardeña et al., 2001)(Li et al., 2005)(Cheng et al., 2006)
Osteoporosis	Osteoblasts	(Klein-Nulend et al., 2003)
Myopia and glaucoma	Optic neurons and fibroblasts	(Cui et al., 2004)(Johnstone, 2004)
Asthma and lung dysfunction	Endothelial cells and alveolar tissue	(Uhlig, 2003)(Ichimura et al., 2003)
Development disorders	Multiple cell types and tissue	(Hove et al., 2003)(Lecuit and Lenne, 2007)(Krieg et al., 2008)
Cancer	Multiple cell types and tissues	(Paszek et al., 2005)(Huang and Ingber, 2005)(Chen et al., 1997)
Immune system disorders	Leuokocytes	(Coughlin and Schmid-Schonbein, 2008)(Ji et al., 2008)
Potential central nervous system disorders	Neurons	(Jacques-Fricke et al., 2006)

Understanding the mechanism of cellular signaling thus is inherently tied to understanding molecular level functions all the way up to protein level. An irony in

cell biology is the fact that while we have sequenced genomes of multiple organisms including us humans, this development has outpaced characterization of the cellular components that these genomes encode and far exceed our ability to reassemble these these components into the types of complex systems that can provide mechanistic insights into cellular behavior. That being said, the field of cytoskeleton research best illustrates the biological importance of establishing order over diverse length scales and time scales as well as understanding how systems of self organizing molecules carry out cellular functions. It is this reason why the field of mechanotransduction has gained high priority in cell signaling labs all over the world.

One of the commonly cited examples of the role of mechanotransduction is in hearing and balance. Sound waves, pressure and gravity cause small displacements in the *sterocilia* of hair cells in the inner ear. These deflections causes tension in the tip links connecting one sterocilia with the adjacent sterocilia, thereby pulling open mechanically gated ion channels. The rapid influx of calcium and other ions can then initiate further downstream signaling. Similarly, mechanotransduction is pivotal for touch sensation and proprioception which is the internal sensing of the relative position of one's body parts.

Since most cells rely on mechanotransduction signaling for normal functioning, many tissues are affected by impaired "biomechanical" signaling. Table 1.2 lists some of the diseases of mechanotransduction.

1.3   Summary of the Thesis Work

The unifying concept for this thesis is cell mechanics in disease. I have tried to give the broadest possible introduction to this concept in this chapter. My work involves using the magnetic tweezers system combined with high resolution microscopy to study

the role of the cytoskeleton in disease. Following the "hierarchal systems biology" approach, these tools have also been used to investigate the mechanisms by which these physical properties affect normal cell functioning and mechanotransduction. Due to the width of my work, I have started each chapter with its own more specific introduction and background. One of the greatest benefits of being a part of center for Computer Integrated Systems of Microscopy and Manipulation(CISMM) is the brilliant scientists from different fields that I have had the opportunity to interact and work with. The work is the sum of many such collaborations within and outside our research group. The collaborative nature of my work is hopefully conveyed to the readers of this document.

I first present the tools, techniques and theories used in all my work in Chapter 2. Past and present members of our group have specialized and often prided in their ability to build state of the art instruments and software in the field of forces in microscopy. One of the greatest achievements in this aspect is the 3 dimensional force microscope (3DFM). Spearheaded by an ex graduate student, Jay K Fisher(Fisher et al., 2005), the 3DFM has become one of the main research tool and cores of CISMM. Contributions by computer scientists, biologists, physicists and biomedical engineers have made this system ideal for users from multiple fields to study systems at different scales all the way from tissue to cells to polymers to single molecules. My involvement with the 3DFM has exclusively been in studying biological systems including cilia in our lung and cell cytoskeleton. In this chapter I briefly describe this system and its application specifically in cell mechanics. As mentioned earlier, there is no single unifying theoretical concept describing the cell as a material. The cell is a highly complex, heterogenous and dynamic system and quantifying its properties are highly dependent on the technique and the models used. I will briefly go over the various models and techniques in the literature and then introduce polymer rheology concepts that I use to measure cell stiffness and force response. I wrap up this chapter with all the complex "mechanical

signatures" that I have seen over the past 4 years in cell pulling. The hope is that this document will be a repository of mechanical observations that may aid any subsequent user looking for canonical data to refer to.

The first project I was involved with was to measure the force response and dynamics of cilia in the human airway system. In Chapter 3, I will first present the relevance of this study in understanding the role of the cilia in airway clearance and in diseases such as cystic fibrosis. Motile cilia are unique multimotor systems that display coordination and periodicity while imparting forces to biological fluids. They play important roles in normal physiologies, and ciliopathires are implicated in a growing number of human diseases. In this chapter, I will report our measurements on individual human cilia through a bead coating technology called spot labeling developed in our lab. Our study showed that

- A reduction in beat amplitude on application of force

- A decreased tip velocity proportionate to applied force

- No significant change in beat frequency

We also developed a quasistatic force model, applying which we deduced that axoneme stiffness is dominated by the rigidity of the microtubules, and that cilia can exert 62+18pN of force at the tip via the generation of 5.6+1.6pN/dynein head. The project was led David B Hill in the CF Center at Chapel Hill and also has contributions by a previous graduate student, Ashley Estes who developed lot of the protocols and instrumentation set-ups for these experiments. This work was published in the Biophysical journal in 2009 (Hill et al., 2010).

The rest of the work is focussed primarily on single cell mechanics, cell signaling and cancer. The seriousness of most epithelial cancers are largely defined by their

ability to invade through the basement membrane, a critical step in the metastatic cascade. While increased secretion of proteases, which facilitate degradation of the basement membrane, alteration in the cytoskeleton (CSK) architecture of cancer cells are previously studied hallmarks of invading cancer cells, the contribution of the mechanical properties of a cancer cell in this process is relative unclear. In Chapter 4, I begin with introducing the broad concepts of cancer and metastasis and the describing the known hallmarks of cancer. I follow this by presenting background work done in the field of cell mechanics and cancer. Our work in collaboration with Dr. Mythreye Karthikeyan in the Blobe lab, shows that stiffness of cancer cells measured with the 3DFM proportionally correlated with the ability of primary cancer cells and cancer lines to migrate and invade through a three dimensional matrix. Our results show that the most migratory and invasive cancer cell types are atleast 5 times softer than their non migratory/invasive phenotypes. Cells that with intermediate invasive potentials show a power law dependance to stiffness. Here, I introduce the TGF β signaling pathway and the type III receptor which has been shown by the Blobe lab to be a crucial regulator of the cytoskeleton and cancer metastasis. I also introduce the main tension causing mechanism in the cell which is the actomyosin machinery. Non muscle myosin causes contraction in actin filaments leading to tension in the cytoskeleton. Decreasing cell stiffness by pharmacological inhibitors of myosin II increases invasiveness, while increasing cell stiffness by restoring expression of metastasis suppressor TβRIII decreases invasiveness. Broadly speaking, these correlations show that mechanical phenotypes can be used to grade the metastatic potential of cell populations with the potential for single cell grading. Predicting invasiveness reliably by altering cell stiffness indicate that pathways regulating these mechanical phenotypes are novel targets for molecular therapy of cancer. Further, these measurements take minutes rather than the many hours needed for an invasion assay, which is promising for incorporation of this tech-

nique as a quantitative diagnostic method and as a discovery tool for therapeutics. These results are the foundation for investigation of mechanosensitive pathways discussed in Chapter 4.

As mentioned earlier, the mechanism of mechanotranduction is of considerable interests to biologists because of the role mechanical forces play in many aspects of cell functions. The outermost force sensing layer for the cell is the its extra cellular matrix(ECM). Integrins are transmembrane receptors that are involved in transmitting forces either imposed externally or generated internally by the cytoskeleton. The Rho signaling pathway is the key regulator of the actin cytoskeleton through its affect on actin polymerization and actomyosin contractility. However, the role RhoA in force sensing and mechanical response of the cell has been controversial and not clearly understood. It is this aspect of RhoA and integrin signaling that has been the main interest of The Burridge lab and Dr. Christophe Guilluy. In Chapter 5, after introducing the basic concepts in integrin mediated signaling and RhoA, I present the results of a joint study by Dr. Guilluy and I. By combining biochemical and biophysical approaches, we identified two guanine nucleotide exchange factors (GEFs), LARG and GEF-H1, as key molecules that regulate cellular adaptation to force. Although each GEF contributes to force mediated RhoA activation, both GEFs are necessary for mechanical response to force. We also show that LARG and GEF-H1 activation involves distinct signaling pathways.

One of the most remarkable observations during the work described in chapter 5was the fact that knockdowns that did not show mechanical adaptation also showed a drop in their basal stiffness magnitude. Our results in Chapter 4 show that cell stiffness plays a very important role in metastasis and is correlated to a cancer cells invasive ability. I also showed that the actomyosin machinery has a key role in this stiffness dependent invasion and migration. The key regulator of actomyosin contractility is again, the

RhoA signaling pathway which we were able to completely parse out in terms of force response and stiffness in Chapter 5 (On a fibroblast system). The natural next step was to combine the two, i.e. investigate the RhoA pathway in the ovarian cancer system and predict based on stiffness, the invasive ability and identify the pathway for this stiffness-invasion correlation. The role of RhoA and RhoGEFs has been controversial with many conflicting reports on the mechanism and potential application as therapeutic targets. I briefly introduce these in Chapter 6, and then show the results where we identify that GEF-H1 and only GEF-H1 shows increased expression in stiff cells and knocking down GEFH1 makes less cancerous cells very invasive and highly migratory. 3DFM measurements show definite attenuation in force response of cancer cells as they get more invasive and that, this response is dependent on GEFH1. Using high resolution fluorescence microscopy, one can see distinct differences in the actin structure and focal adhesion size in highly invasive cells. We also find that knocking down GEFH1 or overexpressing it results in consistent changes in stiffness, force response and invasion. These results point to the mechanism of cytoskeleton stiffness dependent invasion to go via GEFH1 and RhoA and also indicates that stiffness or proteins mediating stiffness are good targets for cancer therapeutic research.

Every decade or so, a new technology in biology/medicine completely changes the perspective of experiment design and/or clinical instrumentation. The current technology leading this change is the high throughput technology in imaging. However, while many new high throughput systems have hit the market, these existing systems suffer from slow 3D imaging and more importantly incompatibility with force application or other mechanical measurements. Our lab as been involved with developing a high throughput system which will enable fast 3D imaging and be compatible with a magnetic tweezers system. In the last Chapter 7, I briefly describe the magnetic

high throughput system(MHTS) and discuss potential applications of such a system in a clinical setting(for cancer diagnoses) and in a lab setting (for multi-parameter signaling experiments). I also discuss the future of mechanotransduction and magnetic tweezers experiments in studying different cellular phenomenas in concert with new breakthrough techniques like optogenetics and synthetic biology.

Chapter 2

The 3 Dimensional force microscope and cell mechanics

2.1   Introduction

Tools and strategies to measure mechanical properties of materials have existed for as long as we have existed. In-sync with our understanding of properties and development of new materials, the tools and instrument we use have also undergone an evolution to enable this growth. Perhaps, the greatest steps in development of techniques and models to understand materials has been in regard to gaining access to length and time scales previously unachievable. Nowhere is the impact of this more exciting than in biology. This is a remarkable time to be a biologist interested in physics and a physicist interested in biology. Our understanding of the structure and function of cells and organisms is developing at a startling pace, qualitatively and quantitatively. The latter has been driven by clever and practical applications of biophysical methods to quantify biological phenomena of living cells.

 The development of advanced technology over the past 2 decades, from high precision mechanical probes for measuring forces as small as piconewtons to imaging techniques that allow the visualization of a single protein *in vivo* has provided reliable tools for
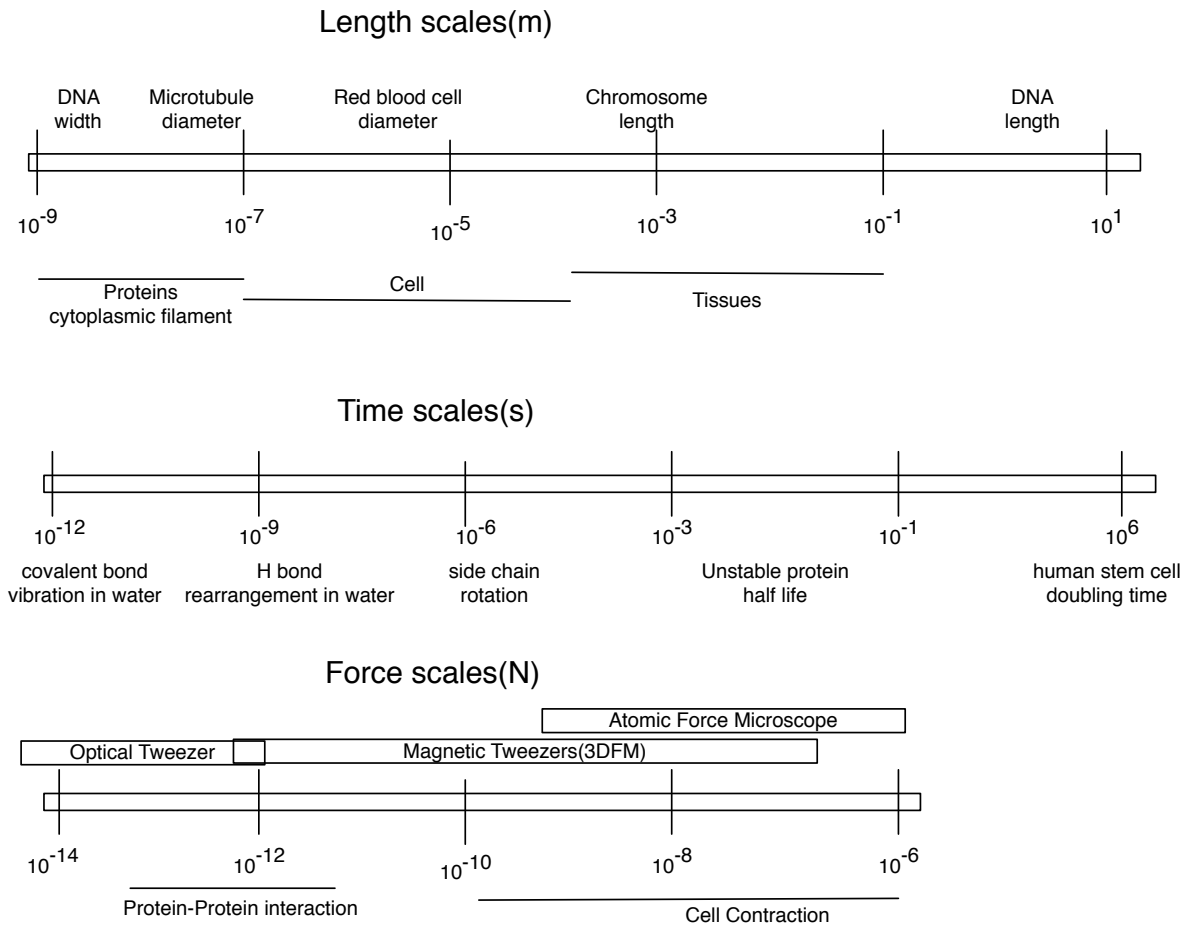
Figure 2.1: Length scales(top), time scales(middle) and force scales(bottom) in biology with the force regimes of different techniques to study cell mechanics.

monitoring the response and evolution of cells, subcellular components and biomolecules under mechanical stimuli. The dynamic nature of the cell and its components makes understanding the length and time scales even more important in cell mechanics.

2.2 Passive microrheolgy

Passive microrheology makes use of diffusion of molecules or small molecules in different materials. Diffusion is a stochastic process arising from motion due to thermal energy or kT of a particle and is key to a variety of different phenomenas in life. Movement of ions into the cell, monomer diffusion to the tip of a growing cytoskeleton filament, binding of signaling molecules to receptors are all diffusion mediated processes. What makes such processes especially intriguing is that despite the stochastic microscopic underpinnings, huge numbers of diffusing molecules over a large number of time steps can give the appearance of purposeful dynamics of particles.

Several methods take advantage of particle diffusion to measure microrheology like Dynamic Light Scattering(DLS)(Maret and Wolf, 1987), Diffusing Wave spectroscopy (DWS)(Mason and Weitz, 1995), Single particle tracking (Mason et al., 1997), Multiple particle tracking (Tseng and Wirtz, 2001)and two particle rheology(Levine and Lubensky, 2000).

Passive microrheology for viscoelastic materials like the cell is based on an extension of Brownian motion of particles in simple liquid(Einstein, 1906). The motion of particles within a viscous liquid can be quantified with the diffusion coefficient, D, which is a measure of how rapidly particles execute a thermally driven random walk. Given the particle size, temperature, and viscosity, η, the diffusion coefficient in a viscous fluid can be determined by the Stokes Einstein relation:

$$D = \frac{k_B T}{6\pi a \eta} \tag{2.1}$$

This relation is valid for thermal fluctuation where no energy consumption, such as ATP-driven motion or convective flows of liquid is present(Mason and Weitz, 1995). This equation is only valid for spherical particle because of the $6\pi a$ factor(Also used in Stoke's law 2.6). The dynamics of the material are usually described by the time-dependent mean square displacement(MSD), $< \Delta r^2(t) >$. When particles diffuse through a viscoelastic media or are transported in a non diffusive manner the $< \Delta r^2(t) >$ becomes non linear with time and can be described with a time-dependent power law, $< \Delta r^2(t) > \sim t^\alpha$. The slope of the log-log plot of the $< \Delta r^2(t) >, \alpha$ describes the mode of motion a particle is undergoing and is defined by the physical processes between $0 \leq \alpha \leq 2$. The generalized Stokes-Einstein relation(GSER) correlates the particle radius, a, and the $< \Delta r^2(t) >$ to provide the creep compliance:

$$J(t) = \frac{\pi a < \Delta r^2(t) >}{k_B T} \tag{2.2}$$

While the bulk of my work is focussed on active rheology, it will become apparent as we move through this chapter, that embedded in my active data is a lot of passive information. Even more remarkable is the fact that, the correlations we see between mechanical properties of the cell and their functions also exist in passive measurements. I will show some representative data for these correlations later in this chapter. Part of the work represented here is now being incorporated into the high throughput instrument that our lab is building(Chapter 7).

2.3   Active microrheology

Unlike the passive measurements approaches, the active microrheology methods incorporate some form of force application either locally at the site of interrogation or to the whole cell. There exist a variety of techniques to manipulate the mechanical

environment of cell population, individual living cells, and individual biomolecules. These approaches differ in three important respects: operating principles, force and displacement phenomena and extent of deformation(i.e., global vs. local; See Table 2.1).

Table 2.1: Application of active rheology techniques in cell studies

Application	Technique	Example
Cell population	Substrate deformation	Effect of global stress on cell morphology (Banes, 2000)
Cell population and single cell	Microfabricated post array detector	Measuring inter/intracellular traction(Tan et al., 2003)
	Magnetic twisting cytometry	Characterizing frequency dependence of cellular component(Bursac et al., 2005)(Navajas et al., 1999; Fabry et al., 2001)
	Magnetic tweezer	Chapter 4 and 5
Single cell	Cytodetacher	Measure cell substrate adhesion forces
	Optical stretcher	See below
Single molecule	Atomic force microscopy	Cell and cytoskeletal protein stiffness(Rotsch and Radmacher, 2000; Radmacher, 2002)
	Optical tweezers	erythrocyte elasticity(Sleep et al., 1999)
	Magnetic tweezer	Viscoelastic deformations of cells and membranes (Bausch et al., 1999)
	High resolution force microscopy	See below

Cell population techniques focus on the mechanical response or mechanical manipulation of entire cell populations. Here, the purpose is often to understand the role that mechanics plays in regulating the structure and function of tissues that comprise organs. Substrate deformation relies on applying strain on substrates that the cells are attached to. The strains are imposed and measured via standard strain gauges or other low resolution displacement sensors. Maximum applied force and displacement are in

the Newton range and millimeter range.

Several cell manipulation technologies have been enabled by the development of thin film lithographic techniques. Micro-patterned substrates are fabricated to allow count wise control of cell adhesion and traction measurements through displacement of the pattern features(Chen et al., 1997) . Arrays of independently deforming posts onto which cells adhere have been produced using standard photolithography to create a silicon replica, then casting an elastomer(PDMS) within the replica to form a pattern of flexible micron-scale cantilever (oriented vertically) and finally microcontact printing the cantilever ends with ECM protein to facilitate cell adhesion. Here, the strain imposed on a particular cell cannot be modulated in a given experiment; it is set by the compliance of the cantilever array. In addition, the deformation is quantified only in the plane of the cell/post interface. Atomic force microscopy(AFM) is a specific example of scanning probe microscopy which has been exploited by the biophysics community because this technique affords Angstrom scale positioning accuracy, the ability to image and mechanically manipulate a single biological structure with better than nm/pN resolution and the potential to track the biological processes in near physiological environments over time. In particular, AFM has been used to explore the elastic deformations of cells and cellular components like the cytoskeleton. The elastic behavior of the cytoskeletal filaments can be explored via AFM as a function of position with the cell, first by creating a contact based image of the cell an then by conducting high resolution force spectroscopy measurements at particular points on that image.

2.3.1 The optical stretcher for imposing force on the whole cell

The basic principal behind all laser based manipulation techniques is that momentum is transferred from light to the object, which in turn, by Newton's second law,

exerts a force on the object. Based on this principal, the single beam laser tweezers have been an invaluable tool in cell biology: for trapping cells(Ashkin and Dziedzic, 1989), measuring force exerted by molecular motors such as myosin and kinesin(Block et al., 1990) or the swimming forces of sperm(Tadir et al., 1990)and studying the polymeric properties of single DNA strand(Chu, 1991). The optical stretcher developed by Guck and Kas in contrast is based on a double beam trap in which two opposed, slightly divergent and identical laser beams with Gaussian intensity profile trap an object in the middle(Guck et al., 2005). The condition of stable trapping is fulfilled if the refractive index of the object is larger than the refractive index of the surrounding medium and if the beam sizes are larger than the size of the trapped object. In object such as cells, the momentum transfer primarily occurs at the surface. The total force acting on the center of gravity is zero because the two beam trap is symmetric and all the resulting surface forces cancer. In elastic objects, the surface forces stretch the object along the beam axis. A simple schematic of the optical stretcher is shown in Figure 2.2. Some of the advantages of this technique is that due to the incorporation of an automated flow chamber, the optical stretcher has the potential to measure elasticity of large number of cels in a short amount of time. This condition is ideal for circulating tumor cell measurements(CTC). The technique also bypasses issues related to localized cell stiffness heterogeneity and mechanical contact of the probe leading to adhesion and active cellular response. An application of this technique in testing for malignant transformation is shown in Chapter 4.

2.3.2   Fluorescence force spectroscopy

Taking a quick diversion from techniques used to apply forces in biology, I want to quickly describe a technique to measure forces in biology.This technique ranks high in many single molecule, protein protein interaction applications and for a lack of a better
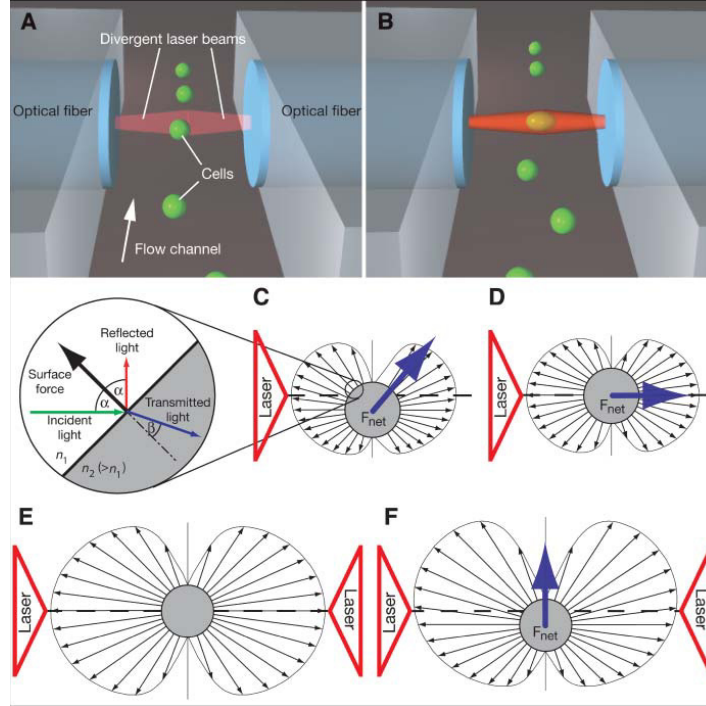
Figure 2.2: From (Guck et al., 2005). Cells flowing through a microfluidic channel can be serially trapped (A) and deformed (B) with two counter propagating divergent laser beams. The distribution of surface forces (small arrows) by one laser beam from the left(large triangles) for a cell that is (C) slightly below the laser axis and (D) on the laser axis. F_{net} is an integration of all the forces. (E) Stable trapping configuration when cell is on axis and (F) when symmetry is broken. (Reprinted with permission)

word, in "coolness" factor.

Mechanical probes have often suffered from the fact that they lack the ability to detect small scale conformational changes unless strong and persistent force is applied. At weak forces, the flexible tether connecting the mechanical probe to the biological molecule is not stretched enough to transmit small movements. Taekjip Ha's group at University of Illinois has been involved in developing single molecule detection techniques for years. In 2007, they combined single molecule fluorescence resonance energy transfer(smFRET) with manipulations using optical trap. smFRET has high spatial resolution ($\leq 5\mathring{A}$) and can be measured at arbitrarily low forces(Hohng et al., 2007). The basic principal of such a system is use a flexible molecule that deforms or unzips at low forces, calibrate it using an optical trap and then insert FRET pairs into the molecule. SInce FRET signals inversely vary with increased stretching or deformation, one can insert this sensor into molecules of interest and detect FRET signals to get forces involved. An application of such a system relevant to this document was the development of the Vinculin tension sensor(Grashoff et al., 2010). Here, the authors designed a tension sensor module that contains a spring like protein segment, based on a sequence from a spider silk protein, that stretches in response to tension. They then positioned the fluorescent proteins at the ends of this spring like protein segment. Application of tension causes the sensor module to stretch leading to decrease in FRET signal and this way the authors were able to measure local tension in the vinculin molecule.

2.4 Magnetic manipulations in cell biology

Magnetic techniques offer a number of advantages over other methods that are commonly used to probe cell mechanics. While a majority of techniques including magnetic tweezers can apply localized forces to molecules on the cell surface, the advantage of
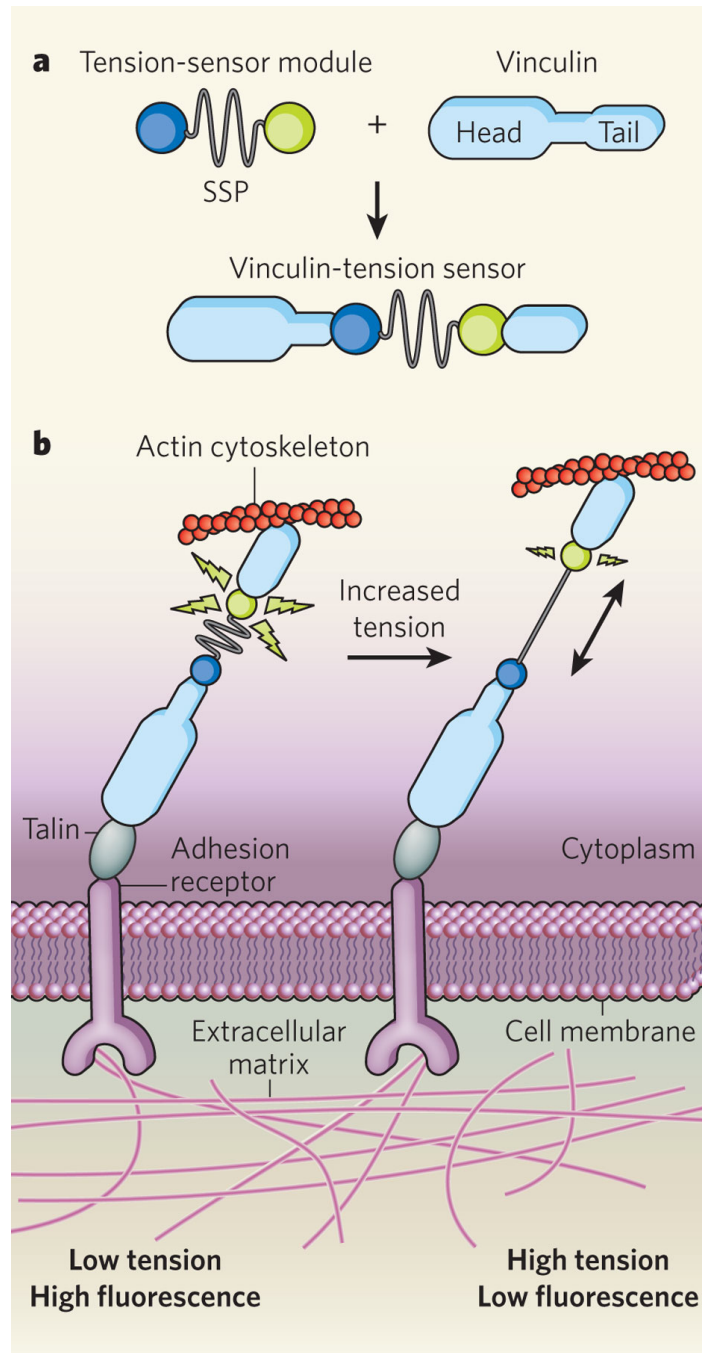
Figure 2.3: From(Doyle and Yamada, 2010). a) Tension sensor module using an 40 amino acid long protein segment derived from the sequence of a spider silk protein(SSP). The sensor module is inserted between the two fluorescent molecule and then reinserted between the head and tail domain of Vinculin. b) Increased tension stretches the SSP region resulting in decreased fluorescence. (Figure not to scale)(Reprinted with permission).

magnetic tweezers include: (1) A much wider range of force (from picoNewtons to nanoNewtons) can be applied to specific cell surface receptors, (2) A much larger frequency range (0-10kHz) of forces can be applied, (3) hundreds of thousands of cells and bound beads can be analyzed simultaneously, (4) cells may be mechanically probed continuously for hours or even days without potential heating problems, (5) forces can applied inside cells by allowing cells to engulf beads, and (6) magnetic systems are more robust, easier to use and cheaper to build.

2.4.1 Magnetic twisting cytometry(MTC)

In MTC, ferromagnetic beads(1-10μm diameter) are used to apply twisting forces to the receptors that the beads are attached to on the surface of living cells. To apply the twisting force, typically a strong (100G) but very brief (10μsec) magnetic pulse is applied using a horizontal Helmholtz coil. This induces and aligns the magnetic dipoles of the beads in the horizontal direction. Within a few seconds, a weaker(0-90G), but sustained magnetic field is applied in the perpendicular direction using a second vertically oriented Helmholtz coil. As a result, the beads are twisted, thus applying a hear forces directly to the bound receptor. The average bead rotation and angular strain can be measured using an inline magnetometer. An important study that came out from MTC was the report of a scaling law that governs both the elastic and frictional properties of a wide variety of living cell types over a wide range of time scales and under a variety of biological interventions(Fabry et al., 2001). Scale free rheology is often found in the class of materials called soft glasses. Further work using MTC also found that large oscillatory shear fluidized the cytoskeletal matrix, which was followed by slow scale free recovery of rheological properties thus establishing a striking analogy between the behavior of the living CSK and that of inert non-equilibrium systems,

including soft glasses(Bursac et al., 2005).

2.5   Magnetic tweezers

In 1950, Crick and Hughes following the suggestion of Dr. Honor B Fell, allowed chick embryo fibroblasts growing in tissue culture to phagocytose small magnetic particles, and then moved these particles in the cytoplasm by means of external magnetic fields(Hughes, 1950). As mentioned in Chapter 1, Seifriz and Heilbrunn had done similar experiments 20-30 years earlier, though Crick's work presented sound experimental and theoretical models for the physical properties of the cytoplasm. The magnetic tweezers functions on the same principles as MTC except instead of applying oscillatory motions on the magnetic probe particle, magnetic tweezers apply linear forces. Force on a magnetic bead is caused by an interaction between the bead's magnetic dipole moment m and the gradient,∇B of an incident magnetic field. For a soft, magnetically permeable bead, m is entirely induced by the incident field. Subject to saturation properties of the magnetic material in the bead,

$$m = \frac{\pi d^3}{2\mu_0} \frac{\mu_r - 1}{\mu_r + 2} B \tag{2.3}$$

where μ_0 is the permeability of free space in SI units, μ_r is the relative permeability of the bead, and d is the diameter of the bead. The magnetic force is then,

$$F = \frac{\pi d^3}{4\mu_0} \frac{\mu_r - 1}{\mu_r + 2} \nabla B^2 \tag{2.4}$$

In a magnetic tweezers apparatus, permanent magnets or electromagnets can be used as source of field. While a permanent magnet generates a static permanent field, electromagnets convert electrical currents into magnetic field and allow the control of

the field through control of the current. The simplest version of an electromagnet is a coiled conductive wire. If multiple coils form a cylindrical geometry, the structure is a called a solenoid. When electrical current runs through the wire, a magnetic field is established in the direction of the solenoid's axis. The strength pf the field produced by an electromagnet is set by the value of the current in the wire and the coil geometry. To amplify the magnetic field, a magnetic core can be positioned inside the solenoid. Cores are typically made from soft ferromagnet materials with high saturation and low remanence. While the amplitude of the field is important, it is the gradient of the magnetic field ∇B that directly factors into the magnitude of the force(Eq. 2.4). The gradient is the strongest close to the magnet, as the field drops in magnitude faster nearer the magnet than further away from it. A convenient rule of thumb in approximating the gradient one can obtain with a magnet is that most of the field will vanish within a distance that is roughly the size of the pole diameter. If the force needs to be constant over an extended range such as the field of view of the microscope, then ∇B needs to be constant over the same area. This can be obtained either by using a blunt large magnet that will generate a slowly decreasing magnet field, that is small gradient or by doing the experiment further away from any type of pole, in the region where the variance of the field tapers off. Generation of large forces require large field gradients. This is typically obtained by tapering off the electromagnet core at the pole on the sample side to concentrate the magnetic flux. If a magnet generates a 0.5T field and the cross section is 1cm, the average gradient near the magnet is on the order of 50T/m and the force is $\mu_{particle} \times 50T/m$. If the magnet is sharpened such that the cross section is $10\mu m$ for a face field of 0.5T the local magnetic gradient is on the order of $5 \times 10^4 T/m$.

2.6 The 3 dimensional force microscope (3DFM)

The 3DFM is the magnetic tweezers system in our lab. Primarily built by Jay K Fisher as part of his graduate work, the system incorporates state of the art magnetic and optics technology for precise, high bandwidth force application with a video and laser based tracking system for measuring probe displacement. The description of this system can be found in multiple publications from the group(Fisher et al., 2006; Fisher et al., 2005)(O'Brien et al., 2008)(Hill et al., 2010). The force acting on a particle in our system depends on a number of factors.

1. **The pole material**: We are currently restricted to 2 different materials, Netic and Co-Netic AA, for our pole plates. Netic material has a high saturation point(2.1T) compared to the Co-netic(0.8T). This should result in a higher achievable maximum force in Netic pole plates. However, the Co-netic has higher permeability(30,000) versus Netic(200), which would cause a faster rise in force in Co-netic for an equal step increase in drive current. Further, the lower coercivity in Co-netic reduces the overall remanence experience after magnetization. In short, even though Co-netic pole plates give a lower maximum force than Netic, their high permeability and low remanence makes them ideal for cell experiments. Co-netics are also more resistant to corrosion making them more suitable for use in cell experiments which are done with low volumes of cell culture media.

2. **Selection of magnetic bead/probe**: A variety of particles, typically superparamagnetic beads, are currently used for physical manipulation of cells and biomolecules. For most magnetic experiments, consistency in the magnetic and geometric characteristics of the particle is very important. Most magnetic particles are commercially available in a variety of size and magnetic content. Our experience so far has been that beads smaller than 1μm are not reliably uni-

form. Thus our lab mostly uses beads of 1μm, 2.8μm and 4.5μm made by Dynal (Invitrogen Corp.). Beads are available with various surface chemistries such as streptavidin, carboxyl, amino or tosyl groups. Streptavidin beads are useful to link to biotinylated antibodies to specific cell surface receptors. This strategy has been used for the cilia experiments in Chapter 3. Tosyl activated beads can simply and easily linked to amino groups on a membrane protein, a stratergy used to coat beads with fibronectin to attach to integrin receptors in Chapters 4 and 5. The calibration section below will show the different forces we get with different beads sized. For my experiments, I use the 2.8μm beads as they give good maximum force for biological experiments with enough resolution in the low force limit.

2.6.1 Calibration

Perhaps, the best way to describe the different components of the 3DFM is by describing the most tightly constrained experiment that is run on the system. Calibration of our pole plates requires running the magnetic system at its highest bandwidth and recording the data at the highest frame rate, which is why I will start by first describing pole plate calibration.

Before running any experiment on systems like the 3DFM, it is important to calibrate the system. Calibration involves finding the force acting on a bead of a particular size at all possible driving voltages and experimental locations with respect to the pole tip. The calibrations are done in samples where the property of the fluid is already well characterized and known. In theory, we can use any Newtonian fluid provided its viscosity is well characterized. Sucrose solutions are good candidates since they are highly water soluble and have predictable viscosities for any concentration below solubility limits and any temperature below 100°C. We also use Karo^{TM} for calibrations that

require high forces because of its relatively high viscosity of 3.4 Pa s. For calibrating 2.8μm magnetic beads with a Co-netic pole plate, we use 2.5M sucrose which has a viscosity of 125mPa s at 23°C.

The variable force calibration software(VFC) was created by Jeremy Cribb to sample the force field around the pole tip as a function of both distance, r, from the pole tip and the drive current, I. The magnet control software, written in MATLAB, allows the user to drive the magnetic amplifier with a series of constant current pulses. As mentioned earlier, the magnet pole tip exhibits remanent magnetization after the application of a magnetic field. We can measure this hysteresis as a velocity of the magnetic bead at zero drive current. To degauss the poles, we apply a drive current

$$I(t) = I_{max}e^{-t/\tau}sin2\pi ft \tag{2.5}$$

where, I$_{max}$ is the maximum applied current since the last degauss, τ is the decay constant, and f is the frequency of the sinusoid. For the 3DFM, the pulse consists of a decaying 10kHz sine wave sampled at 100kHz with a time constant of 1.2ms, equivalent to a 10% decay in amplitude for each cycle. The magnetic drive system that runs the current generation of the 3DFM is capable of driving its full power of 2.5A at a frequency up to 10kHz(Vicci and Superfine, 2004). The material of the pole plate defines the maximum current that one applies during the calibration. Since the Co-netic pole plate saturates very quickly, the highest current applied is 0.6A(Figure 2.5). The *Gluitake* (another Jeremy Cribb masterpiece) program captures and stores video frames in a RAW pixel format (648×484×256) at rates up to 120 frames per second(fps). Tracking of beads in a calibration video gives a data set consisting of bead's velocity at each drive current in each pulse sequence. The only beads included in the analysis are those within an angle of ±30° of the pole's line of symmetry, as the force varies significantly outside of that cone. The pole center is found by extending the bead trajectories to a point of
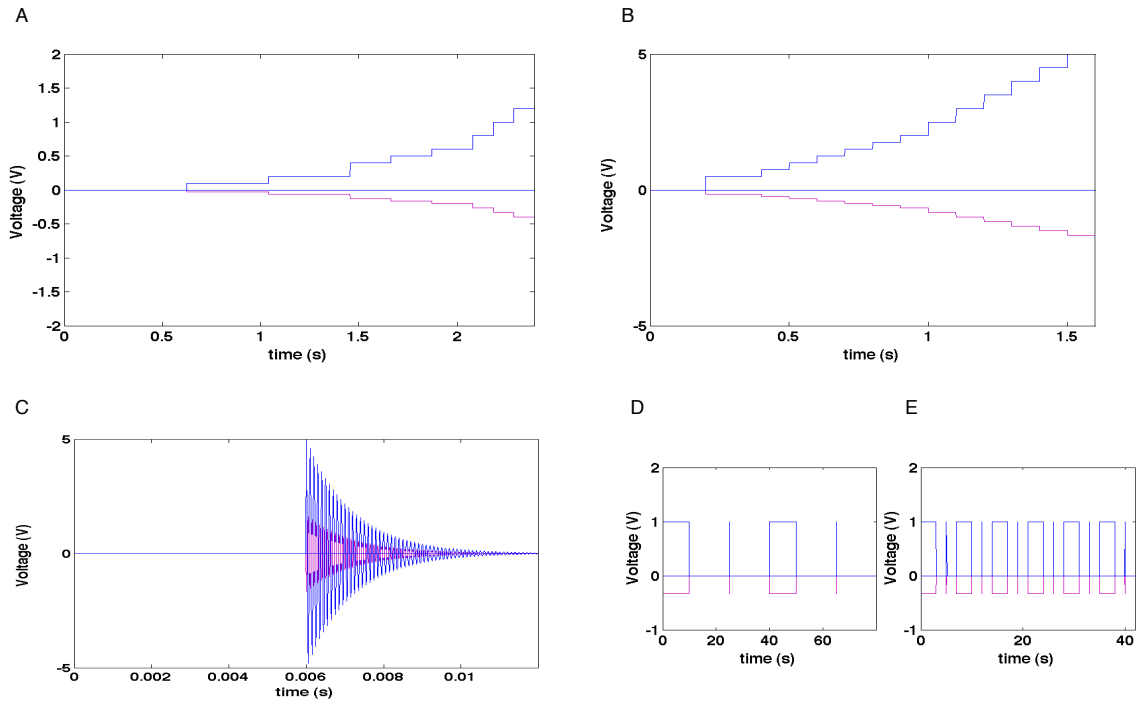
Figure 2.4: Force train: Voltage signals/drive train sent to the magnetic amplifier for A) Calibration of a Co-netic tip, B) Calibration of a Netic tip, C) Degauss routine, D) Compliance measurements(left) and reinforcement measurements(right)

common intersection within the area of the pole tip to determine the origin of this polar coordinate system. The coordinates of $[x(t), y(t)]$ are transformed into this system to find r(t). A linear fit to $r(t)$ at each drive current I reveals the velocity $v(r, l)$.

The tracked particle displacements are synchronized and merged with the magnet drive history to a temporal resolution of approximately 8.6 milliseconds. The velocities are then converted to corresponding forces with Stokes drag for the prescribed particle geometry using the equation:

$$F = 6\pi a \eta v \tag{2.6}$$

where η is the dynamic viscosity of the calibrator fluid, v is the velocity and a is the radius of the bead. The force data, **F** may be displayed as a function of **r** or as a function of the drive current at a given distance, **F(I)**. The saturation of the pole material is evident from the change in the slope of **F(I)**.

Any experiment on the 3DFM system follows the same protocol as the calibration experiment, except that the calibrator fluid is replaced by the material being studied. The experimenter will decide the force profiles that will be applied, the video capturing frame rate and the appropriate model that will be applied to the date to extract properties of the material.

2.6.2 Experimental Procedure

This is detailed procedure for conducting cell stiffness and force response measurements in the 3DFM. Over the past 4 years, I have used different cell types, bead types, force protocols, high resolution fluorescence microscopy etc. However, while there may be variation depending on the cell type(Drosophila versus other cell lines) and bead incubation time(eg. anti ICAM beads versus Fn beads), the general procedure remains
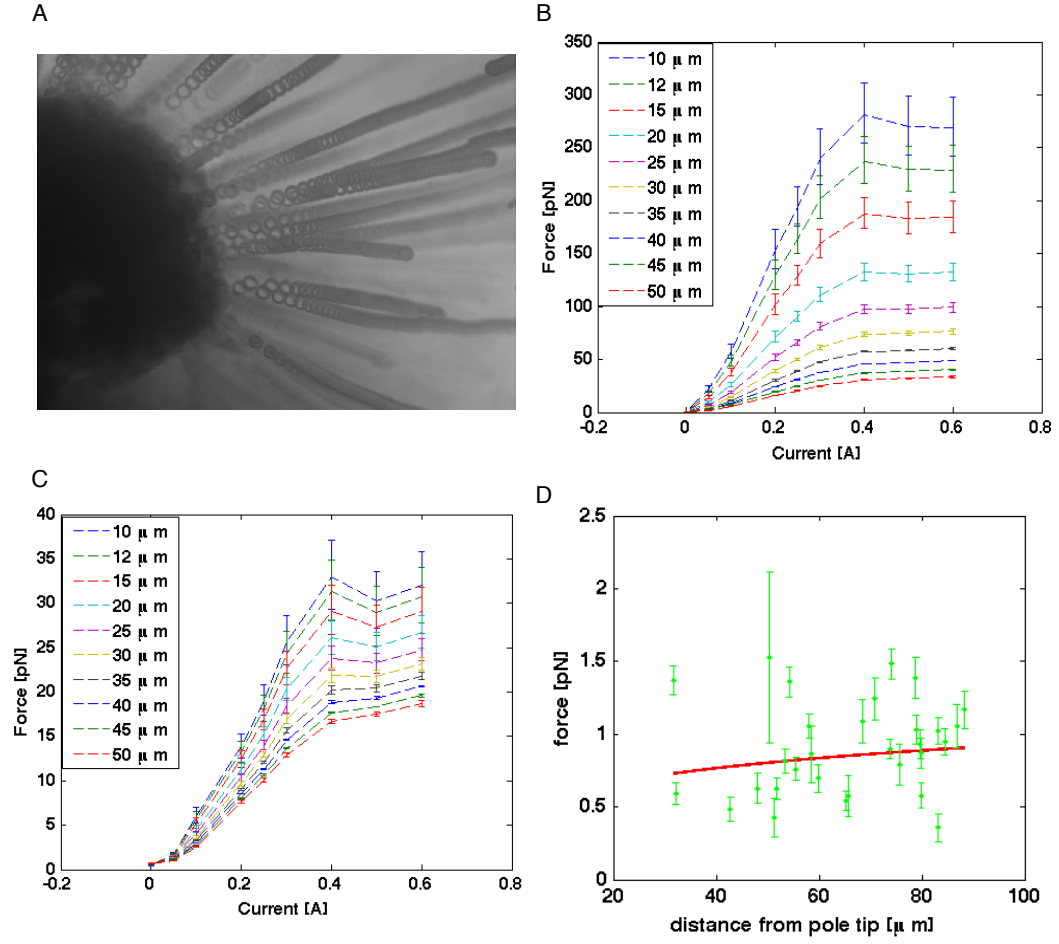
Figure 2.5: A) Maximum intensity projection of a calibration experiment with $2.8\mu m$ beads in sucrose. The shadow of the pole tip is on the left. B) Saturation curve for a Co-netic pole tip at the plane of the tip(Z=0) and C) $40\mu m$ below the pole tip(Z= 40). D) Net remnance in the pole tip prior to degauss.

the same.

1. Before the start of any experiment, we prepare large amounts of magnetic beads coated with the ligand of choice. The pole plate to be used for the experiment is calibrated. Cell experiments start by plating cells on 24×50, 1.5 coverslips typically 12-24 hours before the experiment.The coverslips can be pre treated with fibronectin, other ECM proteins or plasma cleaned. However, while comparing measured values for different cell types or treatment types, care should be taken to keep the cover slip treatment condition the same.

2. On the day of the experiment, after the cells have spread well on the cover slips, the beads are added to the cells 30 minutes before the experiment. The concentration of bead required is pre calculated and typically we shoot for one bead per cell.

3. Before loading the sample on the 3DFM stage, the media on the coverslip is removed and fresh media is added. The fresh media is added in minimum quantities to prevent flow during the experiment.

4. All experiments reported in this document have been done with a 40× objective with a 1.5 multiplier to give a total magnification of 60× or $0.152\mu m$/pixel resolution on the *Pulnix* camera. The various softwares are preloaded and the pole tip is degaussed multiple times before bringing it down on the sample. Initially the pole tip is kept at a high enough height, such that it does not scrape the cells or induce flow.

5. Once a desired field of view is obtained, the pole tip is brought down to a height of less than $20\mu m$ from the bead. The experiment is run by first starting the video and the starting the magnet drive to apply forces. Videos are recorded at either 30fps or 60fps we can get 1 to 5 beads per field of view. Between different runs

we move to a far enough field of view to avoid history dependance on the beads. The pole tip is lifted up(after degaussing) and the sample is then translated to move to a different field of view. The force train or protocol used is kept the same across the measurements that are compared(For e.g. All measurements in Chapter 4 compared have force applied over 10 seconds only.)

6. Once the experiment is completed, the videos are tracked using Video spot tracker(http://cismm.cs.unc.edu/downloads/). Beads which show displacements less than 10nm(detection resolution) and loosely bound beads are eliminated from the analysis pipeline. Custom made MATLAB programs are used for further analysis and cell stiffness quantification.

2.7 Modeling cell mechanics

As a material, the cell is highly dynamic, complex and heterogeneous. Depending on the magnitude, direction and distribution of mechanical stimuli, cells can respond in a variety of ways. Generally, mechanical models for cells are derived using either the micro/nanostructural approach or the continuum approach. The former deems the cytoskeleton as the main structural component and is especially developed for investigating cytoskeletal mechanics of adherent cells. Continuum approach on the other hand, treats the cell as comprising materials with certain continuum material properties. From experimental observations, the appropriate constitutive material models and the associated parameters are then derived. The continuum approach is easier and more straightforward to use in computing the mechanical properties of the cells of the biomechanical response at the cell level is all that is needed. Once a continuum model is established, it can provide details on the distribution of stresses and strains induced on the cell, which in turn can be useful in determining the distribution and transmission

of these forces to the cytoskeletal and subcellular components. This can then assist on the development of more accurate micro and nanostructural components.
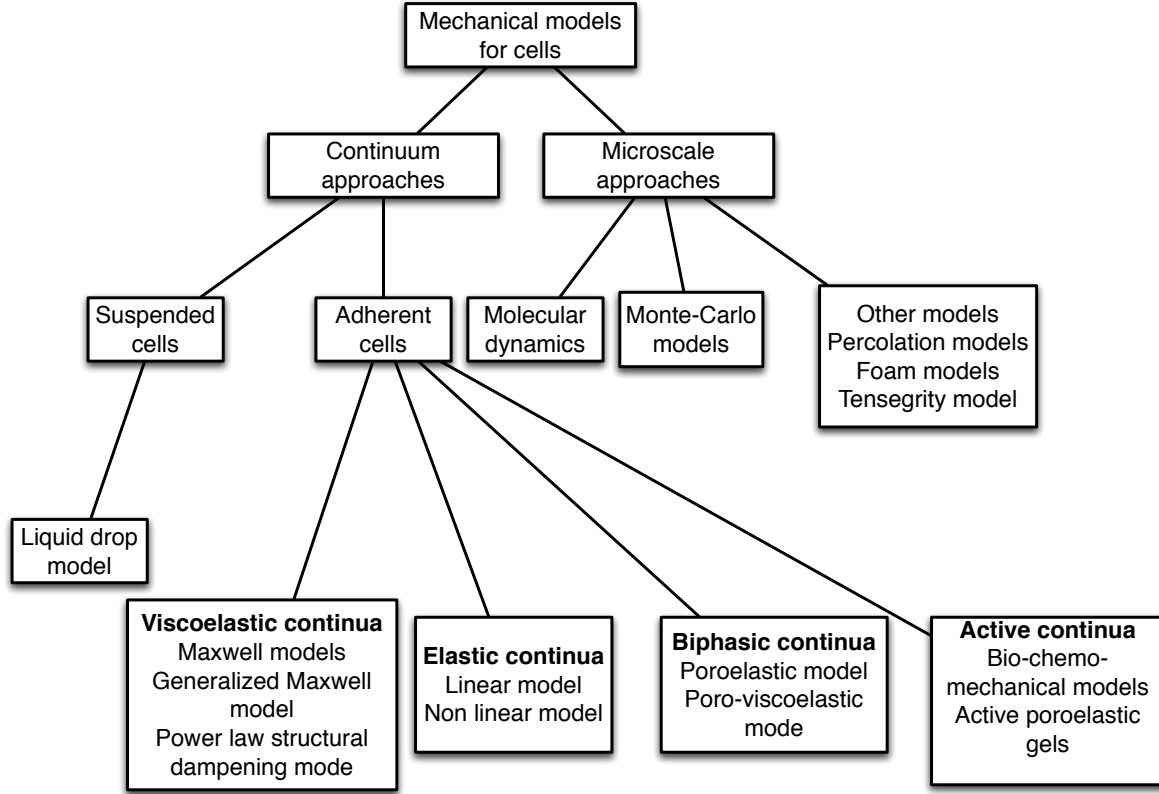
Figure 2.6: Review of mechanical models of the cell.

2.7.1 Mechanical circuits and the Jeffrey's model

The property that rheological studies are designed to quantify is conceptually simple, namely a value that predicts how a material will deform when a force of certain magnitude is applied to it in a defined geometry for a given amount of time. Two different ideal ways in which a material can deform are essentially related to the difference between liquids and solids. When a force is applied to an ideal solid, the material deforms to a certain extent, and then stays put in that deformed state until the force is removed, when it returns to its original state. Ideal liquids on the other hand, will

deform without limit for as long as the force is applied and the liquid will remain in the deformed state when the force is removed. Real materials like the cell are neither ideal solids or liquids, nor even ideal mixtures. Biological materials exhibit both elastic and viscous responses and are therefore called viscoelastic. An ideal elastic system follows Hooke's law, $\sigma = G\gamma$, where G is the elastic shear modulus and $\gamma = \delta x/h$ is the simple shear. For ideal liquids or Newtonian liquids, σ is independent of strain but is proportional to the rate of strain where the proportional constant η is the viscosity giving $\sigma = \eta\dot{\gamma}$.

The use of mechanical models such as the spring and dashpot as analogues of the behavior of real materials enables us to describe very complex experimental behavior using a simple combination of models. Models can be applied to extension or bulk deformations and need not be restricted to application of shear stress. Typically one would like to predict the stress response to all possible deformations and time scales. These expressions are called constitutive equations of the body. As mentioned above, viscoelastic materials exhibit behavior which can be described using a combination of elastic and viscous elements. The elastic element is represented as a spring and the viscous as a dashpot. The 2 simplest arrangements that we can visualize is the models in series(Maxwell model) and in parallel(Kelvin-Voigt model). When we apply a stress to the parallel elements of a Kelvin model, both elements respond. Thus, linear addition of the stresses describe the model: $\sigma = G\gamma + \eta\dot{\gamma}$. For a Maxwell model, it is the strain rates that linearly add:$\dot{\gamma} = \frac{\dot{\sigma}}{G} + \frac{\sigma}{\eta}$. All these relationships are derived from fundamental Newton's laws of motions, where if F_{ext} is the external force being applied on a body resulting in a displacement x, velocity v and acceleration, a, then:

$$F_{ext} - f_v v - kx = ma \tag{2.7}$$

The *ma* factor arises from the inertial effect of the body due to its mass. At the length and time scales of biological measurements, this effect is negligible and ignored. This assumption results from a dimensionless quantity known as the Reynolds number and for the present discussion it is adequate to state here that this number is less than 0.01. Edward Purcell's lecture on "Life at low Reynold's number" is a must read for all biophysicists(Purcell, 1977) and goes into the reason for this assumption. The f_v factor is due to the viscosity, η of the system and for a spherical body can be solved using the Stoke's flow equation:

$$\eta = \frac{F}{6\pi r_s v(t)} \tag{2.8}$$

where r_s is the radius of the sphere. The shear modulus can be computed by first computing the compliance, J,

$$J = \frac{1}{G} = \frac{6\pi r_s x(t)}{F} \tag{2.9}$$

Thus, by substituting these quantities into the equations for Kelvin-Voigt or Maxwell models, we can describe the constitutive equation for a spherical body under the effect of a step external force, $F(t)$.

Creep or step stress experiments with beads on cell exhibit responses which are more complex than pure Kelvin-Voigt and Maxwell bodies. The closest constitutive model describing their behavior in my experiments is the Jeffrey's model. The Jeffrey model shown in Figure 2.8 with its step response, captures behavior typically seen in viscoelastic liquid. The η_0 damper accesses viscous only modes of the material. The stress controlled step response, $J(t)$ is

$$J(t) = \frac{1}{G} + \frac{t}{\eta_0} - \frac{1}{G}exp\left(\frac{-Gt}{\eta_1}\right) \tag{2.10}$$

39
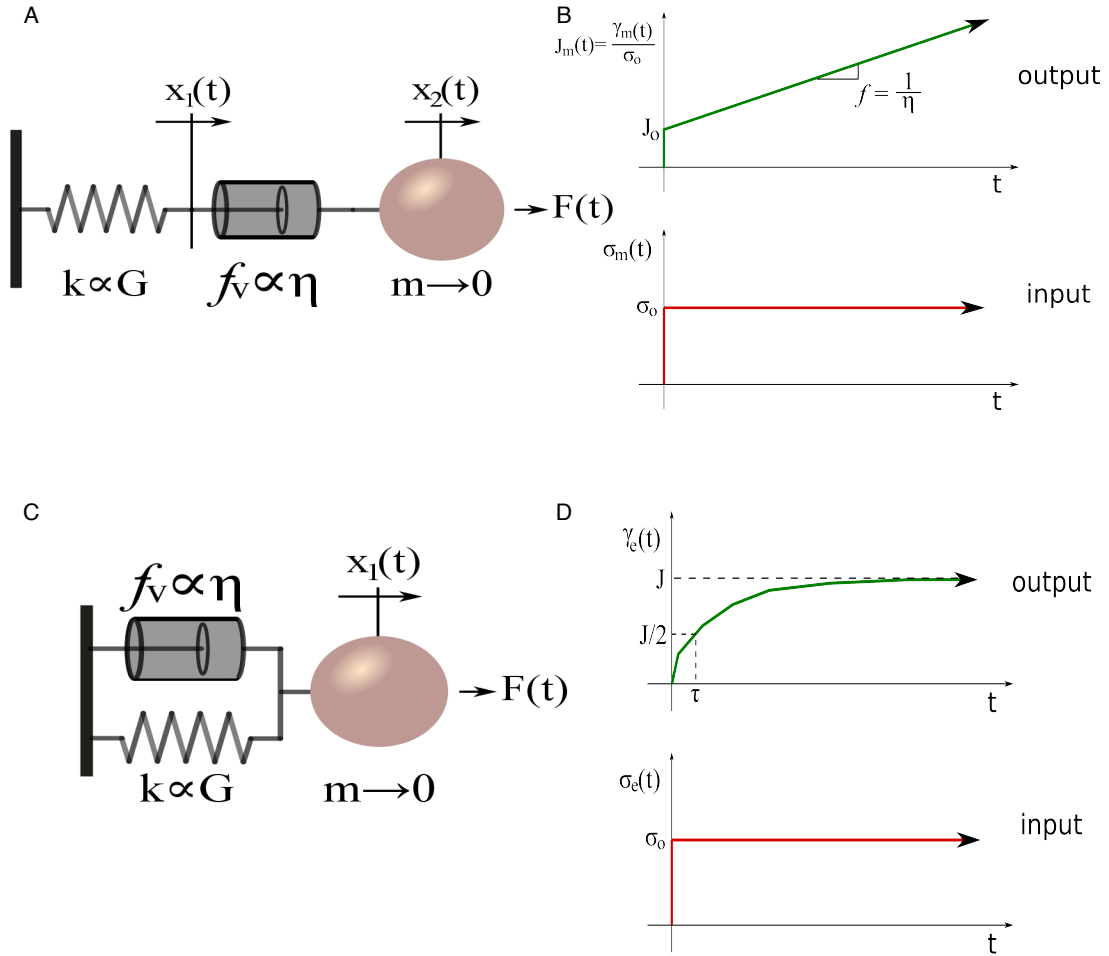
Figure 2.7: Maxwell and Kelvin-Voigt model(From(Cribb, 2010): A) Maxwell model and B) Strain response for a step stress application. C) Kelvin Voigt model(Viscoelastic solid) model and D) Step strain response for a viscoelastic solid.

The steady state, zero-shear viscosity is extracted from the slope of the material's step response while the modulus, G, can be estimated from the projected intercept(Maxwell approximation). The advantage of using a Jeffrey's model is that it can reduce to a Kelvin-Voigt or a Maxwell model easily by changing either one of the 2 dashpots in the model.
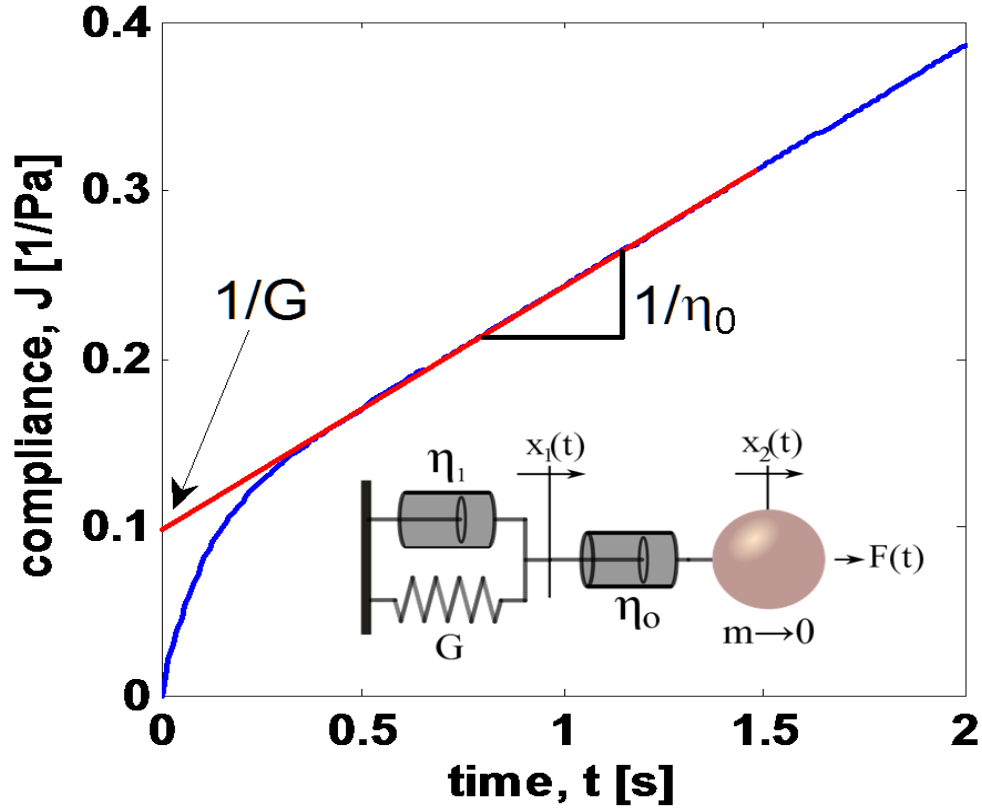
Figure 2.8: The Jeffrey model(From(Cribb, 2010)): The compliance response to a step stress application.

2.7.2 Other models for cell mechanics

The continuum approach as the one used in these studies and described above use a finite number of springs and dashpot, giving a model of the cell as a viscoelastic medium with several distinct relaxation time constants(Desprat et al., 2008). The

relaxation times attributed to a cell often vary depending on the measurement method, and the time and length scale used in the experiment. The lack of consistent results between experiment type suggests that using several distinct relaxation regimes to describe the rheological properties of the cell may not be ideal. More recently the cell has been described by a dense continuum of relaxation times to give a weak power law description of the cell (Icard-Arcizet et al., 2008)(Balland et al., 2006)(Chauvière et al., 2010). Using a power law description of the cell shows strong agreement between experimental methods, including agreement between time and frequency measurements as well as active and passive measurements(Desprat et al., 2008). Power law fitting has also been shown to hold across several cell types, time decades and length scales. The agreement in measured values across many experimental parameters suggests that the continuum of relaxation times is a central feature of cell structure, and that cells may fall into the category of soft glassy rheology .

For a viscoelastic material with a single relaxation time, the creep function $J(t)$ is proportional to $1 - e^{-t/\tau}$ and $\dot{J}(t) \propto e^{-t/\tau}$, where $\dot{J}(t)$ is the time derivative of $J(t)$. Rather than attempt to describe the material using one or a few relaxation times, a distribution $P(\tau)$ is used. The density of relaxation times is assumed to follow a power law $P(\tau) = B\tau^{\alpha-2}$ because of the self similarity of the cytoskeleton structure in the cell. A relaxation time independent $\dot{J}(t)$ is found by integrating across all relaxation times using probability density $P(\tau)$:

$$\dot{J}(t) = \int P(\tau)e^{-t/\tau}d\tau = B\Gamma(\alpha - 1)t^{\alpha-1} \tag{2.11}$$

where Γ is the Euler gamma function. Integrating Equation 2.11 gives a power law equation for the creep function $J(t)$

$$J(t) = \frac{B\Gamma(\alpha - 1)}{\alpha}t^{\alpha} = A_0\frac{t}{t_0}^{\alpha} \tag{2.12}$$

where, A_0 describes the elastic cell property in unites of compliance or Pa^{-1}, α describes the dissipative cell property and t_0 is a reference time usually set to 1second(Mierke et al., 2008). The inverse of the force specific constant A_0 is related to stiffness and α represents the stability of the force bearing structure in the cell, where $\alpha = 1$ describes a newtonian fluid, and $\alpha = 0$ describes a elastic hookean solid (Mierke et al., 2008). Similar to the time dependent creep function, the frequency dependent viscoelastic complex modulus related to the Young's modulus behaves as a power law with respect to frequency:

$$\mid G_e \mid (f) = G_0 \frac{f}{f_0}^{\alpha} \tag{2.13}$$

The relationship between $J(t)$ and $G(\omega)$ is given by:

$$G_e(\omega) = \frac{1}{j(\omega)J(j\omega)} \tag{2.14}$$

where $j^2 = \sqrt{-1}$ and $J(s)$ is the laplace transform of $J(t)$. Using Equation 2.12 for $J(t)$, $J(s)$ can be explicitly solved to be:

$$J(s) = \frac{A_0\Gamma(1+\alpha)}{s(st_0^{\alpha}} \tag{2.15}$$

Combining Equations 2.14and 2.16 and finding the amplitude of gives an expression for $\mid G \mid$ in the form of equation 2.16:

$$\mid G_e \mid (\omega) = \frac{\omega^{\alpha}t_0^{\alpha}}{A_0\Gamma(1+\alpha)} \tag{2.16}$$

By converting Equation 2.17 from angular frequency to frequency a direct relationship between G_0 and A_0 and α is established:

$$G_0 = \frac{(2\pi t_0 f_0)^{\alpha}}{A_0\Gamma(1+\alpha)} \tag{2.17}$$

Measurements of both creep function and the viscoelastic modulus of a single living cell show very good agreement between A_0, α and G_0 using equation 2.17 and between the values of a measured for the creep function and the viscoelastic modulus, suggesting that the power law behavior is an intrinsic feature of cell mechanics.

To measure the rheological properties of the cell, the position of a bead undergoing a constant force while attached to a cell substrate is measured. The creep function of the bead pull is given by equation 2.18 where $x[t]$ and $y[t]$ are bead positions in μm, F is the applied force in pN, r is the bead radius in μm, and $f(\theta)$ is a geometric factor determined by equation 2.19:

$$J(t, F) = 2\pi r f(\theta) \frac{\sqrt{x[t]^2 + y[t]^2}}{F} \tag{2.18}$$

The geometric factor $f(\theta)$ is dependent on how deep the bead being measured is embedded in the cell. θ is given by one half the angle of the submersion cone of the bead in the cell, from this $f(\theta)$ is calculated by :

$$\frac{1}{f(\theta)} = \frac{9}{4\sin\theta} + \frac{3\cos\theta}{2\sin^3\theta} \tag{2.19}$$

Since we have no way of measuring the bead embedding in our experiments, we assume the bead to be halfway embedded in the cell, giving $\theta = \pi/2$ and $f(\theta) = 4/9$.

To be able to measure the consistency of our data and extracted material properties with this model, we fitted power laws to a set of 26 compliance data for 2 different cell types, IGROVs and Skov3. Fitting the Jeffrey's model for the 2 cell type shows that IGROVs are stiffer compared to Skov3(Chapter 4).

A_0 and α were calculated for each bead measurements by doing a regression fit of the

logarithm of creep and time data for the beads, and applied the equation:

$$lnJ(t) = lnA_0 + \alpha ln(t/t_0) \tag{2.20}$$

G_0 for each bead was calculated from A_0 and α using Equation 2.17. The error values for G_0 comes from using geometric mean and standard deviations for the calculated values whereas for A_0 and α, the error is the standard deviation from the spread of the fitting to the data values. The results for the 2 cell type are listed in the below table 2.2 and shown in Figure 2.9. This model is only used here to show consistency in relationship. A more rigorous modeling effort will be required for validating our data with this power law model.

Table 2.2: Material properties of IGROV and Skov3 using time scale independent model

	$A_0(Pa^{-1})$	$G_0(Pa)$	α	Total $A_0(Pa^{-1})$	Total $G_0(Pa)$	Total α
Skov3	0.4 ± 0.3	5 ± 2	0.24 ± 0.08	0.48	3.1	0.18
IGROV	0.06 ± 0.09	103 ± 6	0.5 ± 0.3	0.08	21.3	0.22

2.8 *Cell pulling* signatures

As mentioned earlier, the cell as a material is extremely heterogenous and dynamic. These variations are the reason for large error bars observed in most published reports. While, the large standard of deviations are also present in "whole cell" measuring techniques like the optical stretcher, one can partially argue that some of the variation arises from spatial heterogeneity which is not parsed out by locally measuring probes. One can imagine that, the material near the nucleus is stiffer than the material further away since the nucleus is denser and has its own membrane reinforcing the cytosol and the networks. Temporal variations in measurements also substantially contributes to variations in measurements as was explained in the above section.
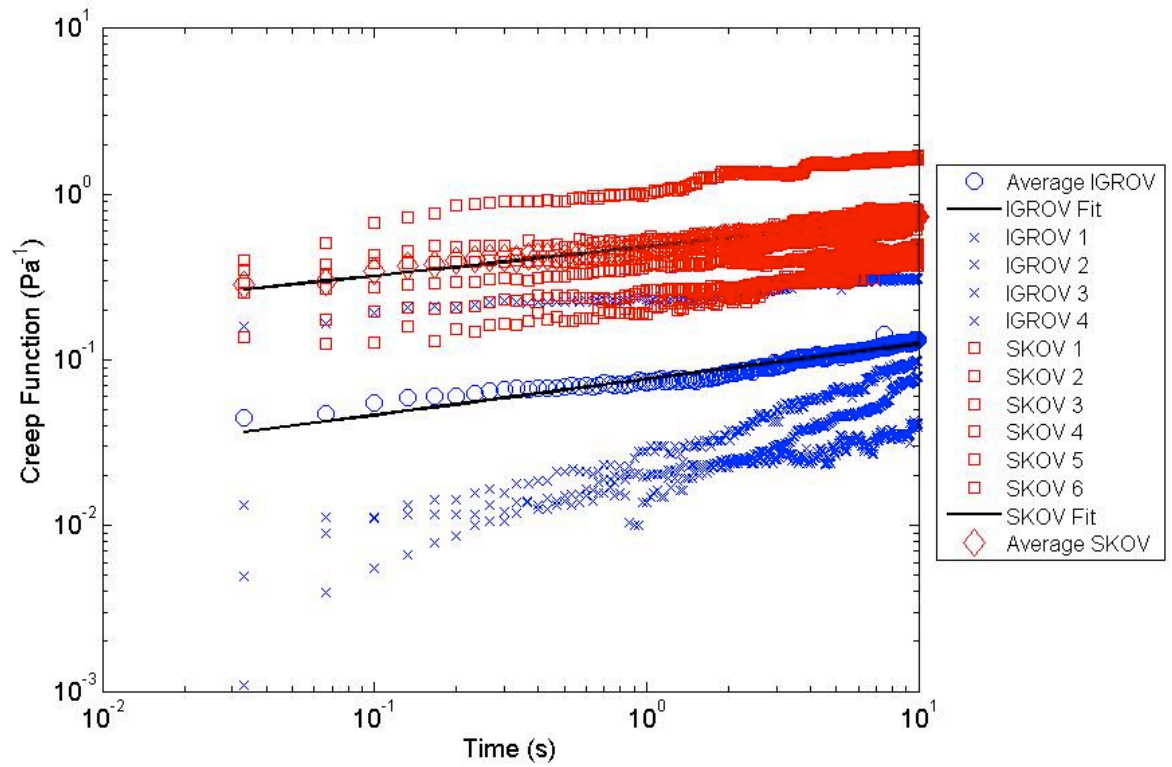
Figure 2.9: Using the model described above, the creep function was calculated for 2 cell types, IGROV and Skov3. The relative difference difference in the mechanical properties of the cell type is consistent with those calculated using Jeffrey's model

Over the past 4 years, there have been multiple signatures of bead displacement that I have observed during creep experiments. Figure 2.10 shows the 4 most common types of bead displacements signatures which highlights the complexity of fitting these responses to mechanical models as explained before. For the same cell type and force train, one can see beads which show viscoelastic solid and viscoelastic liquid response. If we look further in detail at these responses, one will notice that while the bed shows VE solid like features in the relaxation part of the response(complete recovery), the active part of the response does not show a complete roll over or zero slope region as it should for a solid. It may be that the different responses are a function of bead location and this needs further investigation. An interesting experiment to do will be to see the bead response in blebs which are actin depleted. If the viscous part of the response is due to the cytosol and the spring part due to structure and the cytoskeleton, blebbing cells will be a good model to parse this out.

The implication of the magnitude of the spring or the dashpots that we get by fitting these mechanical models is debatable and needs further investigation. However, under same experimental conditions, comparing magnitudes between cell types, phenotypes, knockdowns etc. is very reasonable and scientifically informative. A good validation of for these magnitudes is by comparing the passive diffusion data and the active rheology data of the cell types to see whether the behavior is consistent between cell types or other phenotypes. Using the protocol described above, it is possible to do both, passive and active measurements at the same time. The bead diffusion data comes from the part of the total video data just before the 1st pull. The plot on the right shows the average mean square displacements of 20 different beads on three different cell conditions. The MSD curve in blue is control fibroblast, red is with siRNA knockdown of RhoA and green is siRNA resistant mutant of RhoA(See chapter 5 for more explanation). The

47
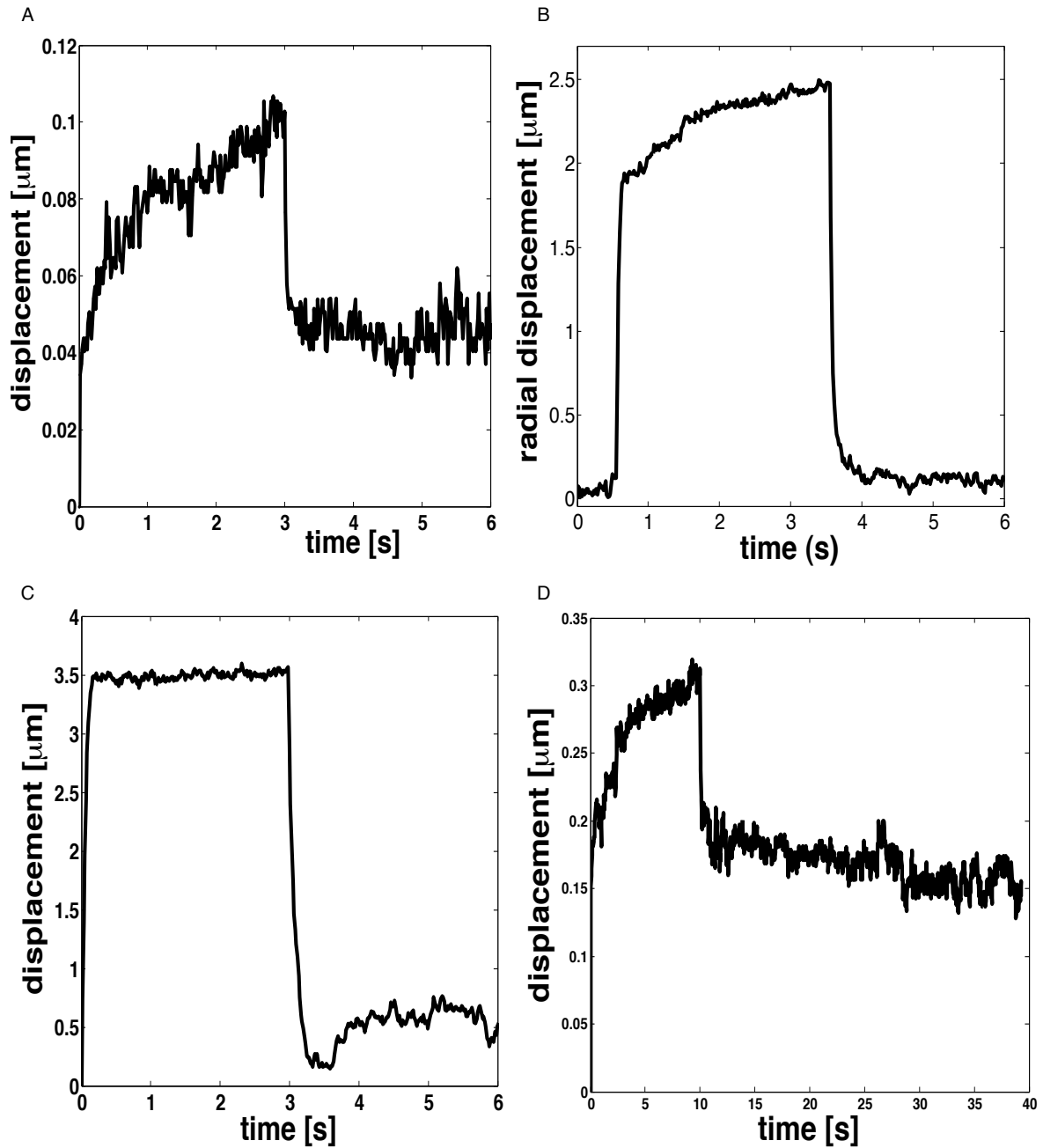
Figure 2.10: Different cell pulling signatures in 3DFM experiments. A) For a 3 second pull, the bead shows a viscoelastic liquid response marked by incomplete recovery and a non zero slope at top. B) The bead here shows complex behavior with almost complete recovery and yet a non zero slope at top. C) A viscoelastic solid signature indicated by the 0 slope and complete recovery. D) A viscoelastic liquid signature for a 10 second pull. In all the data above, one can notice that smaller bead displacements for around the same magnitude of force(indicating stiff material) show more noise.

stiffness calculated by fitting Jeffrey's model to the three different conditions are shown in Figure 5.4C. In both measurements, the control cell type is the stiffest and knocking down RhoA reduces this stiffness which can partly be rescued by introducing mutant siRNA resistant RhoA back in the system. Active and passive techniques inherently measure different properties for the same material. Typically, its hard to access non linear modes of materials using passive techniques. Consistent correlation between Jeffreys model and passive bead rheology for different cell conditions indicate that these approximations are dependable as long as we have good controls.
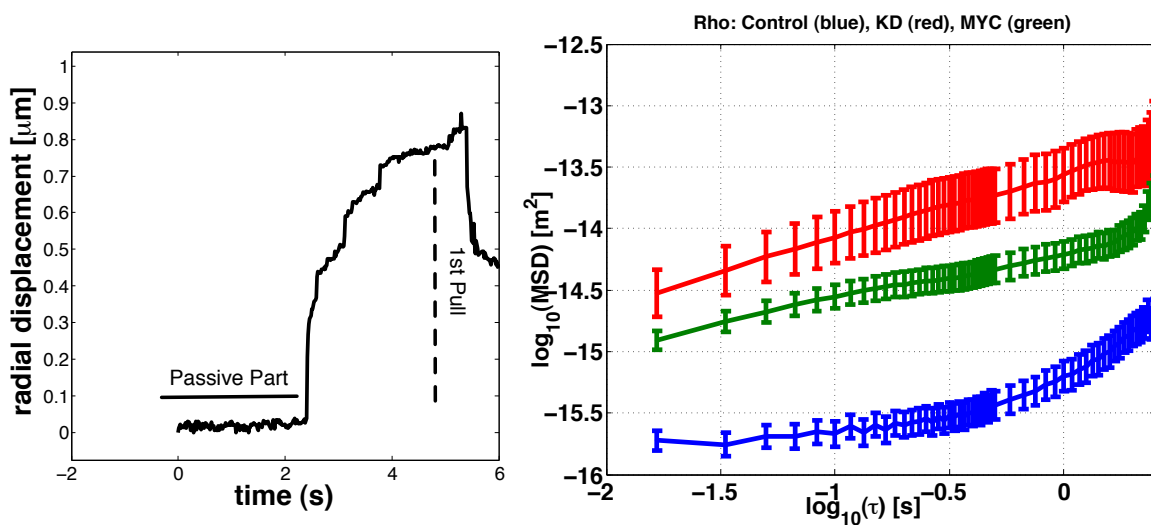
Figure 2.11: (left) Passive bead diffusion data is extracted from the part of the data just before the 1st pull. (Right) MSD plot for 3 different cell types explained in the text. Higher the MSD, more diffusive the bead and softer the material.

2.9   The next step: High throughput systems

This year we celebrate the 10 year anniversary of the completion of the draft sequence of the human genome. The White House press statement articulated the hope felt by many, that this landmark achievement would "lead to a new era of molecular medicine, an era that will bring new ways to prevent, diagnose, treat and cure dis-

ease". The first post genome decade saw spectacular advances in science. The success of the original genome project inspired many other 'big biology' efforts-notably the International HapMap Project, which chartered the points at which human genomes commonly differ, the Encyclopedia of DNA Elements(ENCODE), which aims to identify every functional element in the human genome. Over the 10 years though, one thing has become evident. With the discovery of high volume The gap between basic research and clinical application has not escaped the notice of funding agencies, many of which are now investing serious money in a bid to close it. The NIH, for example, has established a string of major clinical and translational science centers over the past few years and in February it established the joint council with the Food and Drug Administration aimed at promoting translation. The biggest mismatch in the current field of biological sciences is the rapidly increasing ease of gathering genomic and proteomic data versus the continuing difficulty of establishing what these elements actually do. Efforts would require even more imaginative ways to visualize and draw meaning from the flood of data, interdisciplinary teams that can provide the know how for this level of research.

In the next 3 chapters of this document, I will present results which show that probing mechanical properties has 2 very exciting applications. Our results show that the cell stiffness is an important biomarker for metastatic potential in cancer. Cancer is just not one disease but many pathologic conditions that differ widely in aetiology, molecular biology, clinical course and prognosis. Nevertheless, in all cancers malignant neoplasia- uncontrolled growth, invasion and metastasis occurs. Thus, these diseases are experienced as one even though a prognosis is sometimes substantially better than for diseases such as heart failure. Recent results in conjunction with the results in Chapter 4 indicate that all three pathomechanisms of malignancy require changes in active and passive biomechanics of the tumor cell and its stroma. Biomechanical changes can

therefore be a general prerequisite for malignancy independent of the peculiar molecular manifestation in individual cancers. Nanomechanical approaches thus, provide a potentially powerful means for detecting cancer along with the other ancillary biomarkers currently used for diagnoses.

In Chapter 5, I show that using the approach described here, one can dissect signaling pathways which are known to regulate and alter the cytoskeleton. As described later, this regulation is key to multiple cell processes and functions like migration, division, polarization, invasion and others and one can envision using a proteomic or genomic approach to study these processes using this tool.

Techniques for applying forces in biology like those describe above have traditionally suffered from extremely low throughput. Under the direction of Richard Spero, our lab has been involved in transitioning the 3DFM into a magnetic high throughput system(MHTS) for force application in biological materials(Spero et al., 2008). We have demonstrated a biocompatible, multiwell magnetic force system compatible with HTS standards. The system can apply forces comparable to the single specimen 3DFM and is based on a standard microplate geometry and is designed to be scalable to 96 wells. The technology and design of this system described in the Review of scientific instrument publication comprises 16 independently controlled magnetic force generation system which may be operated in a variety of modes. For example, identical forces may be applied simultaneously to a range of specimens or different force profiles may be applied to each well(Spero et al., 2008).

In a collaboration with Steve Rogers' lab here at UNC, we were able to test the system as a tool to study cell mechanics using the *Drosophila* model. Part of the motivation was the availability of the complete siRNA library for this model. *Drosophila* derived cells were and plated on the microplates which show biocompatibility with
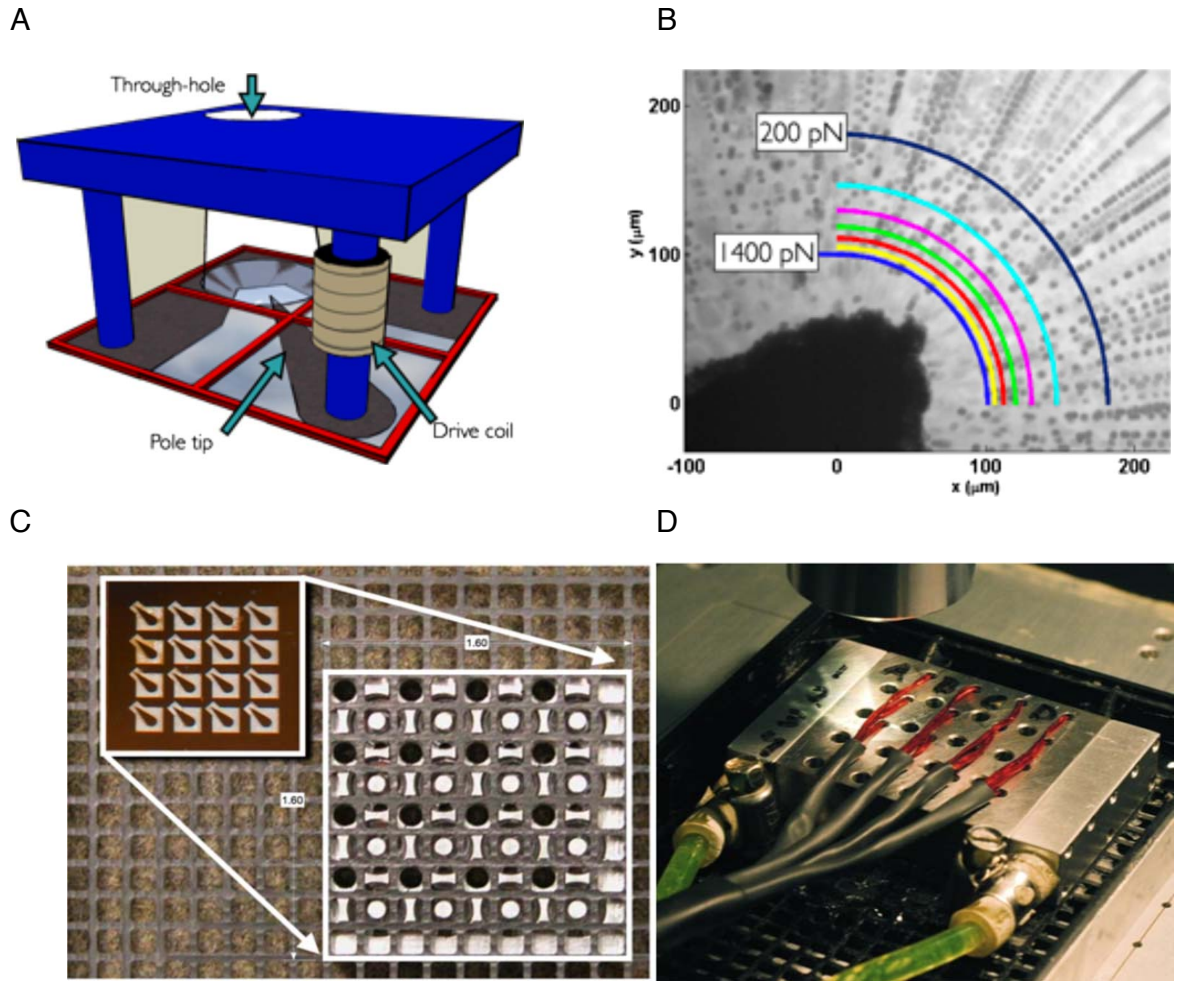
Figure 2.12: From (Spero, 2010).A) A cartoon of a single well's magnetic system. The substrate is a pole flat affixed to the glass. A through hole above the specimen gap provides access for dosing of the specimen during an experiment and illumination for brightfield transmission microscopy. B) A contour plot of force on a $4.5\mu m$ bead, overlaid on a time lapse image of force calibration video. The contour step is 200pN. Each contour line is the average force measured on all beads at that distance from the pole tip with an axis of symmetry. C) The fully assembled MHTS seen from below, the magnetic block drops into the 384-well microplate from above, and the pole plate creates the bottom of the specimen well. D) In operation, tubing provides fluid flow for temperature control , and a condenser objective provides transmission illumination from above.

cells. Identical procedures to those described above were used with regards to bead and incubation time. Half of the wells with cells in them were treated with a protein phosphatase inhibitor(PTPase) cocktail, with a final concentration of $0.5\mu M$. Tyrosine phosphatase have been known to play an important role in force sensing, but there were no quantitative studies on the changes in mechanical properties of the cell due to inhibition of PTPases at the time of these experiments. Using MHTS technology, a single experiment enabled mechanical measurements on cells in four independent cell cultures.
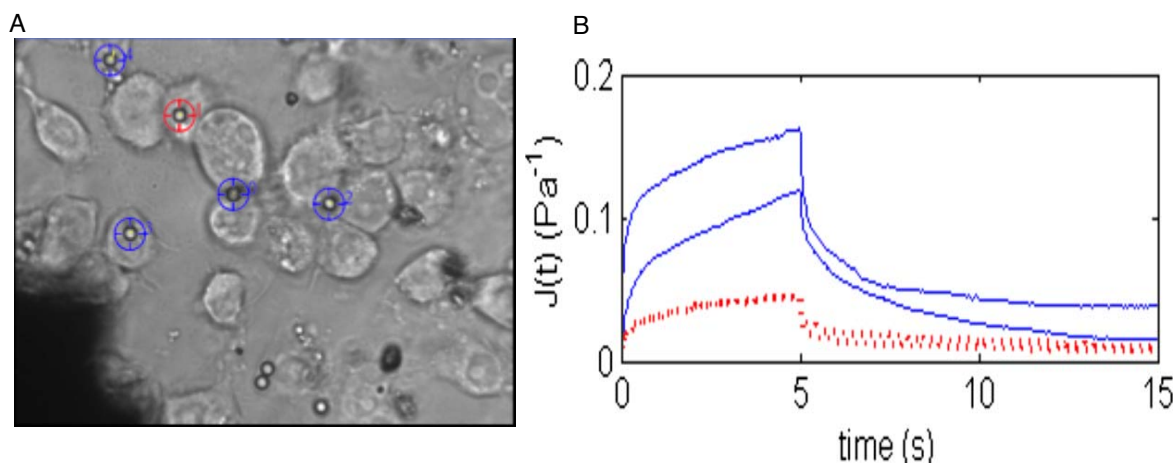
Figure 2.13: A) Image showing biocompatibility with cell cultures. The shadow of the pole tip is visible, bottom left. The brightfield image is taken with a 60X objective. Magnetic beads are observed on the cells , and their trajectory is tracked as described above. B) Compliance curves under control(dotted) and PTPase inhibited conditions(solid).

2.10   Conclusion

We have an impressive array of experimental tools that can be utilized to further our understanding of whether and how the mechanical environment and mechanical behavior of a cell affects its biological function. Rigorous interpretation of how force, stress and energy can be imposed and measured via these approaches will enable more

accurate assessment of current results and also more lucid comparisons of results among different experimental tools. As described above, unlike engineering materials with characteristic length scales, subcellular and molecular structures of biomaterials are not amenable to characterization through continuum formulations because of small dimensions, mechanochemical coupling and difficulties in ascribing local stresses and strains to different structural units of cells and biomolecules. Protein interactions and diffusion in the cytoplasm, protein DNA interactions and energy conversion processes in the cell are all known to be influenced by brownian motion as well as stochastic processes and non equilibrium thermodynamics which should be taken in to account in overall interpretation of the mechanical response.

Despite the lack of a true *consensus* on a mechanical model of the cell, there has been remarkable progress in the field to date. With suitable resources and data, this progress will pick up even more pace because cell mechanics has application to all human disease and its inclusion into health related research efforts represent a major opportunity.

Chapter 3

Force generation and dynamics of

single cilia

Cilia now joins the list with peroxisomes, lysosomes and mitochondria as organelles which when defective in their functioning, cause disease. While cilia has been studied for almost 300 years, cilia related diseases also called ciliopathies, have just recently been appreciated and studied. In this chapter, I present work done under the umbrella of the Virtual Lung project, where we used force microscopy tools to unravel the mystery of a cilia with our results having implications in a wide range of ciliopathies like cystic fibrosis and primary cilia dyskinesia.

The Virtual lung project(VLP) is a highly multidisciplinary collaboration between research labs at UNC in applied mathematics, physics, chemistry, biology and medical doctors from the UNC cystic fibrosis center. The goal of VLP over the years has been to model airway functions to better understand clearance in the lung and that would allow for computational predictions on the effects of treatments. One of the critical cogs in mucociliary clearance wheel is the airway epithelial cilia. These hairlike projections are responsible for generating flow through synchronized beating ultimately pushing the fluid to the upper branches in the lung and nasal cavity for eventual clearance. Critical for lung modeling is the quantitative assessment of a cilia beat. How much force does

it exert, what implication does that have for clearance, what's the mechanism of a cilia beat. The truly remarkable thing about cilia is their omnipresence in various parts of the human body. In that aspect, these questions have relevance to not just the lung but to all parts where cilia are present and have a role. In this chapter, I will introduce the cilium and its role in various functions including airway clearance. I will then present the results of the work I did with David Hill, a former post doc in the lab and now at the UNC Cystic Fibrosis Center.

3.1   The amazing cilia

Starting from the late 17th century, the observance of motion in the microscopic living world has caught the fascination of many observers and researchers. Said Anthony Van Leowenhoek when he first saw ciliary motions, *"One can't be satisfied with just looking at so wonderful a structure: chiefly because one can't get clear on how such an unbelievable motion is brought about...'* . Even though we have spent 300 years trying to understand how cilia move, a consensus explaining ciliary motion is lacking. Major breakthroughs however have provided us with many clues into this complex and ubiquitous process. Sir James Gray's work on cilia and locomotion spanned 40 years from the 1900's and led to discoveries including showing that cilia were active organelles, consisting of a number of filaments. He was also instrumental in the development of the stroboscopic technique with which he was able to show phases of a single ciliary beat, calculate beat frequency and that metachronal wave is essentially a series of ciliary beat(Gray, 1930). The mystery of the cilia structure was unravelled with the advent of electron microscopy as Don Fawcett and Keith Porter were able to show in 1954 that the "9+2" structure of cilia was universal for all motile cilia(Porter and Sale, 2000). The importance given to cilia over 300 years is clearly obvious considering that Anthony van Leeuwenhoek is called the "Father of microbiology", Sir James

Gray "Father of cytology and animal zoology" and Don Fawcett "Father of electron microscopy".

As mentioned earlier, cilia are hairlike centriole-derived extensions of a eucaryotic cell which are membrane bound and contain a core bundle of microtubules also known as the axoneme. Mammalian ciliary axonemes, like axonemes elsewhere in the animal kingdom, are formed with two major patters: 9+2, in which the nine doublet microtubules surround a central pair of singlet microtubules, and 9+0, in which the central pair is missing. The 9+0 also lack the molecular motors, axonemal dyneins, which are responsible for ciliary motion. Thus, the 9+0 are usually non motile whereas the 9+2 are motile. The other major difference between the 9+2 and the 9+0 is that epithelial cells may possess several hundred 9+2 motile cilia, 9+0 are usually solitary.

The 9+0 or non motile cilia are now called primary cilia. They are found on epithelial cells such as the kidney tubule, the bile duct, the endocrine pancreas, and the thyroid, but also on non epithelial cells such as chrondrocytes,, fibroblasts, smooth muscle cells, neurons and Schwann cells. Many people considered primary cilia to be vestigial till very recently. This all changed with research on Polystic kidney disease(Pazour et al., 2000). Pazour et al. demonstrated that the mouse homolog of IFT protein 88 in Chalmydomonas is the mutated protein of the TG737 gene and that with this defect the primary cilia of the mouse kidney are abnormally short or absent. Long primary cilia can be bent by fluid flow or mechanically. These bendings were shown to cause intracellular calcium increase and removal of the cilium abolished this flow sensing response (Praetorius and Spring, 2001)(Praetorius and Spring, 2003). Subsequent research has now shown that mechanotransduction via the primary cilium is necessary for continued normal function and cell differentiation of the kidney epithelial and the loss of the cilium leads to abnormal functions and Polycystic kidney disease.

Similarly, the primary cilia has now been shown to play crucial roles in many other

cell functions. A variant of the 9+0 cilia is the nodal cilia found in the embryo. Like primary cilia, nodal cilia exists individually per cell and a 9+0 axoneme, however they possess dynein arms with dyneins and are motile, generating leftward flow across the node(Nonaka et al., 1998). Exactly how nodal flow induces LR asymmetry is still uncertain, but one of the hypothesis involves the mechanotransduction ability of the cilium leading to calcium influx to one side of the node and a chemosensory pathway including hedgehog signaling(McGrath et al., 2003).
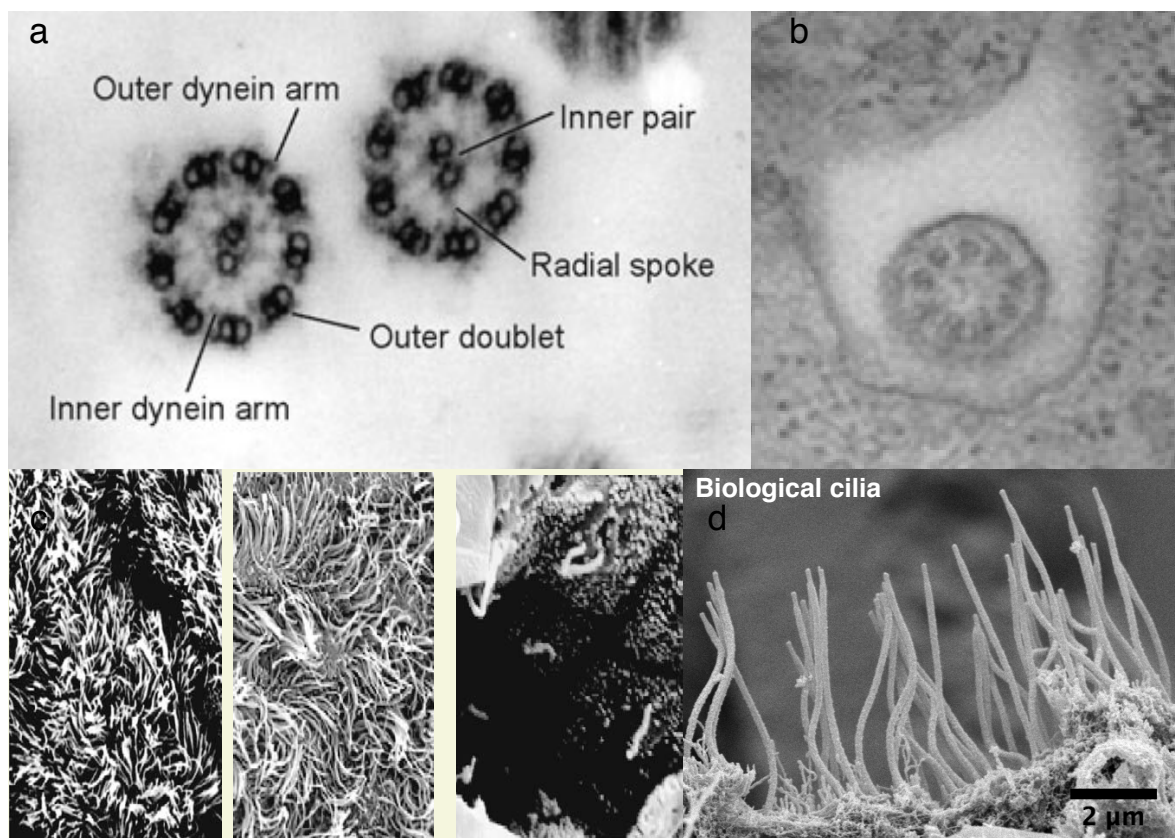
Figure 3.1: Structure](a) and (b)From (Salathe, 2007). The cross sections reveal the classic 9+2 structure in (a) and the 9+0 structure in (b). c) From (Marshall and Nonaka, 2006). Various cilia in Oviduct, brain ventricle and kidney respectively. d) Image courtesy Jerome Carpenter. Cilia in the lung

3.2   The 9+2 cilia

Motile cilia play a crucial role in clearing mucus and debris from the airways, circulating spinal fluid in the ventricles of the brain and in the fallopian tubes. In the brain, cilia is responsible for circulating spinal fluid in the brain, where abnormal ciliary beating has recently been linked to hydrocephalus and other developmental cerebral abnormalities (Sawamoto et al., 2006). In the fallopian tubes the cilia seem to contribute to the movement of the ovum from the ovaries to the uterus.

Mucociliary clearance is an important innate defense mechanism that protects the lungs from inhaled pollutants, allergens and pathogens. The dysfunction of this mechanism is characteristic feature of a broad spectrum of chronic diseases, including cystic fibrosis (CF), primary cilia dyskinesia (PCD), asthma, and chronic bronchitis. Healthy airway surfaces are lined by ciliated epithelial cells and covered with an ASL, which is partitiioned into a mucus layer that entraps inhaled particles and pathogens, and a low viscosity periciliary layer (PCL) that lubricates airway surfaces and facilitates ciliary beating and efficient mucus clearance from the lungs to the mouth (Riordan et al., 1989)(Davis, 2006)(Becker et al., 2003). In CF airway cilia, with an absence of either molecular or functional cystic fibrosis transconductance regulator receptor (CFTR) in the apical membrane of the epithelia, there is unregulated sodium ion absorption and a decreased capacity to secrete chloride ion. Both these defects combine to produce dehydration on the airway surface, with a collapse of the PCL, concentration of mucins within the mucus layer, and adhesion of the mucus to the airway surface, Ultimately, the dehydrated mucus layer is viscous enough that the cilia fails in clearing this fluid leading to airflow obstruction, inflammation and chronic infection, all features of CF (Boucher, 2007).

3.2.1 Structure

Each motile cilia is approximately 6-7μm long and 200-300nm in diameter. As mentioned above, the motile 9+0 nodal cilia lacks the central microtubule pair and beats in a rotational movement rather than the back and forth motion of the 9+2 cilia. Thus, the central microtubule pair may be required for normal, but asymmetric back and forth beat observed in these cilia. Most of our information about the structure of the 9+2 comes from flagella found in Chlamydomonos. Along with the microtubules, dynein arms, radial spokes and one pair of interdoublet links provide the cilium with its unique electron microscopic fingerprint (Figure 3.1). A longitudinal section reveals that the axoneme itself is composed of a repetitive unit with a length of 96nm. These repetitive units consists of four outer dynein arms, three inner dynein arms, one spoke group (three radial spoke), and pair of interdoublet links (Satir and Sleigh, 1990). The outer dynein arms is a two headed molecule(three in Chlamydomonas) with a molecular size of 1-2 million Da(Hastie et al., 1988b) which is attached to the doublet microtubule every 24nm(Taylor et al., 1999). Researchers estimate that the cilium must contain more than 4000 inner and outer dynein arms.

3.2.2 Mechanism of motion

The mechanism of cilia beating has been very controversial, with multiple models and hypothesis out there in the literature. Dyneins can move microtubules only unidirectionally. The ciliary stroke however is bidirectional which requires the effective dynein activity alternate between the two halves of the axoneme. The switch point hypothesis(Satir and Matsuoka, 1989) , was proposed to explain this switch in activity, though till today the exact mechanism of switch remains unclear. It may be, that the bending of the axoneme results in alteration of the structural relationship between the dynein and the microtubules. What is however known is that the IDAs primarily
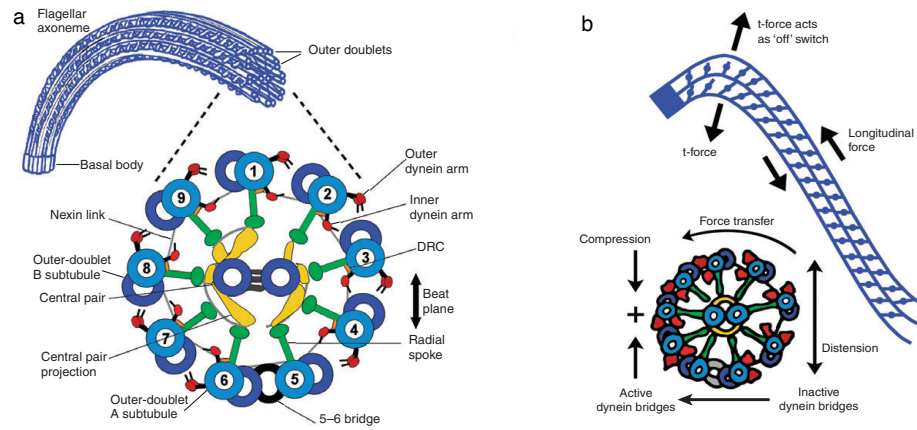
Figure 3.2: From (Lindemann, 2007) a) Structure of the 9+2 axoneme. b) Geometric-clutch hypothesis. Top- The dynein 'off' switching mechanism. Accumulated tension from the active dyneins bends the flagellum and produces a transverse tension in the bent region. When the t-force felt by individual dyneins become large enough to overcome the adhesive capacity of the dynein bridges, the doublets separate and dynein action is terminated. Bottom- Active bridges on one side of the axoneme exert a negative bias on the formation of active bridges on the apposite side of the axoneme. This effect is also enhanced by the spokes, which act as spacer elements.(Reprinted with permission)

control parameters related to bend amplitude that affect the beat form. This may be in part controlled by signaling via kinases and phosphatases that phosphorylate or dephosphorylate radial spoke proteins that act on the velocity of IDA-limited doublet sliding.

The first proposed mechanism of switch point was proposed by Charles Brokaw in 1971 (Brokaw, 1971). His curvature control hypothesis maintains that, when the flagellum bends to a sufficient curvature, it triggers the inactivation of one set of dyneins and the activation of of the opposite set. Based on this curvature control hypothesis, Lindemann proposed the geometric clutch hypothesis (Lindemann, 1994a). According to this model, motor proteins are positioned just far enough from their binding site on the adjacent doublet that when the cilia is straight, the dynein heads a very small but finite probability of forming a bridge to the next doublet. The bending of the axoneme stretches the nexin links that hold the nine outer doublets in a ring and results in the development of a force transverse to the bend (the t-force) that squeezes certain doublets towards each other. Moving the doublets together increases the likelyhood that a dynein bridge will be formed. When the dynein bridge attach, they translocate upon the adjacent doublet and apply a longitudinal force to both of the doublets involved. This longitudinal force exerted across the diameter of the axoneme provides the torque that is required for the axoneme to bend and generate the t-force that pries the doublet apart. When this t-force is high enough, the dyneins no longer function in a processive manner because they are pulled away from their binding site. This is the switching mechanism that according to this hypothesis, terminates dynein action.

There are other mechanistic models to explain the beat cycle based on the dynein cross bridge cycle (cycle of dynein attachment to microtubules, power stroke and detachment). These models are outside the scope of this work, though I should add that

new evidence suggests that nucleotide regulation of the dynein tubulin binding affinity is directly connected to the switching mechanism(Frey and Omoto, 1997). There are, at present, three contending views for the axoneme beat cycle, a mechanistic view as described above with the geometric clutch, the enzymatic view and the view that the it is the behavior of the dynein motors that contributes to the beating.

3.3 Force generation and dynamics of single cilia

.

As mentioned earlier, our interest in cilia lies in its role in mucociliary clearance and pathology of lung including CF, COPD and chronic bronchitis. It is in this system that we applied our force technology to answer fundamental questions:

1. What force can a cilium exert?

2. Is a decrease in ciliary beat frequency (CBF) a necessary consequence of loading?

3. At what viscosity should mucus propulsion begin to fail?

Having said that, our technology provided us with the unique opportunity to answer some basic questions about the mechanism of cilia beating also. We got some very interesting results and extended these experimental results into a simple one dimensional picture of an axoneme. This model let us make conclusions on the mechanism of beating in a cilium with implications on the switch point hypothesis and contradictions with the geometrical clutch hypothesis which were initially met with criticisms from reviewers of our work(Hill et al., 2010).

Much of the methods of this work are described in Chapter 2. One technology that I will describe here literally single handedly made our experiment unique from others and let us make measurements on a single cilia and that is the development of the spot

labeled bead. Much of this protocol was developed by a previous graduate student, Ashley Estes who started working on this project as a Master's student.

3.3.1 Spot labeled beads

A cilia is 7μm in length and only 200μm in diameter at it's tip. For the magnitude of force required to potentially stall the cilia, we needed a bead of 2.8μm diameter. This size mismatch would result in the bead binding to many cilia at a given time. To accomplish binding to a single cilium, we came up with a strategy to reduce the functionalized spot on the 2.8μm bead to around 200nm called spot labeling. 2.8μm beads, functionalized with streptavidin were dried on a cover slip and then sputter coated with a thin layer of gold. Due to contact, a small spot on the bead remained uncoated. The beads on the coverslip were then coated with thiol-PEG (Polyethylene glycol)(Nektar Therapeutics, USA) and then released from the coverslip. To test the single spot functionalizing of the beads, small biotinylated targets (200nm fluorescent beads) were added to spot labeled beads and then imaged Figure 3.3.
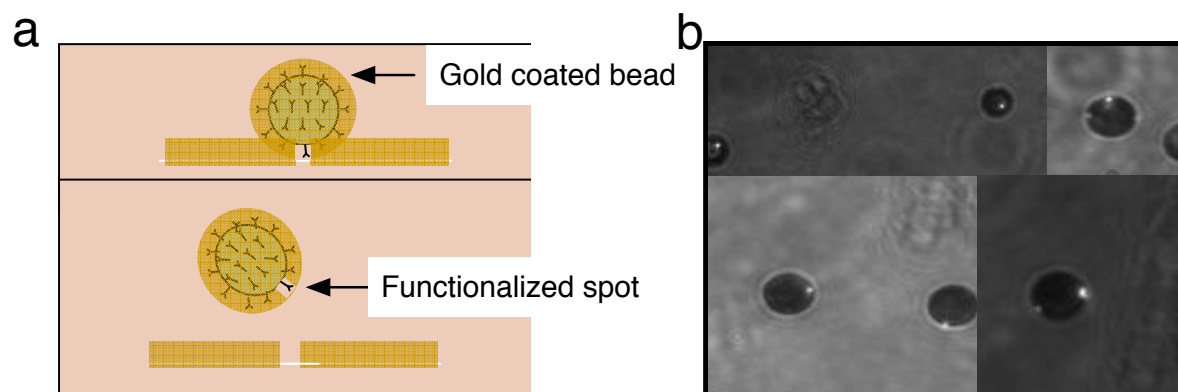
Figure 3.3: (a) Illustration of the spot labeling process. (b) Brightfield and fluorescence images of spot labeled beads that have been mixed with 200nm biotin labeled fluorescent beads.

3.3.2   Baseline Ciliary Pattern

We attached a spot-labeled 2.8μm diameter magnetic bead to the cilia tip, both to transmit force to individual cilia and to track the 2-D projection of the cilias motion with high spatial and temporal resolution(Figure **??**). Prior to the application of magnetic force by the 3DFM, the average ciliary beat amplitude (CBA) for cilia attached to a bead was 5.5μm$\pm$0.3μm (n=15), which is in good agreement with published results (Afzelius, 2004). The average ciliary beat frequency (CBF) of the cilia in our experiment was 8.5 Hz 0.3hz, also in agreement with published results at 23°C(Yager et al., 1978). As expected from earlier work (Sanderson and Sleigh, 1981), an asymmetry was observed in the beat pattern, shown in Figure 3.4 c,d. Based on extrapolations from the beat shape of rabbit tracheal cilia as a function of time (Sanderson and Sleigh, 1981), and human airway cilia(Davis and Sears, 2009), we believe the effective stroke to be the stroke in which a cilium reaches the highest velocity and begins to slow gradually about 2/3 through that stroke (dark arrows, Figure 3.4 c). In contrast, the velocity during the recovery stroke was more constant, with a more rapid transition between the recovery and effective strokes (lighter arrows). The average maximum velocity reached during the effective stroke, was 198μm/s$\pm$15μm/s and during the recovery stroke the average maximum velocity, , was 155μm/s$\pm$11μm/s (n=15). We found that the baseline motion of cilia-bound beads was largely planar, with the lateral excursion of the cilium tip being 5% of the principal beat amplitude, consistent with previous measurements (Chilvers and O'Callaghan, 2000). We also note that the drag force calculated for a 2.8μm bead at the maximum velocity reached during the power stroke of the cilias beat ($\approx$200μm/s) moving through buffer is $\approx$5 pN. As presented below, this is less than 1/10th the effective cilia force determined by our measurements. Taken together, these results argue that bead attachment does not significantly alter the characteristic cilium beat pattern.
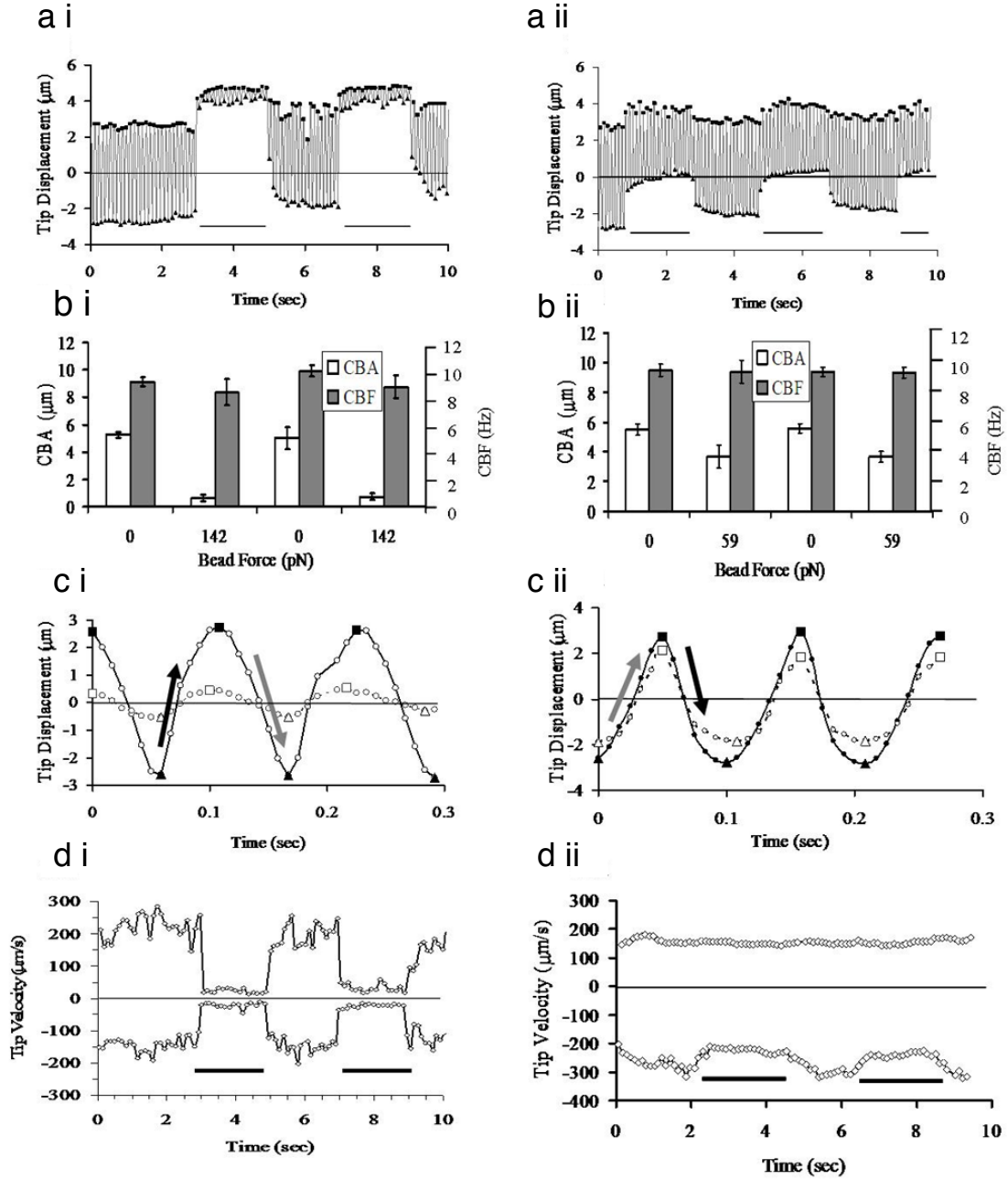
Figure 3.4: (i) Effective Stroke in the Direction of the Bead (magnetic) Force, and (ii) Recovery Stroke in the direction Bead Force. (a)Position vs. time trace of 2.8μm beads attached to an HBE cilium. The line at the base of the graph indicates force on / off. (b) CBA and CBF with and without the applied bead force. (b) Closer inspection of the Cilia Beat Pattern with the force on (solid line) and off (dash line) from (a). The line is the beads motion, the squares are the local maximums and the triangles are the local minimums. The grey arrows indicate the effective stroke of the cilia, and the black arrows the recovery stroke. (d) Instantaneous maximum velocity of beating cilia for the tip position data in (a). In all charts, the position/velocity scale is oriented to be in the direction of the external force.

66

3.3.3 Cilia force response

Forces in our system were applied either toward or against the effective stroke. Parsing the data derived from forces applied toward or against the effective stroke allowed us to determine that the effect of load is independent of orientation. To illustrate the effect of forces toward and away from the effective stroke, we show representative data in Figure 3.4 where the load was towards (i) or away from (ii) the effective stroke, although in this example a different magnitude of force pulses were applied to each (142 pN in i, 59 pN in ii,Figure 3.4). The duration of the applied maximum force was limited by the detachment of the bead from the cilium at longer times and high forces. No matter which way forces were applied, cilia reacted in the same characteristic manner: the center of oscillation moved toward the applied force (Figure 3.4; force oriented toward the top of the page for both i and ii), CBA decreased markedly, and CBF was unaffected. The response to the force applied in Figure 3.4a is shown in Figure 3.4b, and a close-up of the beat pattern in time, before and during a pull, is shown in Figure 3.4c. Note that the period of oscillation was unchanged while the amplitude decreased significantly. Given the constant frequency observed through the experiments, the tip velocity of the cilia must decrease proportionally to the decrease in beat amplitude, as seen in Figure 3.4d. It is noteworthy that the velocity of both the effective and recovery strokes is decreased in response to the application of the external force, and that the ratio of the velocities stays relatively constant, regardless of the orientation of the beat pattern to the external force. Had this not been true, one would expect that the beat pattern shown in Figure 3.4c would have shown a saw-tooth wave when the cilium is loaded, altering the ratio between and depending on the ciliums beat orientation with respect to the external force, which was not the case. Forces were also applied as a slow ramp (Figure 3.5), where coil currents to the magnets were raised as a linear function over 30s to produce ≈170pN force at the bead, and then

removed. This, much longer application of force also did not alter the CBF, while the CBA gradually decreased to less than 10% of the starting value. By analyzing these ramp-type experiments within the context of the model we present below, we were able to deduce the effective motor force exerted by the motor proteins within the cilium.
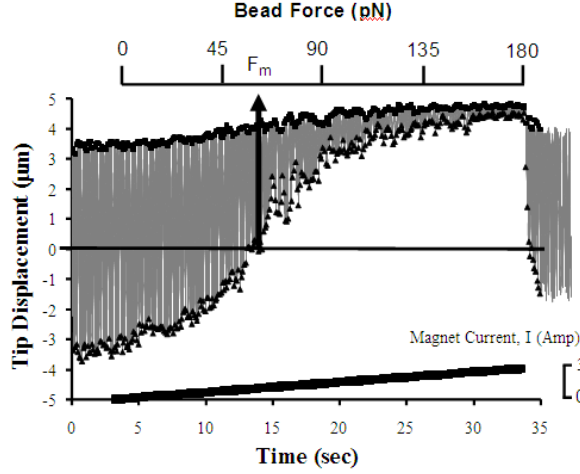
Figure 3.5: The grey line indicates the path of the bead, with squares indicating local maximum and triangles the local minimum. The line at the bottom of the figure shows the magnetic driving current, the bead force is shown on a separate horizontal axis. Using our model, the point at which the bead force is sufficient to limit the minimum excursion of the bead to be the midpoint of the baseline motion is defined as the motor force. The position scale is oriented to be in the direction of the external force.

3.3.4   Cilia do not stall

A comparison of our methodology with that applied to single molecular motors (Howard, 2001), might imply that at some characteristic force the cilium would stop oscillating altogether. However we found that, although CBA declined with increasing force, forces approaching 200 pN did not stall the beat (Figure 3.5 and 3.6). Higher forces tended to pull the beads off of the cilium, but did not appear to stall the oscillation, even briefly. For convenience we define an effective stall force as the point at which the CBA has been reduced to 15% of its baseline. Combining all force/CBA data, we

looked for forces whose error bars overlapped the 15% reduction line. These forces centered on 163pN±18pN (n=15). While our experiment was fundamentally different from previous cilia and flagella force measurements, it is noteworthy that our results are of the same order of magnitude as previous studies on bull sperm flagella. Those studies showed an induced arrest behavior at 250pN (Schmitz et al., 2000) but did not report the detailed amplitude change as the load was increased. Recent AFM measurement of the ensemble average of the normal (i.e. perpendicular to the epithelial) force generated by frog esophageal cilia during their effective stroke was interpreted to be equivalent to 210pN per cilia (Teff et al., 2007).
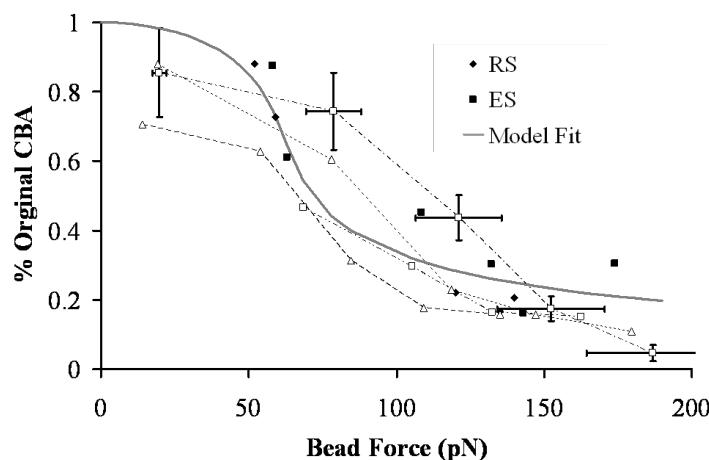
Figure 3.6: Cilia beating with their effective stroke in the direction of the bead force are represented with squares (n = 9), while cilia beating with their recovery stroke in the direction of the bead force are shown with diamonds (n= 6). Closed data points are from pulse type experiments, while open points are from force ramp experiments. Data from the same ramp is connected with a dotted line.

3.3.5 Model

One of the greatest lessons I have learned over my graduate education has been that the greatest insights from experiments comes from application of the most fundamental aspects of science. Stuff one learns in middle and high school. And this lesson

was taught to me by Rich during the development of a simple one dimensional model for an axoneme to apply to our experimental results. The simplicity is reflected in the cartoon of the model which resembles one of the first physics text book I used in India and from application of the basic force balance and spring equation that irrespective of our background, we learn about in school.

It is tempting to conclude that the motors within a cilium together exert a force at least as large as the 162pN near stall force, and that, for example, this force can be applied to propel fluids. However, in our experiment, the external force is applied to the entire mechanical structure of the axoneme and not directly to the internal motor proteins. The external applied force and the internal motors act in parallel against the mechanical stiffness of the axoneme to produce a bend shape, and hence a tip displacement, which must be taken into account in interpreting the true force produced within a cilium. We present a simple mechanical model that allows us to separately quantify the axonemal stiffness and the effective internal force generated by the collective action of the axonemal motors (available for motility or fluid propulsion). The model also allows us to predict the magnitude of fluid resistive force where cilium motion would begin to be compromised. Because ciliary motion appears to be determined by a force balance at all points in its cycle, and inertia can be neglected at this length scale, the cilium can be described as being in quasistatic equilibrium. In such a model, the forces derived from internal motors (F_m), from the mechanical characteristics of the axoneme (F_A), and from the forces applied by the magnetic bead (F_B) sum to zero at all times ($F_B + F_m + F_A = 0$). For simplicity, we reduce the three dimensional physics of the axoneme to a single coordinate, focusing on the tip displacement along a single axis we denote as x_t. We consider the axoneme in this model to be a 1-D spring element with a stiffness k_A that relates the net force on the tip to its displacement through

$K_A = -F_A/x_t$. The axoneme is bent by internal shear stresses that are determined by the magnitude, distribution and direction of the forces the dynein motors generate on neighboring doublet microtubules (Satir and Christensen, 2007). The collective effect of these shear stresses within the model is to bend the axoneme as if a single force (F_m) had been applied at the tip. Finally, the bead exerts a force, F_B, to the cilium through the tip which, once activated, is constant throughout a ciliary beat cycle. This model is diagrammed in Figure 3.7. We consider F_m to be periodic, with an amplitude that is independent of the externally applied force F_B. We also neglect fluid forces at present, which for aqueous environments are calculated to be on the order of 1% of the effective motor force.

Immediately this model allows us to interpret the effective force generated by the internal motors. If we take the midpoint of the unloaded cilium beat as x_t=0, then we can understand the cilia motion without load as due to the internal motor force that is at a maximum when the cilia tip is furthest displaced from the midpoint location, at a turn-around point. Whenever the cilium tip is at x_t=0, then F_A=0. Without the additional load, this will also be the location where F_m=0, as dictated by the force balance assumption. However, when the external load F_B is applied, the beat cycle midpoint shifts in the direction of the applied force. At a particular value of F_B it will be the case that one of the turnaround points will be shifted to the original x_t=0. At this location, F_A=0 and the sum of $F_m + F_B = 0$. Therefore, at this location, we can set F_m= -F_B to find the value of the effective motor force from the value of F_B that pulls one of the beat extrema to the original midpoint. It can be seen from Figure 3.5 that this force for this data sequence is approximately 65 pN, and thus the internal forces provided by the motors within this cilium produce about 65 pN of force.

We now use this model to focus on the beat amplitude and its reduction under load. A model that assumes a linear (Hookean) spring for the axoneme, where is a
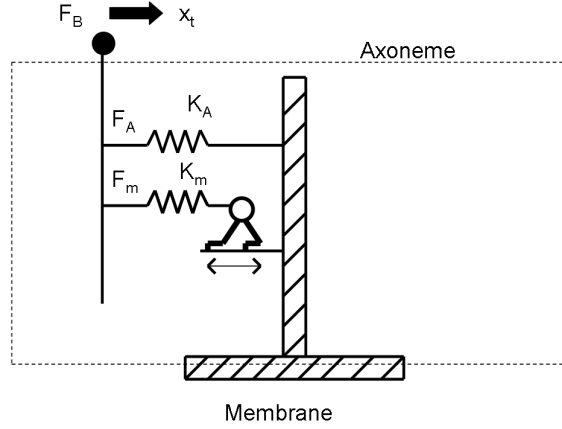
Figure 3.7: Axoneme is represented as a nonlinear spring K_A that applies a restoring force F_A, and an internal force F_m generated by an internal spring K_m extended by a system of stepping motors

fixed constant independent of position, does not produce a reduction in the periodic beat amplitude as the magnetic force is increased. A model with an axoneme that stiffens at large amplitudes, with does capture the CBA reduction, while also allowing the applied force to shift the center of oscillation. The particular form for F_A was chosen for simplicity. It is the lowest power exponent that provides symmetric stiffening of the axoneme (i. e. stiffens similarly in both directions). We use this term to capture the qualitative features of the axoneme under load. We note that the quantitative conclusions of this report are determined from the cilium behavior near , where the non-linear term of the spring constant is not a significant factor. The origin of this term may be due to the mechanical stiffening of the axoneme at large bend angles arising, for example, from steric interactions in the interior of the microtubule structure. We will leave further analysis of this term for another report. This model was applied directly to the data. This nonlinear spring relationship correctly captures the reduction in CBA with applied force (Figure 3.6). By solving our model for the beat amplitude as a function of external force, we find $k_A = 5.4 \pm 1.43$ pN/μm, $k'_A = 0.73 \pm 0.15$ pN/μm^3 and $F_m = 62pN \pm 18pN$, where the errors are the standard deviation of the fit. Thus the

72

fit generates a value for F_m that is in good agreement with that obtained by inspection of Figure 3.5, as described earlier. Moreover, when the data is plotted as a function of $F_B - F_m$ (Figure 3.7), we see that this fit is reasonably good agreement with our data in its entirety. Finally, we note that within our model, the stall force in terms of an applied force that brings the beat amplitude to zero, does not exist. It is F_m that is the fundamental quantity of interest for insight into axoneme dynamics and for understanding the force that the cilium can apply.

$$F_B + F_m = F_A$$

$$F_m = f sin(\omega t)$$

$$F_A = k_A x(t) + k'_A x(t)^3$$

Since our model only captures the end point of the cilia beat cycle under amplitude reductions, we replace the motor force term with an effective motor force f. Substituting the last 2 equations into the first equation, we get a standardized form of our force equilibrium equation given by

$$x(t)^3 + \frac{k_A}{k'_A} - \frac{F_B + f}{k'_A} = 0$$

The above equation is a standard 3rd order polynomial. Solving for x, we get a solution for x given by:

$$x(t) = \frac{\frac{-k_A}{k'_A}}{3\left[\frac{(F_B \pm f)^2}{2k'_A} - \sqrt{\frac{(F_B \pm f)^2}{(4k'_A)^2} + \frac{(k'_A)^2}{(27k'_A)^3}}\right]} + \left[\frac{(F_B \pm f)^2}{2k'_A} - \sqrt{\frac{(F_B \pm f)^2}{(4k'_A)^2} + \frac{(k'_A)^2}{(27k'_A)^3}}\right]^{1/3}$$

The maximum displacement of the axoneme tip is defined by the case when the applied force is in the same direction as the internal effective motor force$(F_B + f)$ and the minimum as the external force acting against the internal force $(F_B - f)$. Thus the change in CBA is given by:

$$\delta x = \frac{x(t)_{max} - x(t)_{min}}{\delta x(t)_0}. \tag{3.1}$$
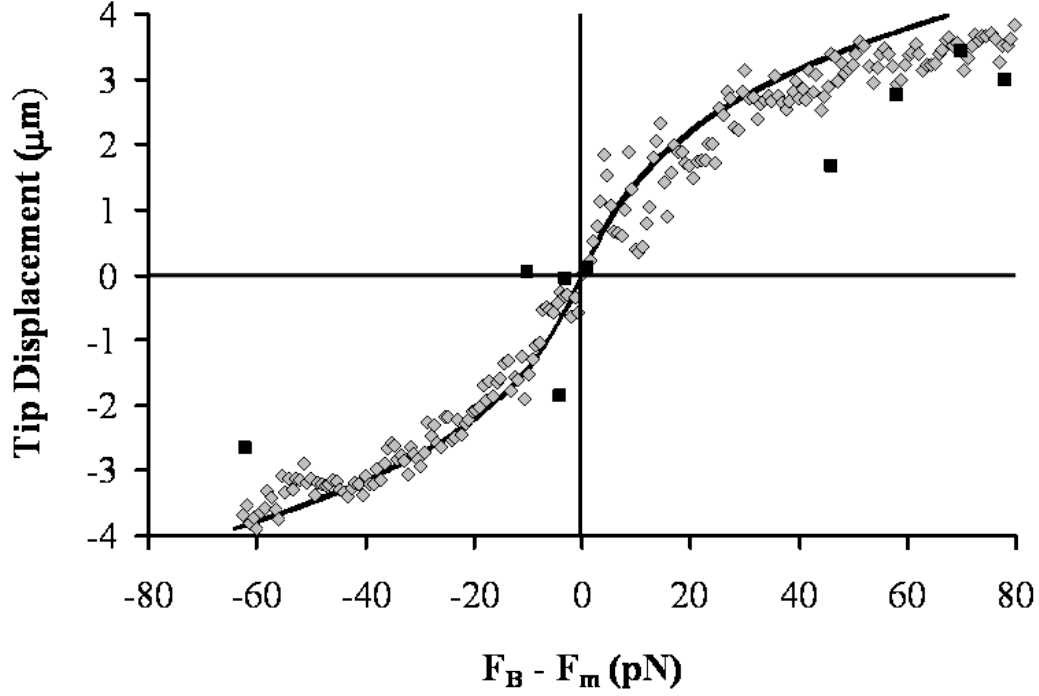
Figure 3.8: Data points (diamonds) are the local minimums from figure 3, and the black squares are the pulse data (n = 9). The data has been replotted such that the applied force (i.e. the sum of the external force F_B, and the effective motor force, F_m) fall at 0,0. Line is from nonlinear model with parameters determined by fit to complete cilia data set of Figure 4, which is in good agreement with the data.

3.4   Discussion

Studies of a variety of model biological systems have left open the question of whether the force generation in axonemes is symmetric with regard to the stroke direction, and whether the timing mechanism that determines the beat frequency is based on an internal timer or on the external curvature of the axoneme (Lindemann, 2007)(Brokaw, 2001)(Dillon et al., 2003)(Mitran, 2007) .These issues play a critical role in computational models of the propulsion of fluids by cilia. For example, most models assume the so-called curvature controlled switchpoint mechanism for determining the beat frequency, which would dictate the maintenance of cilia bend shape upon loading

74

the cilia with a high viscosity fluid (Rikmenspoel, 1976). These models also require the correct value of internal force generation in order to predict fluid propulsion. Thus our results usefully inform several fundamental issues of cilia function. Below we develop the implications of our results with respect to the contributions of MTs on the overall stiffness of the axoneme, the effective total and per-motor force generated by the dyneins, and the control of switching between the effective and recovery strokes. We conclude with the implications of the cilia force in fluid propulsion and in rheological and flow sensing.

3.4.1 Stiffness of the axoneme dominated by the microtubules

The linear spring constant we measured ($k_A = 5.4 pN/\mu m$) allows us to assess the relative contribution of MTs and other structural proteins within the cilium using the theory of simple bending. Assuming small deformation, $k_A = \frac{3EI}{L^3}$, where E is Young's modulus of the material, I the second moment of inertia and L the cilium length, $7\mu m$, we find the flexural rigidity EI (the force required to bend a structure to a unit curvature) is $(6.2 \pm 1.6) \times 10^{-22} Nm^2$. Two previous studies have measured the stiffness of individual sperm flagellar axonemes using microneedles (Schmitz et al., 2000)(Okuno and Hiramoto, 1979). Most relevant to our data is the report using echinoderm sperm, where values of were obtained (Okuno and Hiramoto, 1979). Our value falls within this range. We can now compare our value with that obtained from measured mechanical properties of microtubules and the established geometry of the axoneme. As a lower bound, we calculate the axoneme flexural rigidity assuming that it equals the sum of the flexural rigidities of its component microtubules. This is equivalent to assuming that the microtubules can slide freely past one another during bending. Directly measured values of flexural rigidity of singlet microtubules fall within the range $16 \times 10^{-24} - 45 \times 10^{-24} Nm^2$(Tuszynski et al., 2005)(Nedelec, 2002)(Gittes

et al., 1993)(Elbaum et al., 1996)(Cassimeris et al., 2001). We therefore calculate the ratio of flexural rigidities of an axoneme to a singlet microtubule, $\frac{EI_{axoneme}}{EI_{SM}}$, to be given by the range of 14-19. Assuming a reasonable geometry for the axoneme and assuming that the flexural rigidity of the microtubule doublet can be extrapolated from its geometry relative to the singlet, we calculate $\frac{EI_{axoneme}}{EI_{SM}} = 28$(Cassimeris et al., 2001) . The agreement between our measured value and calculated literature values implies that the flexural rigidity of the axoneme is dominated by the microtubules, with internal proteins providing a relatively minor contribution for small bend angles during beating. We note that our measurements occur during active motion of the motors, and the linear term alone applies for small deformations. A more detailed interpretation will require direct measurements of the mechanical properties of microtubule doublets.

3.4.2 Most of the motors contribute to actuation of the axoneme.

We have obtained an effective internal motor force,F_m of 62pN±18pN by fitting our model to the data in Figure 3.6. To relate F_m to the contributions of individual axonemal motors, we interpret it in the context of a 2D, internally driven, elastic rod-like filament model for the axoneme (Camalet and Julicher, 2000). In this model each motor applies a force with a component parallel to the microtubules, and thus generates a distributed shear stress through the action of the ensemble of motors. The shear stress acts to bend the axoneme. A uniformly distributed shear stress will bend a cantilever as if a single force was applied at the cantilever tip,F_m . We can write $F_m = n.a.f.m$ where a is the microtubule doublet spacing, f is the internal shear force per motor domain, m is the density of motor domains per unit length in the axoneme and n is the effective number of columns of active motors. Solving for f we find:$f = \frac{F_m}{n.a.m}$. The microtubule doublet spacing in the axoneme is known to be ≈24nm, and analyzed cryo-

EM images (Nicastro et al., 2006) of the Chlamydomonas axoneme reveal the number of motor heads per repeat length of 96nm. By counting 4 of the three-headed outer dynein arms (ODAs), 5 single headed, and 1 double headed IDAs, we get a total of 19 motor head domains. There is some evidence to suggest that airway cilia ODAs are double headed (Hastie et al., 1988a) unlike Chlamydomonas, giving a total of 15 motor head domains. To estimate the force contribution of a single active dynein, we used a geometrical argument based on the angles made by the contributing microtubules with the bending direction(Figure 3.9). Based on symmetry, we can assume that there are at most 4 columns of dyneins that contribute to the beat in particular direction (Lindemann, 2007)Each contributing dynein column is is represented as A, B, C, D. Thus the effective contribution of the dyneins is give by

$$F_{PM} = F_A cos 70° + F_B cos 30° + F_C cos 10° + F_D cos 50°$$
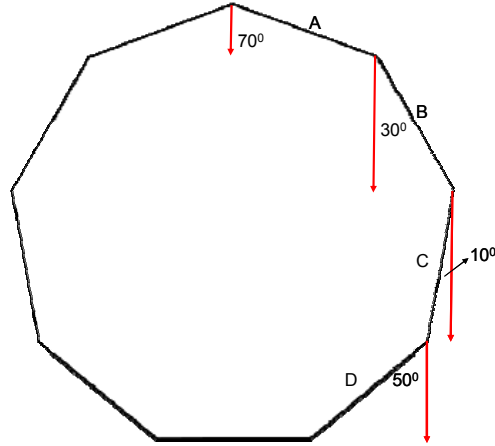
Figure 3.9: Segments A, B, C, D represent columns of active dyneins.

This reduces to $F_{PM} = 2.84.F_{SD}$. F_{PM} is the force per motor domain and from our model is found to be 16pN. This gives us a conservative value 5.6 pN $\pm$1.6pN per motor domain in the cilia, which is in good agreement with the 6pN stall force observed in

single molecule experiments (Shingyoji et al., 1998). To demonstrate the sensitivity of the derived motor force on estimated parameters, we note that, should the number of motor heads per repeat be the same as it is in *Chlamydomonas*(Kotani et al., 2007), our force per motor would be 4.4 pN$\pm$1.3pN. Our results and calculations indicate that during the beat cycle a large fraction of the dyneins are contributing to the shear stress within the axoneme. This conclusion suggests that there is little reserve force available to the axoneme. As the force due to external influences approaches $\approx$60pN, due, for example, to loading from viscous fluids, then the axoneme should begin to significantly change its behavior.

3.4.3 Internal timing mechanism

Our results have significance for the switch point hypothesis (Satir and Matsuoka, 1989), and for the underlying dynamics that control cilia beat frequency. It is widely recognized that some form of strain is necessary to couple the individual motors for their coordination over significant lengths of the axoneme(explained earlier). The cause of the switch-point has been attributed to local curvature control through intra-microtubule shear strain at points of curvature (Dillon et al., 2003)(Brokaw, 2002)(Hines and Blum, 1979)(Machin, 1958) or an avalanche of dyneins releasing as the internal normal strain between MT pairs increases when the axoneme bends (Lindemann, 2007)(Lindemann, 1994b)(Lindemann, 1994a). We observed no change in the beat frequency upon the application of forces that decreased CBA up to 15% of the original amplitude, while causing a dramatic shifting of the tip trajectory away from the center line. Although our experimental geometry prevents the measurement of the axonemes shape, we can infer that the axoneme acquires a different curvature when the tip is displaced microns away from the original center line under external loading. If the curvature of the axoneme caused a triggering of the turnaround, then we should see a reversal at

approximately the same tip positions as the turn-around positions of the unloaded axoneme. Likewise, when CBA drops to 15% of its original value, we expect that the curvature of the axoneme during the beat cycle would be similarly diminished, especially for the stroke beating against the external force. However, the axoneme continues to switch beat directions with the same timing as before the application of the external force. The concept of an internal timing mechanism within the axoneme has previously been suggested (Brokaw, 2001), and is supported by laser tweezers measurements of dynein slipping, indicating a potential oscillating mechanism in force generation at the molecular scale (Shingyoji et al., 1998)(Kojima et al., 2002)(Kotani et al., 2007). Strain coordination between motors may be due to shear strains between neighboring microtubules that do not result in curvature, as may happen if the boundary condition at the basal body allows for sliding (Riedel-Kruse et al., 2007)(Vernon and Woolley, 2002)(Vernon and Woolley, 2004). We conclude that an internal timing mechanism dominates the switch mechanism, and that the coupling needed for coordination is robust over a wide range of external geometries.

3.4.4 Both effective and recovery strokes are driven

Brokaw recently pointed out that models of flagellar and ciliary axoneme motion can be classified as either active effective with passive recovery, or active for both (Brokaw, 2005). Our data strongly supports an active motion for both effective and recovery strokes in airway-derived cilia, especially with the observation that the midline of the tip velocity plot remains essentially the same during pulls as it was before, implying that velocity is not biased in the direction of the magnetic force. This is true whether the direction of force is toward or away from the effective stroke. Thus the tip velocity in both directions appears to be determined by the endogenous biochemistry and biophysics of the activation and release of the dynein motors during all phases of

the beat.

3.4.5 Cilia can generate sufficient force to propel healthy mucus

The effective force that we measure for cilia has implications for the physiological role of cilia in propelling fluids and in force sensing. We can use the simple model for the force of a surrounding fluid on a moving rod to understand the ability of cilia to propel high viscosity fluids such as mucus. The maximum torque needed to rotate a rod about its end in a viscous fluid through an angle of $\pm\ 45°$ is given approximately by $T = \frac{\pi^3.\eta.L^3.f}{24}$ (Howard, 2001). Assuming that this torque is generated from a point force at the rod end, we find that the critical viscosity where the effective internal force can generate the necessary torque is given by $\eta_{crit} = \frac{24}{\pi^3}\frac{F_m}{L^2 f}$. For a 7 micron axoneme beating at 10Hz with $F_m = 62pN$, we find $\eta_{crit} = 100mPa.s$. It is noteworthy that this viscosity is comparable to the measured viscosity of normal human respiratory tract mucus (Baconnais et al., 1999)(56-58)(Matsui et al., 2006), and lower than the viscosities reported for mucus and sputum from patients with Cystic Fibrosis (Braga et al., 1992) and Chronic Bronchitis (Puchelle et al., 1981), and is roughly 100x of the viscosity of buffer. The reports of viscous effects on ciliary beat phenomena include studies of CBF, beat shape and metachronal patterns in the ciliary fields of paramecium (Machemer, 1972) and three reports of viscosity effects in airway epithelia (Gheber et al., 1998) (Andrade et al., 2005)(Johnson et al., 1991). All four studies report a drop in CBF with increasing viscosity of the surrounding solution. The three studies on airway cilia show an initial decrease in CBF at low viscosities (down to 65% at 30mPa-s) that remains nominally constant at higher viscosities, with the eventual loss of consistent beat shapes at viscosities above 180mPas (Johnson et al., 1991). The usual interpretation of these results is that the drop in CBF is an inherent mechanical effect

on the cilia, while the maintenance of the CBF at higher viscosities is due to a regulatory mechanism correlated to Ca+ influx, channel activity and other biochemical effectors (Salathe, 2007). Those interpretations are consistent with curvature control models that maintain an internal force mechanism whose amplitude is unchanged under load. Such an interpretation is additionally supported by the observation of a constant amplitude under viscous loading (Johnson et al., 1991). However, it is difficult to reconcile these models with our results that show a constant CBF independent of beat amplitude. Our results may be consistent with previous measurements of viscous effects if we consider an induction period for the onset of the CBF decrease. Our measurements in this report are limited to under 30 seconds due to the force-induced release of the bead, while all three airway cilia studies note the reduction of the CBF over a few minutes after dosing with higher viscosity. This also may indicate a switchover between control modes, from frequency control to geometry control, as has been observed in flagellar beating (Ohmuro and Ishijima, 2006). Alternatively, altering the viscosity of solutions to change the effective load at the cilium tip changes a large set of variables, including ionic strength and effective mobility of nucleotides and other cofactors, which may or may not be effectively addressed. Our system allows all other variables to remain constant, except for increased loading at the tip. Finally, the forces experienced by the axoneme under viscous loading are fundamentally different than those experiences in our experiment. In viscous loading experiments, the external drag force on the axoneme is proportional to the instantaneous axoneme velocity. In our system, the external force is constant, and it is therefore possible that these two types of experiments elicit different responses from the axoneme. Within the contexts of a dynamical systems model for the axoneme, altering the dissipative term through a change in viscosity can dramatically change the filament dynamics in a highly non-linear manner (Camalet and Julicher, 2000).

3.4.6 Cilia generate sufficient force to stimulate stretch activated channels

Within the context of a flow system such as lung epithelia, homeostasis may be enabled by a feedback mechanism whereby cilia act as sensors of some combination of mucus flow, rheology and volume (Sanderson and Dirksen, 1986). If the cilium tip end were constrained by a static, high modulus mucus layer, then a simple model of cilia dynamics would predict that the internal drive mechanism of the axoneme would cause a force of F_m= 62pN to be exerted on the membrane at the base of the axoneme. We can compare this point force to shear stresses that have provoked responses in epithelia by calculating an effective membrane shear stress σ through $\sigma = F_m.c$ where c is the area density of cilia. Taking c = 5cilia/μm^2 (Dirksen, 1982), we find $\sigma = 325 Pa$. This value is four orders of magnitude larger than the values of shear stress caused by fluid flow that have been shown to provoke responses in cell culture systems where values below 10^{-2}Pa were effective(Resnick and Hopfer, 2007)(Winters et al., 2007). Therefore we would expect that a field of cilia with their tips constrained by high viscosity mucus could cause a response through a mechanism similar to shear sensing, perhaps through strains within the membrane or underlying cytoskeleton.

3.5 Conclusion

Forces are ubiquitous in biology. They drive systems, act as stimulus and manifest as responses in cellular systems. The force driving mechanism in flagella and cilia are one of the most sophisticated biophysical systems in the body. What is truly remarkable is that evolutionarily speaking, these organelles have been conserved in their structure and function across species and times lines as is evident in Chlamydomonos, paramecium and other organisms. Understanding human cilia is especially critical as we take steps

to understand the molecular aspects of various diseases including those of our lungs which are now the number three killers in the United States.

Here I have presented the dynamics of individual airway epithelial cilia under load using the magnetic bead methodology. The implications of these results in pathologies like CF are multifold. Our measure of the force generated by the axoneme sets quantitative bounds on the propulsion of viscoelastic fluids, and provides a measure of the ciliary forces on the membrane that may play a role in biochemical feedback regulation of epithelial phenomena. These numbers are also critical input parameters for various computational models of the lung that are under development in different research centers in the world. Within the VLP, these numbers have provided valuable insights into the study of mucus rheology, cell signaling in the lung and biomimetic cilia systems.

The presence of cilia in multiple cells and tissues in our body implies that our results have implications which are just not restricted to the lung. Mechanistic understanding of these amazing molecular machines have suffered from reliable quantitative data from single cilium which our work provides. Our results imply that the mechanical stiffness of the axoneme is dominated by the microtubules during activation. The shear stress that bends the axoneme, assuming measurements of in-vitro assays, is generated by a large fraction of the dynein motor proteins activated at any one time. The frequency of the cilium is unchanged upon loading even when its motion is suppressed to less than 15% of its original value. This challenges existing models which have been designed to account for observed decreases in cilia beat frequency with increased viscosity of the surrounding fluid. These curvature-dependent models have relied upon geometry-dependent switchpoints between effective and recovery strokes. In contrast, our measurements highlight the role of an intrinsic mechanism that allows the axoneme to maintain its beat frequency under external loading.

Chapter 4

Cell mechanics and Cancer

Cancer accounted for 7.9 million deaths in 2007. That's 13% of all deaths for that calendar year. The estimated number for 2030 is 12 million. It encompasses more than 100 distinct diseases with diverse risk factors and epidemiology. The National Institute for Health(NIH) gives out 6 billion dollars every year to cancer related grants. If one types "cancer" in Pubmed, there are close to 3 million hits. Approximately 100,000 somatic mutations from cancer genomes have been reported in the quarter of a century since the first somatic mutation was found in HRAS. It is estimated that in the next few years, several hundred million more will be revealed by large scale, complete sequencing of cancer genomes.

Cancer is a disease of intimidating numbers. I begin this chapter by introducing the fundamental cellular processes leading to cancer and list what are now the accepted properties or hallmarks of cancer cells. Research on material properties of the cell and cancer has undergone a revival over the past 10-15 years and I will review a few which are closely related to my research and represent the current state of the art in cancer mechanics research. I then move on to results of our work done in collaboration with the Blobe lab at Duke where we show that invasiveness which is a property(hallmark) of metastatic cells shows a strong correlation with the mechanical property of these cells and one can tune the metastatic potential by altering the mechanical properties

through alterations in different signaling pathways. These results have strong implications in two aspects of oncology. Firstly, understanding signaling pathways that affect cell mechanics can give us new therapeutic targets, and secondly, in clinical settings, the mechanical grading or *Mechanical phenotyping* shown here has a great potential in replacing traditional metastatic potential assays like 2D cell motility assays, 3D migration and invasion assays which typically take hours compared to minutes for these mechanical measurements.

4.1 Introduction

As a society, cells function very differently from other societies and ecosystems. While survival of the fittest has driven species through time, cells follow the rule of "self sacrifice". All somatic cell lineages are programmed to undergo cell suicide or apoptosis, a process that ensures propagation of genetic copies. Human cells rely on strong collaboration to survive, a collaboration based on cell communication and signaling. Each cell behaves in a socially responsible manner, resting, growing, dividing, differentiating and ultimately dying for the good of the organism. What is truly remarkable is the fact that, of the 10^{14} cells in our body, about 10^9 cells undergo perturbations or mutations daily. If the society is unable to tackle one of these mutations, giving a cell some advantage over the others, this cell becomes a founder of a mutant clone. Over time, repeated mutations, competition, natural selection leads to complete disruption in the harmony of the cell society. This is the onset of cancer. Individual mutant clone of cells, begins by prospering at the expense of its neighbors, and descendants of this clone disrupt the overall cellular society(Alberts, 2008).

85

4.2 Hallmarks of cancer

Almost 10 years ago, Hanahan and Weinberg published a seminal paper summarizing the six essential alterations in cell physiology that collectively dictate malignant growth, termed the hallmarks of cancer(Hanahan and Weinberg, 2000). By 2010, this paper has 6,352 citations, which reflects the enthusiasm with which this guidance was accepted. Considering that there are 100 distinct types of cancer, and countless subtypes, summarizing the vast catalog of cancer cell genotypes into six essential alterations in cell physiology is truly significant. The six hallmarks defined were:

1. Self-sufficiency in growth signals - No type of normal cells can proliferate without mitogenic growth signals(GS) and move from a quiescent state into an active proliferate state. Acquired GS autonomy was the first of the hallmarks defined by cancer researchers.

2. Insensitivity to antigrowth signals - Growth inhibitory signals, like their positively acting counterpart, are received by transmembrane cell surface receptors which maintain cellular quiescence and tissue homeostasis. The TGFβ pathway discussed later, is one such pathway important for this regulation.

3. Evading apoptosis - We discussed this aspect earlier, one of the fundamental laws broken by cancer cells is their ability to resist programmed cell death or apoptosis. Once triggered by a variety of signals, the program unfolds led by cellular membrane disruptions, breaking down of the cytoplasmic and nuclear skeleton, extrusion of the cytosol, degradation of the chromosomes, finally concluding with the fragmentation of the nucleus. Within 24 hours, shriveled cell corpses are engulfed by nearby cells. Cancer cells resist apoptosis through a variety of mechanisms including mutation in certain genes like the p53 tumor suppressor gene.

4. Limitless replicative potential - The three above mentioned capabilities leads to uncoupling of a cell's growth program from signals in its environment. However, research has shown that acquired disruption of cell cell signaling is not enough to ensure expansive tumor growth. Since most types of tumor cells that are propagated in culture appear immortalized, as opposed to cells showing senescence, this suggests that limitless replicative potential is a phenotype acquired in vivo during tumor progression.

5. Sustained angiogenesis - The process of angiogenesis or the growth of new blood vessels is requires oxygen and nutrients supplied by the vasculature. Incipient neoplasias develop angiogenic capability to progress to a larger size.

6. Tissue invasion and metastasis - Metastasis, or the spread of cancer cells to distal sites is responsible for 90% of all cancer related deaths. This highly complex cascade of events is also the least understood aspects of cancer. Once an abnormal cell grows and proliferates out of control, it gives rise to a tumor called a *neoplasm*. As long as the neoplasm is confined at its primary site and does not undergo metastasis, the tumor is said to be benign and removing of the mass leads to a complete cure. However, cancer cells in tumors achieve the ability to breakthrough the tissue barrier and start penetrating the basement membrane, a process called *invasion*. A tumor is considered malignant only if the cells have acquired this ability to invade surrounding tissue. From here on, these cells enter the blood or lymphatic vessels, and eventually invade through barriers at other tissue sites and form secondary tumors. The more widely a cancer spreads, the harder it becomes to eradicate it. Invasiveness, or the ability of cancer cells to penetrate blood vessels, lymphatic vessels, basal lamina and the endothelial lining is thus one of the defining properties of malignant tumors. This penetration of cancer cells into the basement membrane is in itself a multistep event with

hallmarks that include secretion of proteases, alterations in adhesion receptors, and changes in cell morphological and migratory properties.

For the purpose of work described in the chapter, changes in cell morphology is the most crucial signature for invasiveness and metastasis. Any material that undergoes a change in its structure or in the organization of its elements also undergoes a change in its mechanical property. A cell is not unlike any composite material like fiberglass or Kevlar. As an example, consider the composite, fibre reinforced concrete or FRC. FRC is concrete containing fibrous materials that contains short discrete fibers that are uniformly distributed and randomly oriented. The mechanical characteristics of FRC change with varying concretes, fibre materials, geometries, distribution, orientation and density. This is fundamental hypothesis for mechanics in cancer cells. If cancer cells undergo changes in orientation, distribution and density of its cytoskeleton, this will also directly affect the mechanical property.

4.3 Role of the cytoskeleton in Invasion and Migration

Eukaryotic cells depend on their cytoskeleton for a number of different functions. The internal spatial organization, shape, structural properties, external interaction, internal signal transmission, all depend on cytoskeletal filaments. Importantly, the cytoskeleton provides the cell with all the mechanical linkages that allow a cell to bear stresses and strain that would otherwise rip apart with changes in its environment. It is dynamics of cytoskeleton assembly and disassembly, combined with an intricate system of signaling that also drives the cell, literally. It is therefore not surprising that any changes in cell motility is due to the change in regulation of the cytoskeleton. Metastatic cancer cells acquire invasive capabilities which essentially involves two

steps. Aberrant cell migration and secretion of proteases. Proteases like matrix metal-loproteases(MMP) are important and widely studied phenomenas in oncology and the contribution of cell stiffness and cytoskeleton in secretion is unclear in secretion but is outside the scope of this work. To understand the role that cell stiffness may have in cytoskeleton mediated migration/invasion, we need to first understand the role of the cytoskeleton in migration.

Cell motility is a complex and highly coordinated process and it is likely that changes in the expression of several genes are required for the cell to become motile. It is hypothesized that, for a cell to become motile, it needs deregulation of more than one gene combined with the correct microenvironment. Intravital imaging of experimental tumors has shown that only a small proportion of tumor cells are motile (<0.1% of tumor cells) and are not uniformly distributed but are observed in localized areas of the tumor(Ahmed et al., 2002)(Wyckoff et al., 2000)(Wang et al., 2002).

Cells respond to several internal and external stimuli which promote cell migration. The initial reaction involves cell polarization and protrusion formation. These protrusions are either large branching dendritic actin networks called lamellipodia, or spike-like organized long actin filaments called filopodia(Welch and Mullins, 2002). The structures are driven by actin polymerization and are stabilized by adhering to the extracellular matrix(ECM) through integrin receptors or adjacent cells via junction receptors. Adhesions are important in mechanotransduction and will be discussed in detail in subsequent chapters. The adhesions form sites bound to which, the cell can produce traction and move the cell body forward. The traction is mediated through actomyosin contractility machinery of the cell.
In vivo and in vitro experiments have shown that tumor cells show multiple mecha-

nisms of motility. *Mesenchymal* cell motility is one of the better understood motility mechanisms because they are well suited to movement on rigid 2D substrates that are used in most in vitro studies .Mesenchymal mode is characterized by an elongated cell morphology and established cell polarity and is dependent upon proteolysis to degrade the ECM(Friedl and Wolf, 2003)(Friedl, 2004). Cell speeds are relatively slow in mesenchymal mode($0.1\mu m$/min-$1\mu m$/min). It is estimated that between 10% and 40% of carcinomas undergo an EMT and use this form of motility. High resolution intravital imaging and other such approaches have demonstrated that some carcinoma cells move at very high speeds with an amoeboid morphology(up to $4\mu m$/min)(Wyckoff et al., 2000)(Friedl, 2004). *Amoeboid* movement of cancer cells is likely to use mechanisms similar to migrating leukocytes and Dictyostelium(Friedl et al., 2001). In Dictyostelium, a wave of actin polymerization propagates around the cell cortex(Vicker, 2002). Cortical actin contraction driven by Rho-ROCK signaling might promote rapid remodeling of the cell cortex characteristic of amoeboid movement. A third form of motility is *collective* cell motility. This involves movement of whole clusters or sheets of tumor cells. This is similar to a collective form of mesenchymal motility, with the cells at the front producing MMPs and generating a path for the following cells(Nabeshima et al., 2002). In contrast to single cell motility, which requires the loss of adherin junctions, the maintenance of adherin junctions is important for this form of movement.

It is clear that the cytoskeleton plays a very important role in any migrational mode. The dynamics of the cytoskeleton through signaling, actomyosin contractility and polymerization drives cell motion. One of the key regulator is the small GTPase family of Rho, including RhoA, Rac and Cdc42. I will introduce this family of proteins in the next chapter. For the work presented in this chapter, it is sufficient to say that the cytoskeleton mediates migration and invasion through its effects on cell polarity,
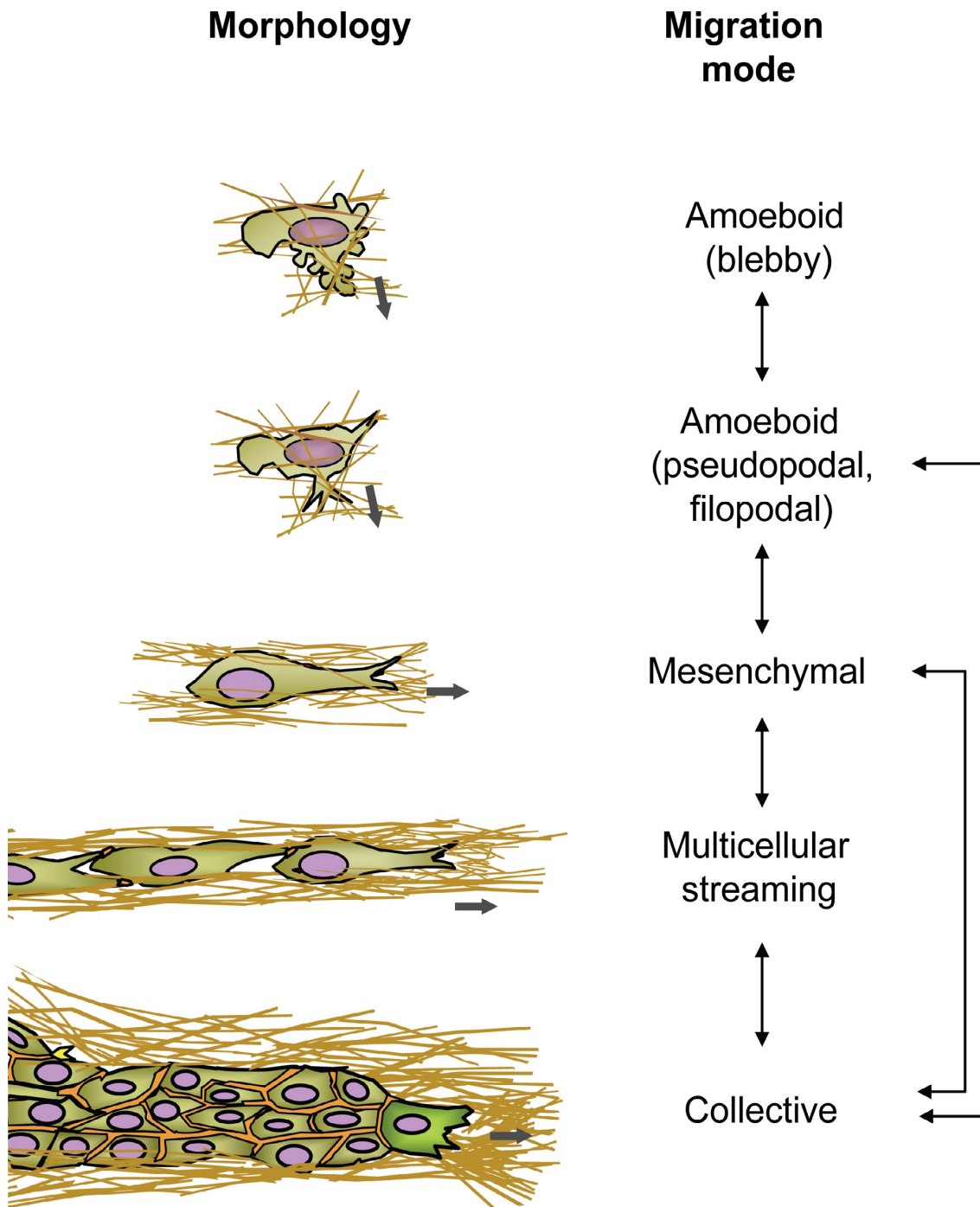
Figure 4.1: From (Friedl and Wolf, 2010). The migration modes is based on typical cell morphology (rounded or spindle shaped) and pattern (individual, loosely connected, or collective). Thick arrows indicate direction of migration. (Reprinted with permission)

polymerization and actomyosin contractility. The key to cell stiffness playing a role in migration is the fact that actomyosin contractility in the end is also responsible for the tension in the cytoskeleton and its mechanical properties.

4.3.1 Actomyosin Contractility

Myosin molecules walk along and propel the sliding of and produce tension in the actin cytoskeleton. The energy required for this process is provided by the hydrolysis of ATP at the catalytic amino-terminal (head) region of the molecule. The C-terminal domains of some myosins self associate into filaments, which allow their heads to tether actin filaments and produce tension. Non muscle myosin (NMII) which is the main motor of interest in my studies, comprises of three pairs of peptides: two heavy chains of 230 kDa, two 20 kDa regulatory light chains (RLC) that regulate NM II activity and two 17 kDa essential light chains (ELC) that stabilize the heavy chain structure(Figure 4.2).

Due to it's ability to dynamically remodel the actin cytoskeleton, NM II regulates multiple cellular processes. While NM II does not reside in or play a part in the physical organization of the lamellipodium, it can affect the net rate of cell protrusion which drives cell migration (Vicente-Manzanares et al., 2007)(Ponti et al., 2004)(Cai et al., 2006). NM II is also required for maturation of focal adhesions, which is a critical step in migration as well as cell-ECM interaction. The integrin actin linkage translates the effect of NM II to adhesions and mediates adhesion formation and maturation. Finally, NM II plays an integral part in cellular response to mechanical stimulation through cellular signaling pathways that regulate its activation. For example, application of external force produces post-translational modifications such as phosphorylation, or conformational changes in different signaling molecules, which inhibit protrusion formation and lead to adhesion maturation and actin filament bundling (Galbraith et al.,

2002). Studies have also shown that cells sense substrate stiffness, in part through the activation of NM II by RLC phosphorylation (Beningo et al., 2001; Beningo et al., 2006).

Thus, overall through its effect on actin bundling and contractility, NM II acts as an important integrator of processes that drive migration, adhesion and mechanotransduction. More importantly and relevant here is the fact that NM II is an important end point on which many signaling pathways converge, largely through the Rho GTPase. NM II is at one end of the regulatory feedback loops that control the activation of NM II's own upstream signaling pathways. As one recent review states, "Emerging evidence strongly indicates that mechanical forces probably remodel the tumor cell microenvironment through NM II to affect tumor progression and metastasis, but the precise mechanism by which NM II responds to and generates the microenvironment remains to elucidated" (Vicente-Manzanares et al., 2009).

4.4   TGFβ signaling

Another factor implicated in regulating invasion, either via the cytoskeleton or via secretion of proteases like the MMPs, is transforming growth factor-β(TGF-β)(Gordon and Blobe, 2008; Dong et al., 2007)(Massagué, 2008). The TGF-β signaling pathways have diverse roles in human disease. In cancer, these pathways act as both, tumor suppressors and tumor promoters(Gordon and Blobe, 2008; Dong et al., 2007) (Massagué, 2008). By inhibiting cell proliferation and inducing senescence and apoptosis, the pathway act as a tumor suppressor. This is consistent with the finding that receptors and signaling components of the TGF-β pathway are often deleted or mutated in human cancers (Jakowlew, 2006). However, in later stages of diseases, tumors over express and deregulate TGF-β ligands, which may induce epithelial to mesenchymal transitions (EMT) and enhance migration and invasion(Rahimi and Leof, 2007). The

6S assembly-competent NM II

Globular head domain
(actin binding and
Mg^{2+}-ATPase motor domains)

ELC

RLC

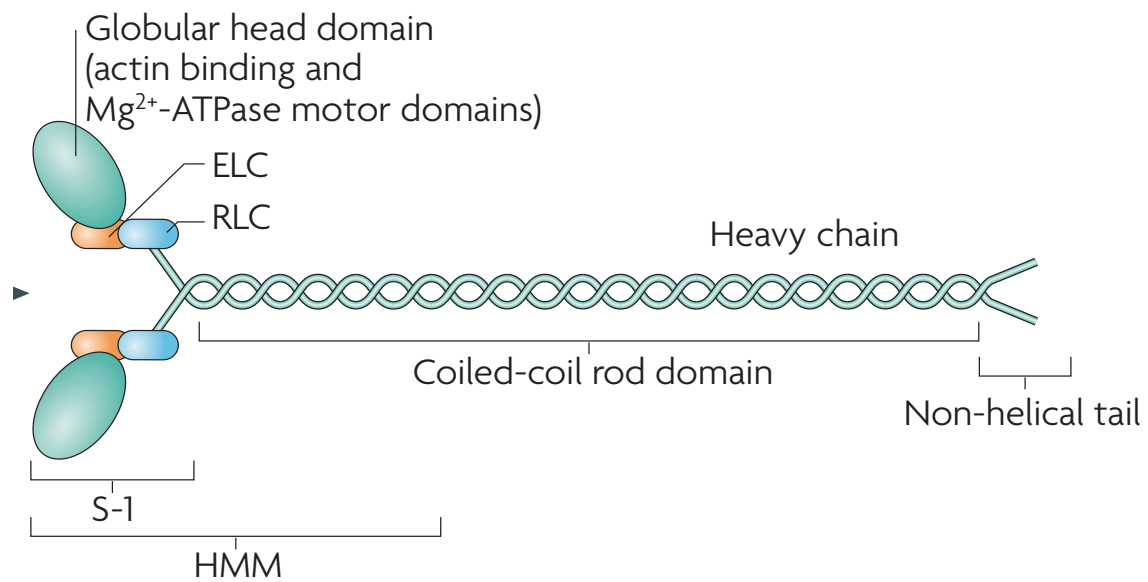Heavy chain

Coiled-coil rod domain

Non-helical tail

S-1

HMM

Figure 4.2: From (Vicente-Manzanares et al., 2009). The subunit and domain structure of non-muscle myosin II(NM II). Phosphorylation of the RLC results in the unfolded structure shown here. (Reprinted with permission)

precise mechanism of this dichotomy is currently unknown.

Our interest in the role of TGF-β in cancers is focussed on the type III receptor (TβRIII or betaglycan). This receptor is lost in a broad spectrum of cancers and importantly the TβRIII receptor has been shown to be an important regulator of cell migration, invasion and cell growth and angiogenesis in both in vivo and in vitro models. Recently it has also been shown that, re-expression of the type III receptor in epithelial cancer cells results in alterations in the cytoskeleton and cytoskeleton mediated signaling(**?**). It is this aspect of the receptor and TGF-β signaling that interests us in terms of effects on mechanical properties of the cytoskeleton. A schematic of the signaling pathway is shown below.

4.5 Cell mechanics in cancer

In a 1998 editorial for Science, Stella Hurtley wrote that "changes in the cytoskeleton are key, and even diagnostic, in the pathology of some diseases, including cancer"(Weinberg, 2007). The study of mechanical properties in cancer cells can be split into 2 broad groups. One group focusses on the changes in the mechanical properties of the ECM as cells become metastatic and other group focusses on the mechanical properties of individual cancer cells. What is known now is that tumor cells have stiffer ECM, a consequence of which is that oncologists usually diagnose cancer by sensing the change in elasticity of tissue by palpation. I want to quickly review recent work elucidating the implication of a stiff ECM in cancer and 2 papers that measure stiffness of cancer cells.

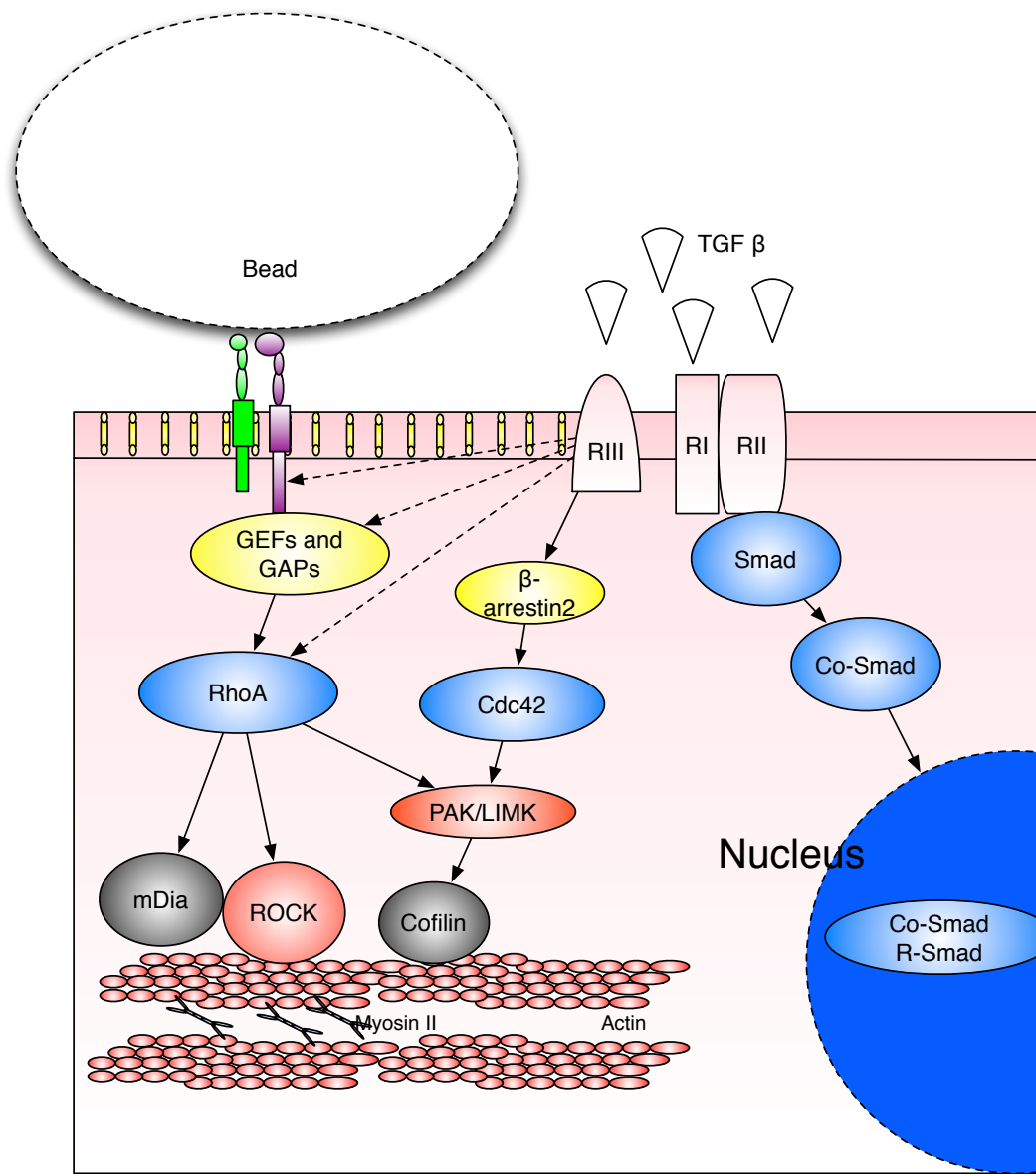Figure 4.3: The TGFβ pathway through the RIII receptor is shown here. Recent evidence has shown that TGFβ results in alteration in the cytoskeleton through the Cdc42 pathway. The dashed arrows show potential downstream pathways which have been hypothesized before. TβRIII mediates cell migration in a β-arrestin2 dependent manner through activation of Cdc42 in a ligand independent manner.

4.5.1 Tensional homeostasis and malignant phenotype

Using an electromechanical indentor to directly measure tissue mechanics, Paszek et al. found that explanted mouse mammary tumor cells are stiffer than healthy mammary gland(Paszek et al., 2005). They cultured normal mammary epithelial cells on ECM gels that varied in mechanical compliance over the range displayed by normal and cancer tissues they measure in vivo. Not only did the stiff ECM gels promote expression of the undiffrentiated malignant phenotype, but they also found elevated levels of Rho activity. Interestingly, overexpression of constitutively active Rho in normal mammary cells on a soft matrix promoted malignancy as they generated more force, disrupted cell-cell junction, spread, increased proliferation and lost acinar organization. This dedifferentiated phenotype was reversed by blocking tension generation through pharmacological inhibition of ROCK or myosin II. The hypothesis that has emerged from this study and subsequent work is that increased stiffening of the ECM may promote integrin clustering, ERK activation and Rho mediated contractility. This increase in tension will further increase ECM stiffness by tensing or realigning ECM components, thereby creating a deadly, self sustaining positive feedback loop shown in Figure 4.4.

4.5.2 Nanomechanical analysis and Optical deformability.

This paper was the first work reporting on stiffness of live metastatic cancer cells taken from pleural fluids of patients with suspected lung, breast and pancreas cancer(Cross et al., 2007). Stiffness measurements were carried out using an atomic force microscope and done on population of cells. To confirm the selected cell populations actually represent tumor and mesothelial cells, immunofluorescence triple labeling assays were performed. They found that metastatic cancer cells ere 70% softer, with a standard of deviation over five times narrower, than the benign cells that line the body cavity.
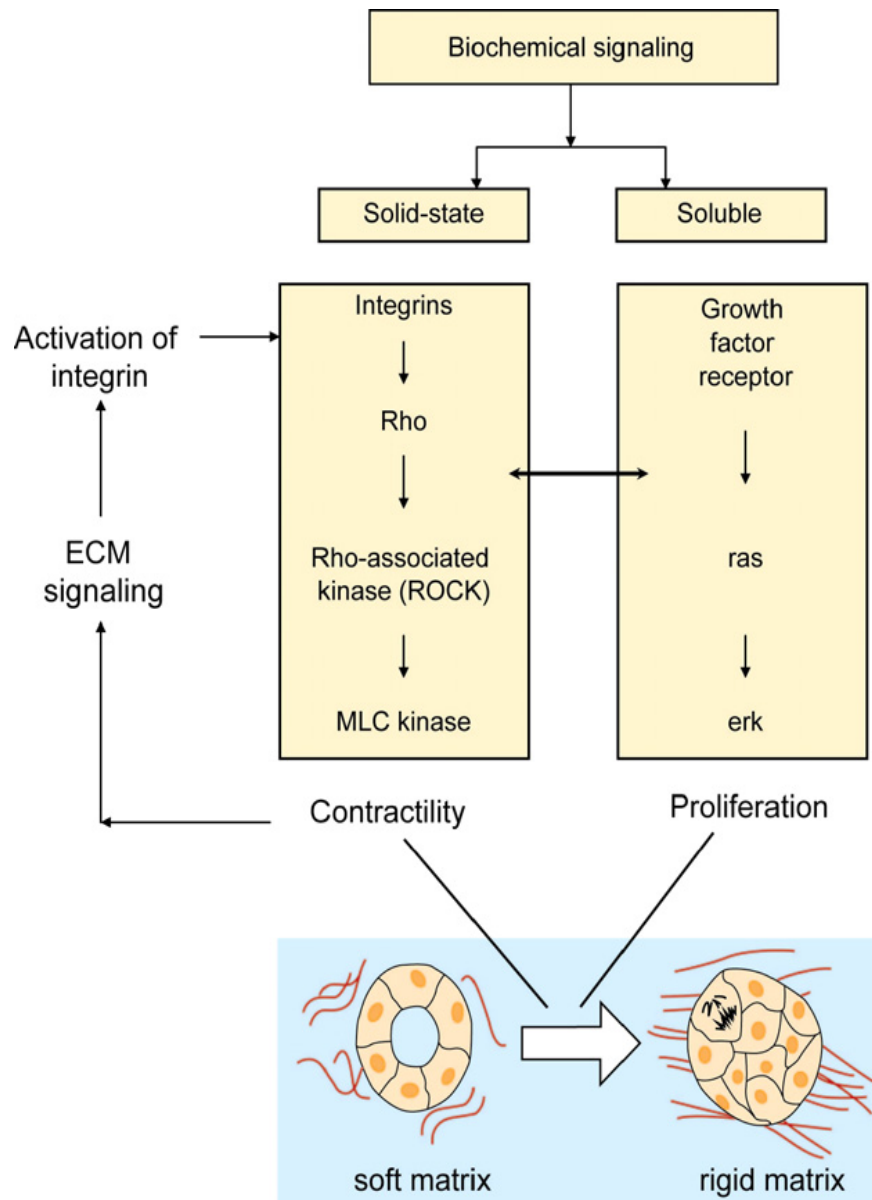
Figure 4.4: Adapted from (Suresh, 2007a). Illustration of how mechanical signaling from the ECM acts in concert tumorigenic signaling to activate malignant transformation. (Reprinted with permission)

Guck et al. used a microfluidic optical stretcher to measure stiffness of the breast cancer cell line MCF 10 and MCF 7(Guck et al., 2005). The optical stretcher is a coaxially aligned dual beam laser tweezers system which can sequentially suspend, trap and deform isolated cells. Using this technique, they found that cancerous MCF 7 cells are more deformable than the normal MCF 10. The reduction in elastic rigidity appeared to arise from reduction in F-actin concentration of as much as 30%. The width of distributions were consistent with Gimzewski's observation with the normal cells showing a wider distribution compared to the cancerous MCF 7 cell line.

While these measurements show that cancer cells are softer than their malignant counterpart, the exact relationship between stiffness and metastasis is not explored in any of these studies. In fact very little is known about the relationship between the two. The fundamental question we wanted to answer with our studies was whether cancer progression correlates with stiffness.

4.6 Results

4.6.1 Ovarian cancer cells and primaries have a varied invasive potential

As mentioned earlier, metastasis of cells requires both motility and invasion through a basement membrane, which can be modeled reproducibly in vitro using reconstituted basement membrane in a transwell format(Lefkowitz and Shenoy, 2005). Cells (50,000-70,000 for invasion and 20,000-30,000 for migration) were seeded in the upper chamber of a transwell chamber either coated with matrigel or uncoated for migration. Cells were allowed to migrate or invade for 18 to 24 h at 37°C toward the lower chamber, containing media plus 10% FBS. Cells on the upper surface of the filter were removed and the cells
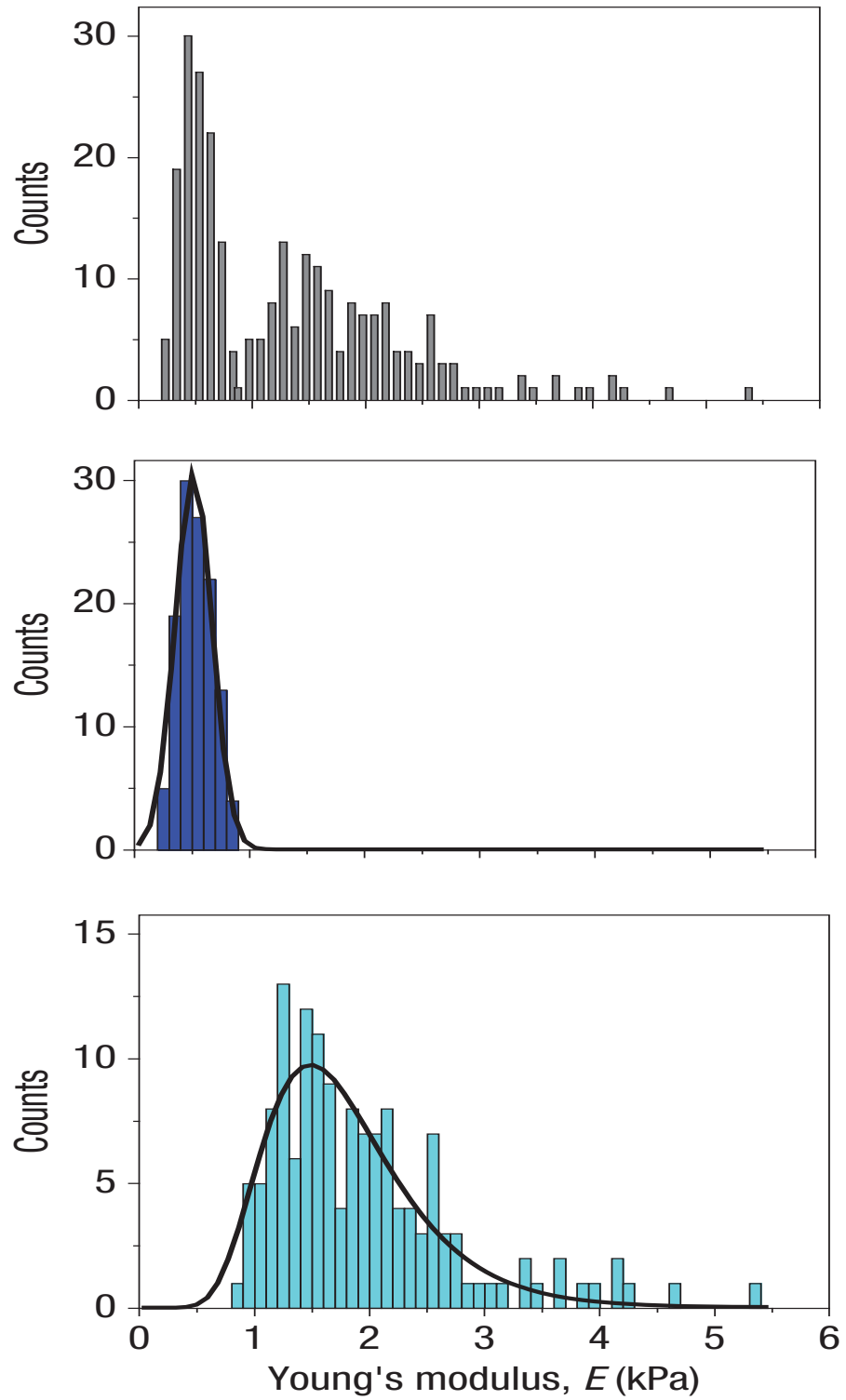
Figure 4.5: Mechanical measurements on pleural fluid from (Cross et al., 2007). *Top* Histogram of young's modulus, E for all data collected from seven different clinical samples. *Middle* Gaussian fit for all tumor data from the seven samples. *Bottom* Log-normal fit of normal cells. (Reprinted with permission)
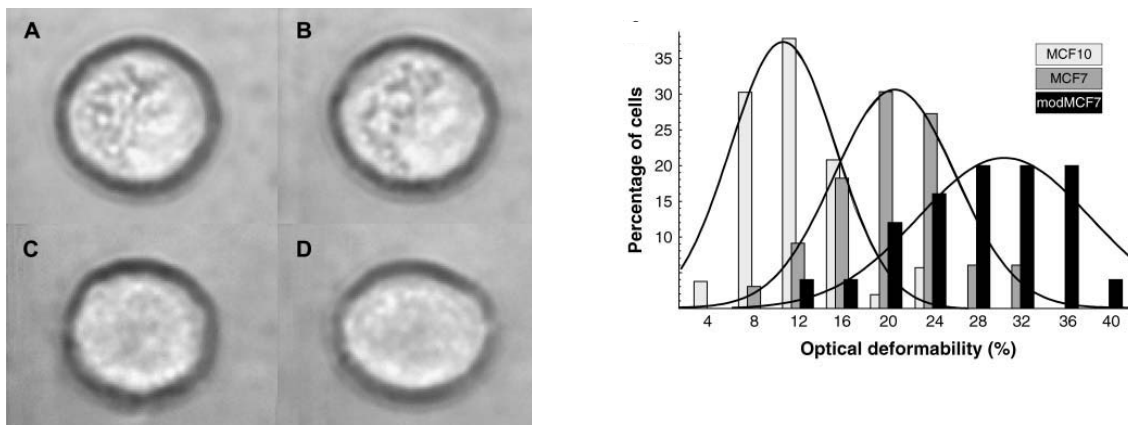
Figure 4.6: Optical deformation data from(Guck et al., 2005). *Left* Typical examples of stretching of breast epithelial cells. A and C are taken at incident light power of 100mW in each beam and B and D are images at 600mW light power. *Right* Optical deformability of normal, cancerous and metastatic breast epithelial cells. (Reprinted with permission)

that invaded/ migrated to the underside of the filter were fixed and stained using the 3 Step Stain Set (Richard-Allan Scientific). Percent cell migration or invasion was determined as the fraction of total cells that invaded through the filter. Each assay was set up in duplicate, and each experiment was conducted at least 3 times with 4 random fields from a 10x magnification analyzed for each membrane. The migratory capacity of the panel of cells was also determined using Transwells in the absence of reconstituted Matrigel. We used a series of ovarian cancer cell lines and primary cells. Primary short term epithelial ovarian cancer cell cultures were established from the ascites of patients with Stage III/IV epithelial ovarian cancer as described previously(Katz et al., 2009). Briefly, ascitic fluid was centrifuged at 4°C for 10 min at 2000 rpm and hemolysis of erythrocytes was done by resuspending cells in 0.17M NH_4Cl for 10 min on ice. Cells were then washed three times in Hanks Balanced Salt Solution (HBSS) and finally resuspended in 30mL RPMI media per 1cm pellet. Cell suspensions were layered over 10mL Ficoll and centrifuged for 25 min at 25°C at 2500 rpm. Cells were seeded on 10mg/mL fibronectin coated culture dishes in RPMI media containing 20% FBS and

1% penicillin/streptomycin solution at 37°C in 5% CO_2. Adhered cells were subject to limited dispase digestion for the first passage to remove fibroblasts and stained with a pan-cytokeratin antibody to confirm epithelial origin.

While both ovarian cancer cell lines and primary ovarian cancer cells were able to invade through Matrigel, the degree of invasiveness varied widely among individual cell types. We found that the most invasive and migratory cell line, HEY, was two orders of magnitude more invasive ($I_{HEY} = 0.85\%$, $I_{IGROV} = 0.006\%$) than the least migratory and invasive cell line, IGROV(Figure 4.7). Similarly, while primary cells were all obtained from patients with either stage III or stage IV disease, the most invasive primary cell line, OV207, was an order of magnitude more invasive than the least invasive primary cell line, OV445 (Figure 4.7; $I_{OV207}= 0.193\%$, $I_{OV445}= 0.006\%$).

4.6.2   Cell stiffness measurements of ovarian cancer cells.

The broad range of invasive potential among these cancer cell lines and primary cancer cells suggested that their invasiveness might reflect the biology of the tumors from which they were derived. To assess the changes in mechanical properties of the cancer cells that exhibited different invasive potential, we used the 3DFM system. We found that the most invasive cell line, HEY, was 10 times more deformable than IGROVs, which was our least invasive cell line (Figure 4.7). In addition, the most invasive primary ovarian cancer cells, OV207, which exhibited 30 fold greater invasion than OV445, was 10 times more deformable than OV445 cells (OV207-J_{max}= 3.1 Pa^{-1}; OV445-J_{max} = 0.3 Pa^{-1} (Figure 4.7). The cell stiffness was derived as explained in Chapter 2, using the Jeffrey's model. The stiffness for each cell line and primary cell type was then plotted against their invasiveness (Figure4.8). We found that the stiffness showed an inverse correlation with invasiveness (Pearsons correlation coefficient (p); p$_{celllines}$= -0.7, p$_{primaries}$=-0.9). The cell types within each box were not significantly
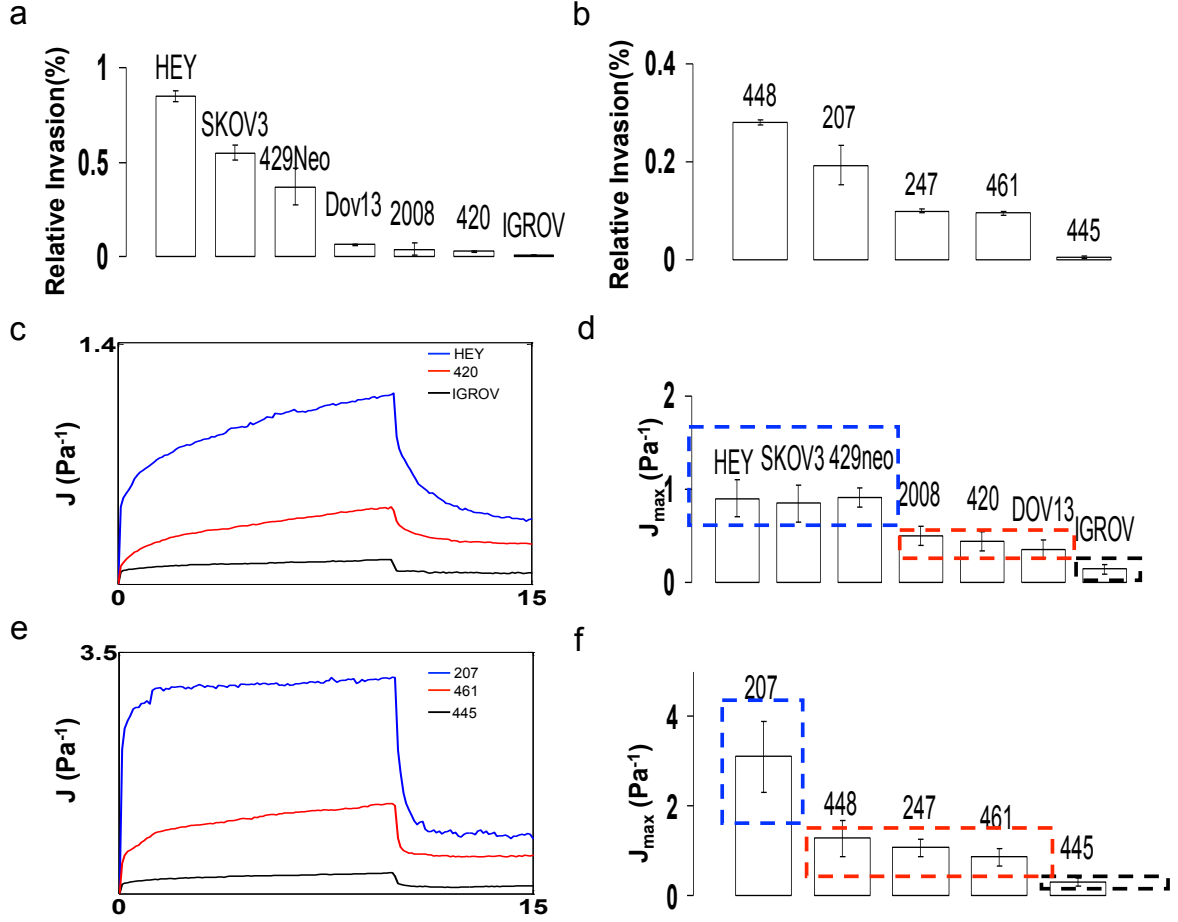
Figure 4.7: (a) Percent invasion relative to each for the series of cell line. Data represented as the mean±SE.(b) Invasion data for the primary cells. (c) Compliance curve for cell lines, IGROVs(least invasive), HEY(most invasive) and 420(medium invasiveness). (d) Maximum compliance for all the cell lines is presented. The three boxes encompassed by dashed line indicate the different scored regions based on relative invasion with cell lines within a box not being statistically significant from each other mechanically(p≥0.05). (Blue- high invasion, I≥0.4, Red- medium invasion, 0.2<I<0.4, Black- low invasion, I≤0.2). (e) Compliance curve for three primary cells, OV207(high invasiveness), OV445(low invasiveness) and OV461 (medium invasiveness). (f) Maximum compliance for primary cancer cells as described in (d). (Blue- high invasion, I≥0.15, Red- medium invasion, 0.1<I<0.15, Black- low invasion, I≤0.1). All mechanical measurements represent mean±sem.

different in their stiffness but fell within a region scored as high invasion ($I \geq 0.4$ for cell lines and $I \geq 0.15$ for primaries), medium invasion ($0.2 < I < 0.4$ for cell lines and $0.1 < I < 0.15$ for primaries) and low invasion ($I \leq 0.2$ for cell lines and $I \leq 0.1$ for primary cancer cells). Cell lines from different scored regions were significantly different from each other ($p \leq 0.05$) making this a very robust comparison. Consistent with results from Gimzewski and Guck(described above), stiffness for cell lines with the lowest invasiveness showed a log normal distribution whereas the highly invasive cell lines showed a normal distribution (Figure4.10). When each of the correlations were scaled by their corresponding stiffest cell type (or least invasive), each corresponded to a single parameter power law (Figure4.8). These data demonstrate that the stiffness of the cell scales inversely with their invasive potential and that aspects of the biology of the cancer cells could be captured by these biomechanical measurements.

4.6.3 Role of Acto-myosin remodeling

To investigate the role of structure and actomyosin contractility in stiffness dependent invasion, we examined the distribution of actin and phosphorylated myosin light chain (pMLC). Visualization of the actin network and pMLC (Figure 4.11) in the most stiff (least invasive) cancer cell line, IGROV, revealed strong cortical actin filament staining with few or no cell protrusions or lamellepodial structures. In contrast, the more invasive cell lines, including SKOV3 and HEY cells, exhibited distinct lamellipodial structures (Figure 4.11) and protrusive structures that are very elongated, with limited cortical actin staining. In addition pMLC was localized along the cell periphery in IGROVs (Figure 4.11), while SKOV3 and HEY cells had little to no peripheral pMLC (Figure 4.11). To investigate the role of stiffness in cancer cell invasion, we looked at the actomyosin machinery and its effect on this process. Since cells with differential invasiveness (IGROV vs. HEY) had distinct differences in pMLC localization and cy-
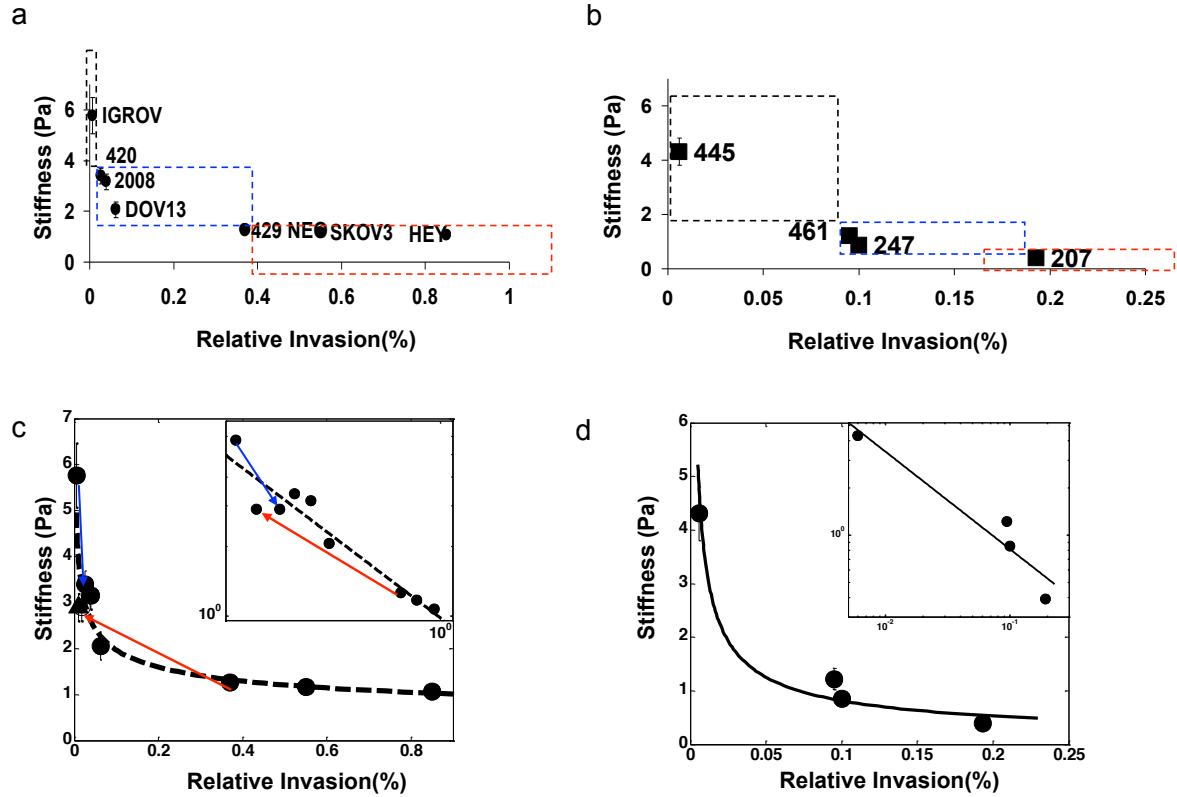
Figure 4.8: Stiffness calculated by fitting a Jeffrey's model to compliance curves for cell lines (a) and primary cancer cells (b) and mapped with the relative invasion from Figure 4.7. (c) Power law showing the correlation between the stiffness of cell lines and their invasion. IGROV when treated with blebbistatin (open circle, blue arrow) and OVCA429Neo with OVCA429TβRIII (triangle, red arrow) move on the line consistent with the correlation. (INSET) Power law on log log plot. (d) Power law correlation for the primary cell lines. (INSET) power law on a log log plot.
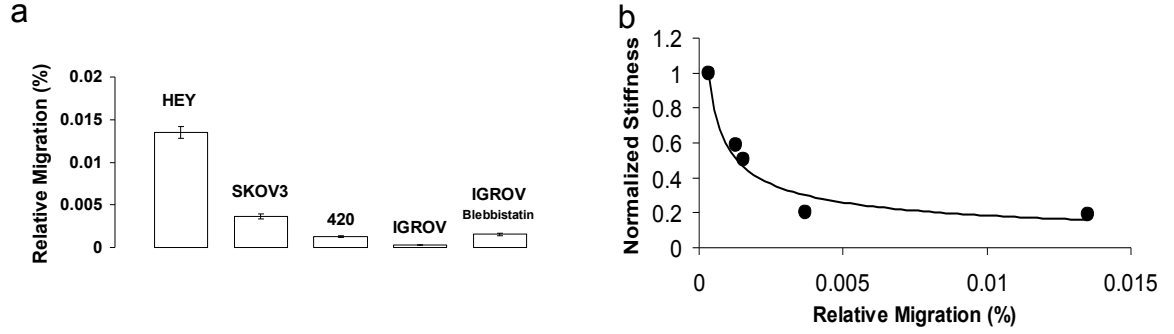
Figure 4.9: Transwell migration assay done as described in the text show migration results for 4 different cell lines and the effect of treating the stiffest or the least invasive/migratory cell line with IGROV with blebbistatin. (b) Plot showing proportional correlation between the stiffness of the cell lines and their relative migration.
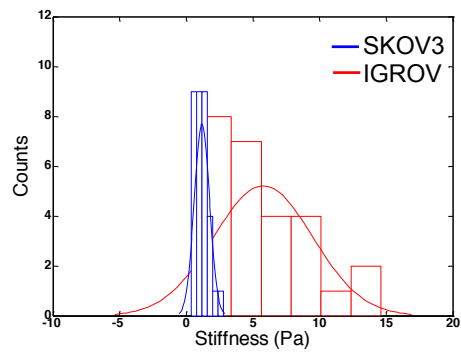
Figure 4.10: Distribution shows that IGROV's show a log normal distribution whereas SKOV3 shows a normal distribution.

toskeletal architecture, we used blebbistatin, a Myosin II inhibitor on the stiffest and least invasive cell line, IGROV, and examined how an artificially reduced cell stiffness affected invasion. While blebbistatin did not effect cell viability, it disrupted cortical pMLC localization (Figure 4.12), increased cell invasiveness 2.5 fold, and decreased cell stiffness by 2, suggesting that reducing cell stiffness is sufficient in itself to adopt the invasive phenotype.
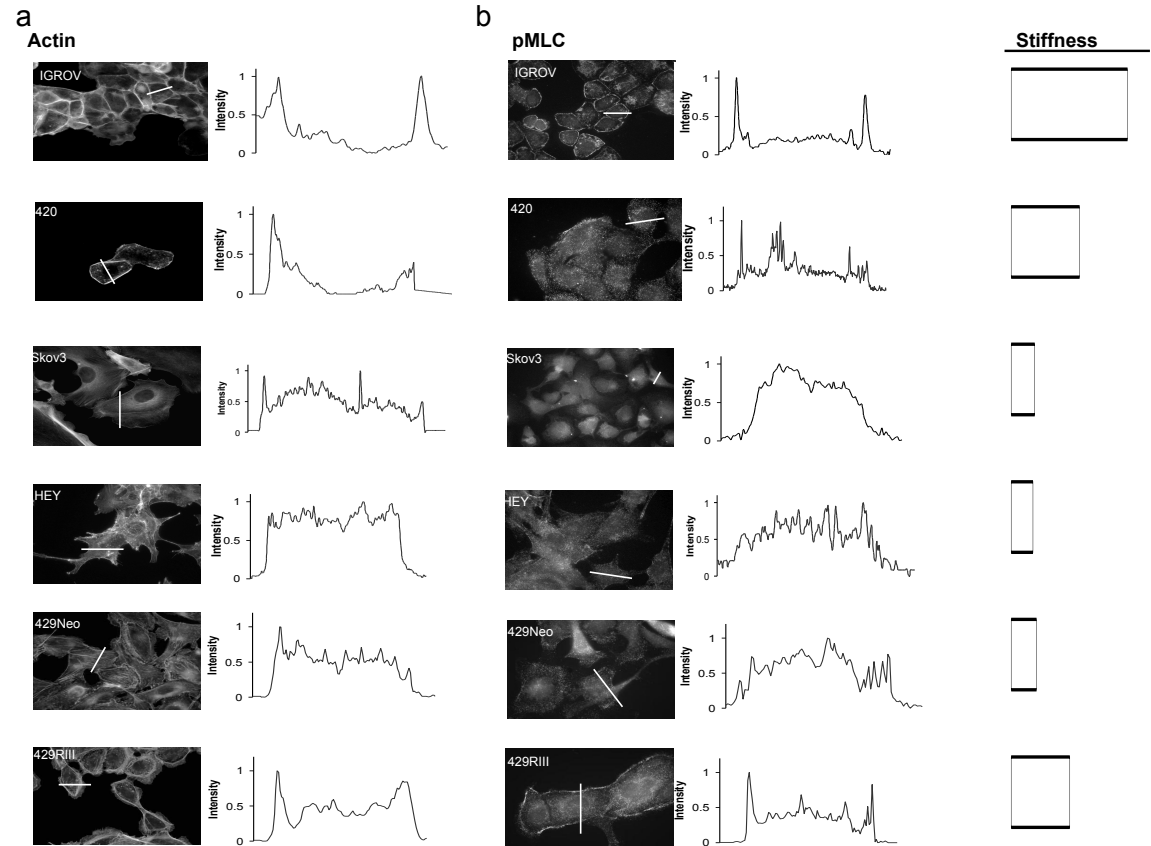
Figure 4.11: $1X10^5$ cells of the indicated cell lines were plated on coverslips and stained either for (a) actin or (b) phosphorylated myosin light chain (pMLC). Quantification of fluorescence intensity using Image J software across the line shown in the corresponding panels on the left are indicative of stress fiber density incase of actin or cortical pMLC localization. (c) Stiffness of the respective cell lines.

As mentioned earlier, the Blobe lab has previously demonstrated that TβRIII decreases ovarian and breast cancer cell motility and invasiveness via alterations in the
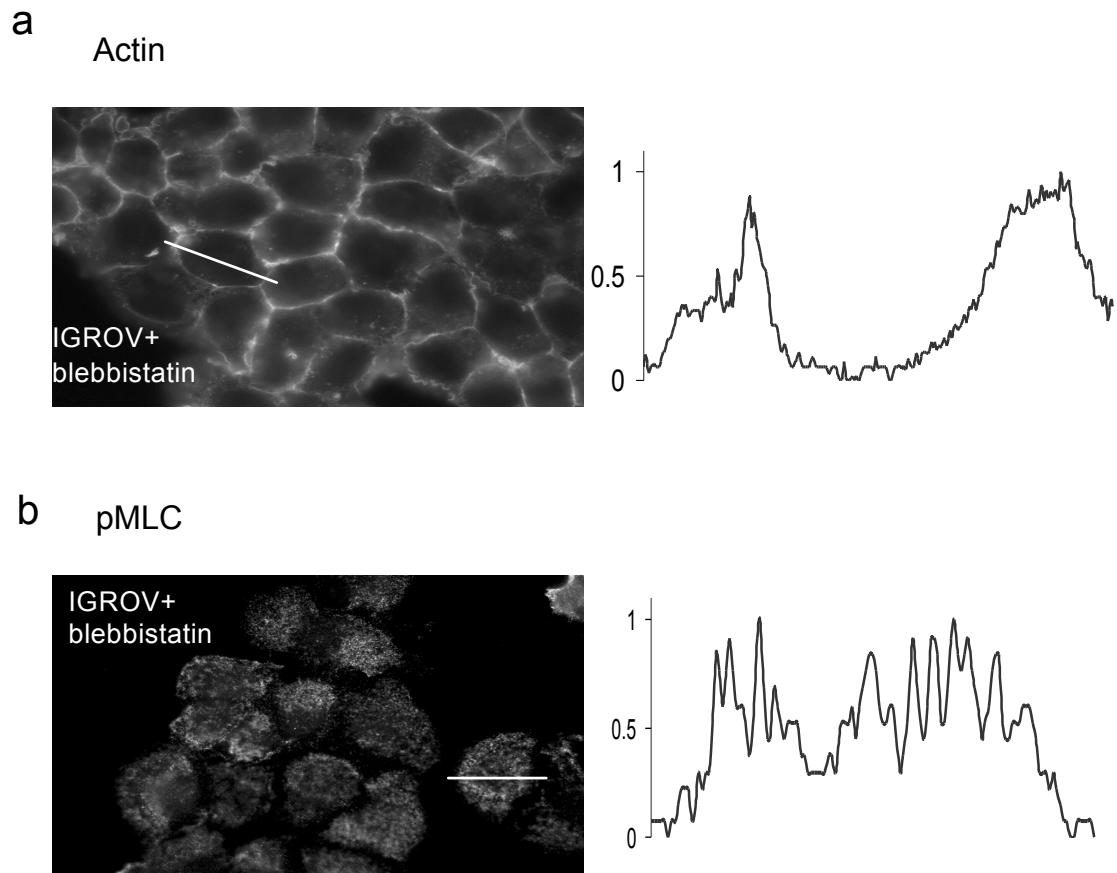
Figure 4.12: (a) Actin staining on the stiffest cell line IGROV treated with blebbistatin similar to Figure4.11 shows diffusive cortical actin due to treatment. (b) pMLC staining of he same cell line and treatment shows concomitant alteration in Myosin II.

actin cytoskeleton(**?**). To determine the role mechanical properties in the suppression of invasion, we examined the effect of TβRIII/betaglycan expression on cancer cell stiffness using Ovca429-Neo, with low levels of endogenous TβRIII expression, and contrasted their stiffness and invasiveness with the Ovca429-TβRIII, which is the Ovca429-Neo cell line that has had its TβRIII expression restored. We found that Ovca429-TβRIII cells had a stiffness of 2.9Pa, which corresponded to a two-fold increase in the stiffness of these cells over the Neo cell line (Figure 4.13). Further, this increase in the stiffness was consistent with the proportional decrease in invasiveness observed with the panel of ovarian cancer cell lines and plotted onto the power law in Figure 4.8. Moreover, treating Ovca429-TβRIII cells with blebbistatin increased their invasion by four fold (Figure 4.13), while decreasing their stiffness by two fold, similar to effects seen with the IGROVs. These data demonstrate that alteration in the cytoskeleton, using either pharmacological agents or biological alterations (TβRIII) that regulate the cytoskeleton, have a direct and inverse effect on cellular invasiveness and stiffness.

Intriguingly, while Ovca420 and IGROV cells exhibited high cortical actin staining (Figure 4.11), they exhibited a 1.7 fold difference in stiffness, which corresponded to a 4 fold difference in invasive potential (Figure 4.7 and Figure 4.8). This demonstrates that cell stiffness measurements performed as described may be a more discerning measurement of invasive potential than examining structure. More images of these cell lines will be shown in Chapter 6 examining actin and focal adhesion distributions.

4.7   Discussion

Here we report significant variation in the invasive potential of epithelial-derived cancer cells and show how that variation correlates with their mechanical properties. Our results are the first evidence that metastatic potential measured through cancer cell invasion shows an inverse proportional relationship with cell stiffness. As cancer cells
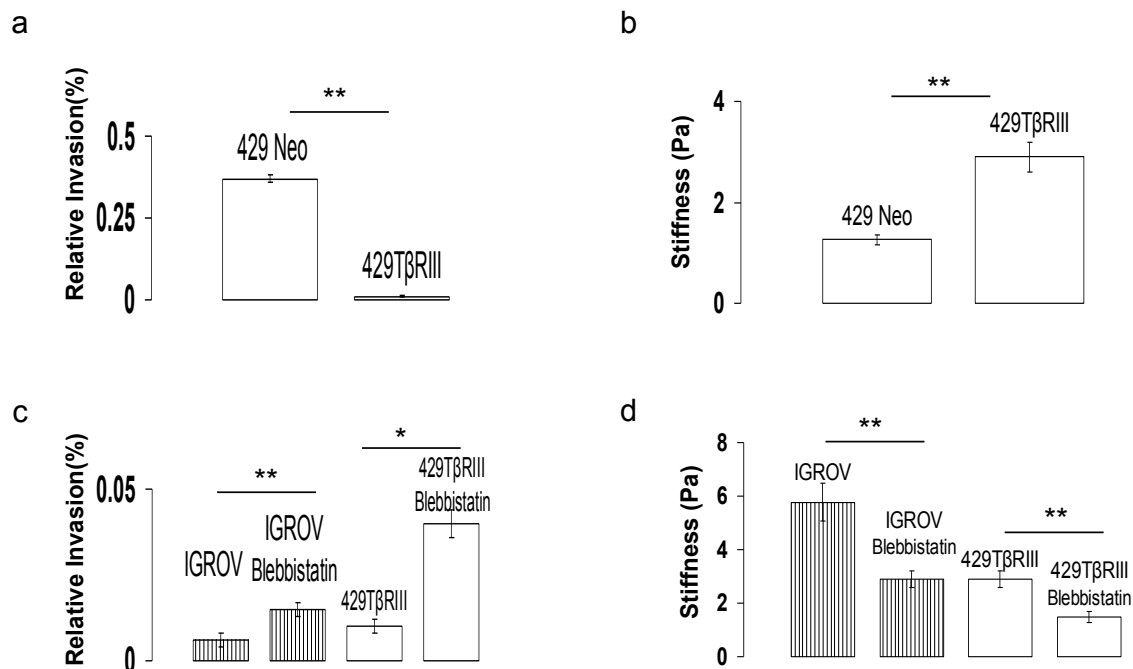
Figure 4.13: (a) Invasion assays of OVCA429-Neo and OVCA429-TβRIII was performed as described in the document. Data are a composite of two independent experiments performed in duplicate. Each column represents the mean±SEM. (b) Stiffness for the corresponding cell type and treatments in (a) obtained as described in the text. (c) Effect of blebbistatin treatment on the invasion potential of IGROV and OVCA429TβRIII cell types. (d) Stiffness for the corresponding cel type and treatments in (c). (**- p<0.01, *- p<0.05).

get progressively more invasive, they display more fluid like mechanical characteristics that result in cell deformation and shape changes suitable for a metastatic population. We also find that cell lines having similar cytomorphology and primary cells from patients with similar stage disease can have widely different invasive potential that correlates with difference in stiffness. Currently, cell based diagnoses in cancer rely on removing and slicing of sample tissue and histologic examination of the sample through antibody labeling of either a specific markers or protein. This complex process is not always reliable and lacks a quantified assessment of the disease state(Suresh, 2007b). Hence, sensitive biophysical measurements such as those demonstrated here, that can be performed in a short period of time, on samples obtained from either ascites or circulating tumor cells, can provide potentially unique information about the patients cancer including metastatic grading.

Insights into biomechanical changes during cancer progression has the potential to lead to novel therapy for treatments(Fritsch et al., 2010). In that respect, our results point to two potential targets. TGFβ signaling has been known to play a central role in tumor maintenance and progression(Gatza et al.,). As mentioned earlier, TβRIII, a co-receptor for TGFβ is lost or reduced in multiple human cancers, including breast, lung, prostate, pancreatic, renal and ovarian cancer and restoration of TβRIII suppresses cancer progression and/or metastasis. In the present study, we find that this mechanism of motility and invasion inhibition by restoration of the TβRIII expression is linked to its effect on the mechanical properties of the cytoskeleton, specifically an increase in cell stiffness.

We also find that cell stiffness and its proportional correlation with invasion are strongly coupled to myosin II mediated contractility. Recent studies have shown that myosin IIA-deficient cells display substantially increased cell migration and membrane ruffling(Even-Ram et al., 2007). Blebbistatin, an inhibitor of myosin II ATPase activity,

has also been shown to have effects similar to myosin IIA gene ablation i.e. increased migration and membrane ruffling(Even-Ram et al., 2007). Consistent with these results, we find that treatment of ovarian cancer cells with blebbistatin increases cell invasion through matrigel and migration through a transwell. At the same time, we are able to measure a markedly reduced cell stiffness, and show that this reduction fits on the same curve as that of native invasiveness vs stiffness. Consistent with this relationship, blebbistatin overcomes the effect of restoring TβRIII by both enhancing invasion and increasing stiffness. Again, the effect of blebbistatin on TβRIII cells merely shifts where the cells end up on the invasiveness-stiffness curve(Figure 4.8).

The fact that the relationship between invasiveness and stiffness is maintained under all of the conditions we tested suggests that stiffness may be an excellent predictor of invasive potential, and that treatments that affect cellular stiffness, independent of mechanism, may be useful anti-metastatic approaches. In other words, whether by approaches that target gene expression, myosin II activity, actin polymerization, Rho GTPases, or many other possible targets, if the final effect of any such treatment changes cell stiffness, then it might be a good candidate to also change invasiveness in the opposite direction. It is this mechanism that I will discuss in Chapter 6.

The residual differences between weakly invasive cells following myosin blockade and highly invasive cells could be the contribution of other mechanisms that regulate invasion, including MMP production which I have not discussed here. While mechanisms underlying cell motility have been extensively studied, the different links between the cytoskeleton and its mechanical properties are current active areas of investigation and remain to be elucidated. The association of malignant transformation and invasiveness with the cytoskeleton and a cells mechanical properties may lead to novel treatments in cancer therapy.

Chapter 5

Integrin mediated force signaling

5.1 Introduction

Communication between species has had an explicit role in evolution, which may explain the long delay between unicellular organism and multicellular organisms(2.5 billion years). This delay has been attributed to cells having the same genome lacking the ability to communicate and organize their function and behavior. Cell communication and signaling, thus, is a fundamental machinery that a cell has to have and regulate for most normal functions.

Cell communication is a complex cascade of events that usually is mediated by extracellular signal molecules. Cells communicate by means of hundreds of kinds of signal molecules which could be proteins, small peptides, amino acids, nucleotides, steroids etc. and the communication is both, short range(to neighboring cells) and long range. The simplest signaling pathway is shown in Figure 5.1. Most cells can emit and receive signals, all depending on the receptor proteins, which binds to the signal molecules. The binding activates the receptor, which in turn activates one or more intracellular signaling pathways. These pathways process the signal and distribute it to the appropriate targets which are called effector or effector proteins. Depending on the nature and state of the receiving cell and the signal, these effectors can be gene regulatory proteins, ion

channels, or parts of the cytoskeleton. The complexity in this function arises from the fact that a typical cell is exposed to hundreds of different signaling molecules in its environment and the cell responds to this mix of signals very selectively according to its character. A cell may respond to one combination of signals by dying and to another combination by dividing or migrating. Infact, because different types of cells require different combination of survival signals, each cell type is restricted to a specific set of environments in the body. Further adding to the complexity is the fact that different types of cells usually respond differently to the same extracellular signal molecules. For example, the neurotransmitter acetylcholine decreases the rate and force of contraction in heart muscle cells but stimulates skeletal muscle cells to contract. These differences are not just because of differences in binding receptors as is the case in the above example. Again, acetylcholine binds to the same surface receptors in heart muscle cells and salivary gland cells, but produces a different effect due to differences in the intracellular pathways in these two cell types.

As introduced in Chapter 1, mechanotransduction is a subset of cell signaling where the extracellular signaling molecules are not chemical but mechanical in nature. These external signals can be transmitted from the ECM or from the neighboring cells to the internal of the cell via adhesion receptors. The primary receptors that bind and interact with different components of the ECM belong to the integrin family. The members of this large family of homologous transmembrane adhesion molecules have a remarkable ability to transmit signals in both directions across the cell membrane. The binding of a matrix component to an integrin can send a message into the interior of the cell, and conditions in the cell interior can send a signal outward to control binding of the integrin to the matrix. Inside the cell, integrins associate with actin filaments through a variety of cytoskeleton linker proteins. Each component of the linkage from the cytoskeleton

114
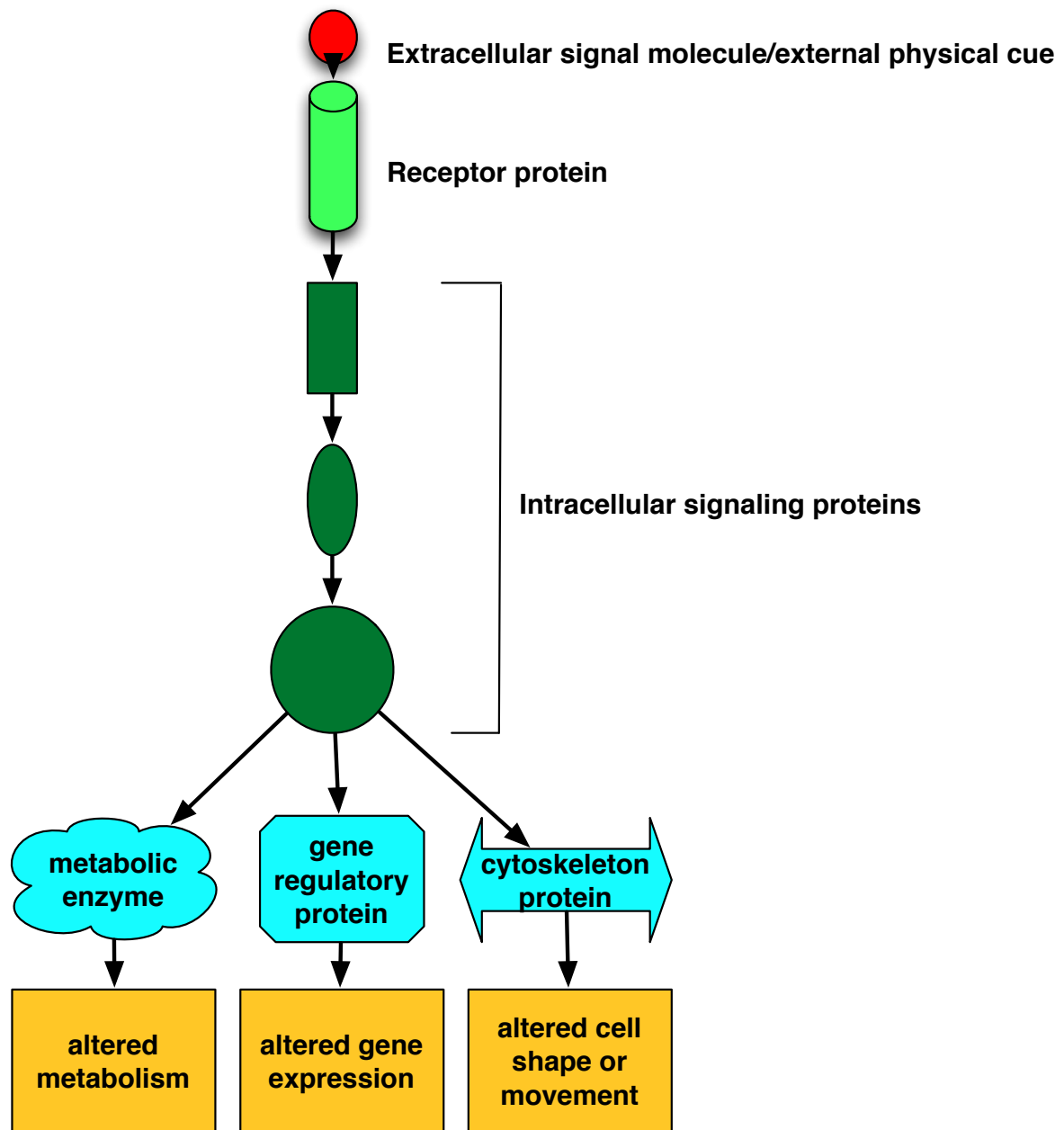
Figure 5.1: The signal molecule usually binds to a receptor protein that is embedded in the plasma membrane of the target cell and activates one or more intracellular signaling pathway. The pathways ultimately alter the activity of effector proteins.

through the integrin mediated adhesion to the ECM therefore transmits forces that may be generated internally through actomyosin contractility(described in Chapter 4 and forces form outside the cell.

5.2 Focal adhesions and integrin signaling

As mentioned above, formation of adhesions by integrins involves binding to ECM proteins and linkage to the actin cytoskeleton; both of which are cooperative in nature(Burridge and Chrzanowska-Wodnicka, 1996). Focal adhesions large elongated structures, typically 2μm wide and 3-10μm long. Cells also contain focal complexes that have similar composition but are smaller and circular. Focal adhesions which are usually distributed on the lower surface of the cell, depend on activation of the small GTPases Rho where as focal complexes which are under actively protruding cell edges require activation of CDC42 or Rac instead of Rho(Schwartz, 2010). Focal complexes mature to focal adhesions on association with large actin structures. Until recently, the exact molecular architecture of focal adhesion was unknown.

5.2.1 Architecture of focal adhesions.

In 2010, using three dimensional super-resolution fluorescence microscopy, Kanchanawong et al. were able to map nanoscale protein organization in focal adhesions(Davidson et al., 2010). The microscopy technique used by them is called interferometric photoactivated localization microscopy (iPALM). iPALM combines photoactivated localization microscopy with simultaneous multi-phase interferometry of photons from each fluorescent molecule. By constructing imaging probes with photoactivable fluorescent proteins fused to focal adhesion proteins, they were able to achieve 20nm

localization accuracy in lateral dimensions and 10-15nm in the vertical axis.

They found that focal adhesions possess a well organized molecular architecture in which integrins and actin are separated by a 40nm core region that contains multiple partially overlapping protein specific strata. The organization indicates a composite multilaminar architecture made up of atleast three spatial and functional compartments that mediate interdependent functions of focal adhesions: an integrin signaling layer, a force transduction layer and an actin regulatory layer (Figure5.2). Focal adhesion kinase(FAK) and paxillin represent a membrane proximal integrin signaling layer that probably relays integrin-ECM engagement into signaling cascades that control adhesion dynamics. Talin and vinculin are observed in the broader central zone , with talin organized into arrays of diagonally oriented tethers that probably link integrin to actin directly. α-Actinin appears to localize predominantly along the actin stress fibers where it may mediate their formation through actin filament cross-linking activity. Interestingly, the authors also hypothesized that the diagonal talin orientation could arise from actomyosin pulling of the talin tails relative to the integrin bound head which may reveal distinct sites along the length of talin for further protein interactions.

5.3   Cellular response to force

The primary response of cells and focal adhesions to force is strengthening or reinforcement, in which the adhesions enlarge or recruit new cytoskeletal proteins that help resist the applied force. Both, focal adhesions and focal complexes require association with the actomyosin contractility to form (Burridge and Chrzanowska-Wodnicka, 1996). Responses to forces clearly occur at multiple level and effect each component of the physical linkage described in the above section.

Cells respond to force on integrin-mediated adhesions by remodeling the ECM by regulating proteins such as fibronectin. Current models propose that fibronectin initially
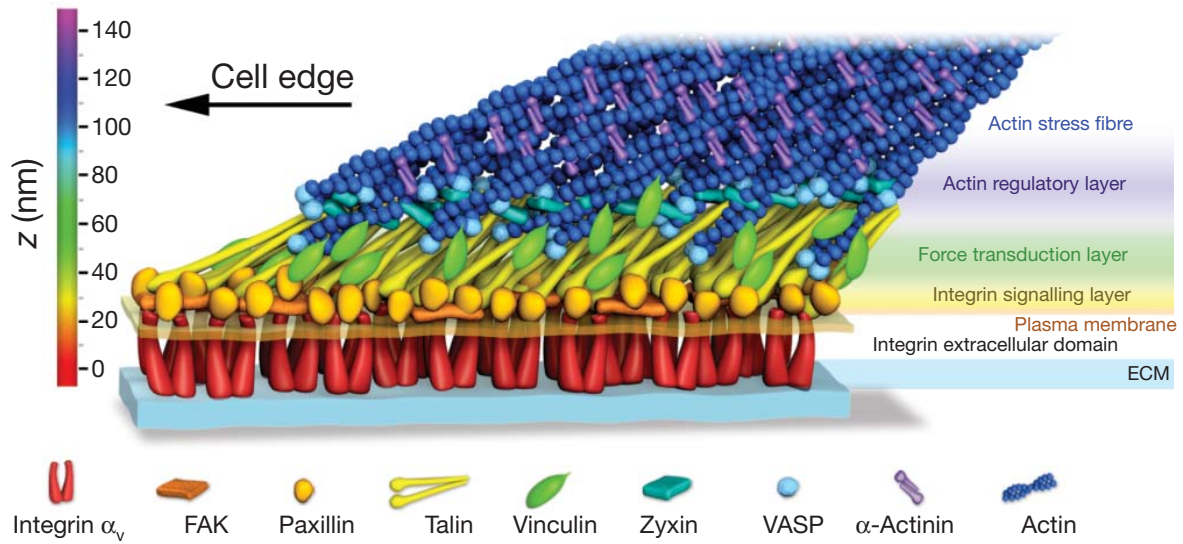
Figure 5.2: From(Davidson et al., 2010). Schematic model of focal adhesion molecular architecture, depicting experimentally determined protein positions.(Figure reprinted with permission)

binds through an integrin, then is subject to tension from actomyosin. Puling on fibronectin opens folded domains to reveal cryptic binding sites that promote its assembly into fibrils(Zhong et al., 1998). There is also evidence that integrins themselves may be mechanosensors. Integrins undergo complex conformational rearrangements that govern both affinity for ECM proteins and association with cytoskeleton proteins. Experiments with optical tweezers showed that adhesions begin to recruit vinculin and increase their strength within seconds of applying force(Galbraith et al., 2002). Seeing the architecture of the focal adhesions, it seems that the interaction of vinculin with talin tail domain regulates this force mediated recruitment. The development of a fluorescence based tension sensor for vinculin showed that adhesion strengthening was associated with high force across this molecule, which was followed by recruitment of additional vinculin and enlargement of the adhesion, resulting in decreased force per vinculin(Grashoff et al., 2010). On longer time scales, it has been shown that entire adhesions in adherent cells lengthen under applied force, indicating the recruitment of

not only vinculin but integrins and other proteins(Riveline et al., 2001).

So overall, applying forces on focal adhesions and integrins may result in confomrational changes in integrin and/or talin, recruitment of proteins such as vinculin and other integrins(clustering) all leading to changes in engagement to the actomyosin machinery and other actin functions like polymerization.

5.3.1 Signaling pathways and force

Force transmission through integrin regulates a wide range of signaling pathways, downstream genes and differentiation programs. Stretching cells triggers activation of signaling pathways that include MAP kinases, Rho GTPases, elevated cytoplasmic calcium, and generation of reactive oxygen(Li et al., 2005). Some of the signaling events are mediated by mechanisms associated with adhesion strengthening. In smooth muscle cells and fibroblasts, stretch triggers integrin conversion to the high affinity state, which leads to increased ECM binding (Katsumi et al., 2002) which activates a variety of signaling pathways. For example, p130Cas, an important focal adhesion adapter protein becomes a better substrate for Src family kinases after stretching cells on elastic substrata or after stretching Cas in vitro(Sawada and Sheetz, 2002). Once phosphorylated on tyrosine residue, Cas recruits SH2 domain adapter protein Crk, which recruits GTPases exchange factors (GEFs).

The master regulators of essentially every aspect of actin cytoskeleton function are the small Rho family GTPases, principally Rho and Rac.

5.4   Rho GTPases

For the actin cytoskeleton, diverse cell-surface receptors trigger global structural re-arrangements in response to external signals. But all of these signals seem to converge inside a cell on a group of closely related monomeric GTPases that are members of the Rho protein family- Cdc42, Rac, and Rho. Rho GTPases constitute a distinct amily within the superfamily of Ras-related small GTPases and are found in all eukaryotic cells. Twenty-two mammalian genes encoding Rho GTPases have been described- three Rho isoforms A, B and C; three Rac isoforms 1, 2, and 3; Cdc42, RhoD, Rnd1, Rnd2, RhoE/Rnd3. RhoG, TC10, and TCL; RhoH/TTF; Chp and Wrch-1; Rif; RhoBTB1, and 2 and Miro-1 and 2(Jaffe and Hall, 2005). Like al other GTPases, they act as molecular switches cycling between an active GTP bound state and an inactive GDP bound state. Thsi activity is controlled by (a) guanine nucleotide exchange factor (GEFs) that catalyze erxchange of GDP for GTP to activate the switch; (b) GTPases activating proteins (GAPs) that stimulate the intrinsic GTPases activity to inactivate the switch; (c) guanine nucleotide dissociation inhibitors (GDIs), whose role appears to be spontaneous activation(Olofsson, 1999). GEFs and GAPs will be discussed later in detail. It is in the active GTP bound state that Rho GTPases perform their regulatory function through a conformation specific interation with target(effector) proteins. Over 50 effectors have been identified so far for Rho, Rac and Cdc42 that include serine/threonine kinases, tyrosine kinases, lipid kinases, lipases, oxidases, and scaffold proteins. Some key targets of activated Cdc42 are members of the WASp protein family. Although WASp itself is expressed only in blood cells and immune system cells, other family members are expressed ubiquitously that enable activated Cdc42 to enhance actin polymerization. Association with Cdc42-GTP stabilizes the open form of WASp, enabling it to bind to ARP(actin related protein) complex and strongly enhancing this complex's actin nucleation activity. Rac-GTP also activates WASp family members,

as well as activates the crosslinking activity of the gel forming protein, filamin, and inhibiting the contractile activity of the motor protein myosin II, stabilizing the lamellipodia and inhibiting the formation of contractile stress fibers.

Rho-GTP has a very different set of targets. Instead of activating the ARP complex to build actin networks, Rho-GTP turns on formin proteins to construct parallel actin networks. mDia1 is a direct target of Rho. GTP and binding of GTPase relieves an auto-inhibitory interaction, exposing an FH2 domain that then binds to the barbed end of an actin filament (Zigmond, 2004). mDia1 also contains an essential FH1 domain, which interacts with a profilin/actin complex that delivers it to the filament end. In addition to elongation, the discrete changes to the actin cytoskeleton induced by Rho, Rac, or Cdc42 require the correct spatial organization of filaments. The best characterized of these is Rho-induced assembly of contractile actin:myosin filaments, which is mediated by Rho kinase (ROCK)(Also introduced in Chapter 4). ROCK is a serine/threonine kinase which has many substrates. The key event appears to be phosphorylation-induced inactivation of myosin light chain(MLC) phosphatase(Riento Ridley 2003). This in turn leads to increased phosphorylation of MLC, which promotes actin filament cross-linking activity of myosin II.
The RhoGTPases play crucial roles in a variety of cell functions including cell cycle, mitosis, cytokinesis and cell morphology. Most pertinent to this document is its role in cell migration. I introduced the role of the cytoskeleton in migration in Chapter 4 from a structural perspective; however most structures and migration modes are a result of complex signaling pathways including the RhoGTPases.

Cell migration is conceptually, a 3 step cyclic process, with the three steps being a) Cell polarization, b) Cell protrusion and polarization, and c) Cell rear retraction.
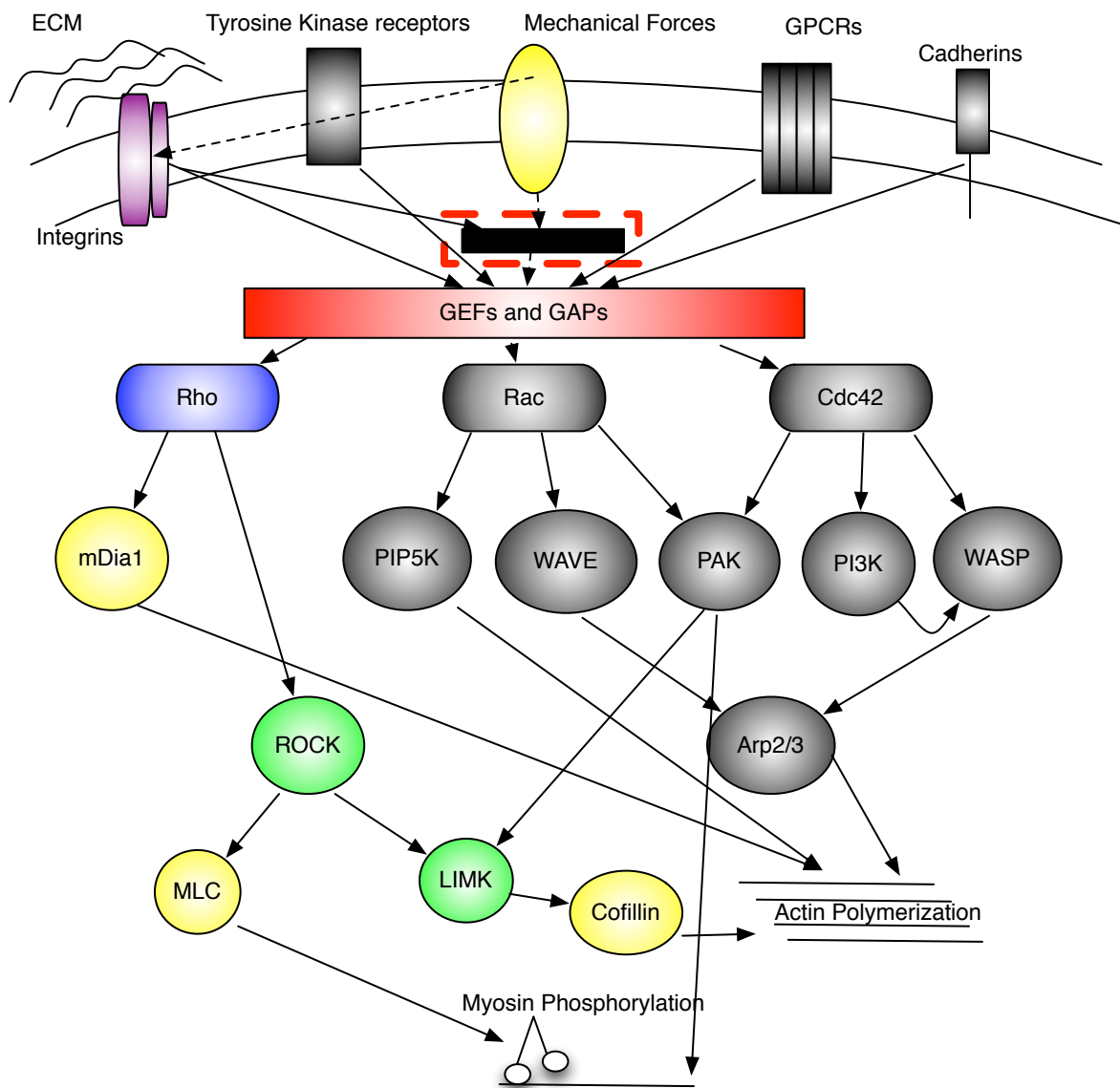
Figure 5.3: A scaled down version of the Rho signaling pathway. Effectors known to affect actin are shown here. The black box shown here represents the unknown regulation of Rho via external forces. The black box along with the RhoA GEFs are the subject of the experiments described in this chapter.

The organization of filaments in protrusions depends on the type of protrusion. In lamellipodia, actin filaments form a branching "dendritic" network wheras in filoppodia, they are organized in long parallel filaments. In lamellipodia, actin polymerization is mediated by Arp2/3 which is locally activated by the WASP/WAVE family members. As mentioned above, WASP/WAVE family of Arp2/3 complex activators are majr targets of Rac and Cdc42. Thus these Rho GTPases are the central regulators of cell protrusions during migration. Rac activates WAVE proteins(Ridley and Cory, 2002) and Cdc42 binds to WASP proteins which subsequently activates Arp2/3 to induce dendritic actin polymerization. WAVE/WASP prteins may themselves regulate the activity of Rac and Cdc42 by binding to GEFs (Alto et al., 2002)(Hussain et al., 2001), and could thereby generate positive or negative feedback loops to regulate the extent of Cdc42/Rac induced actin polymerization.Cell polarization means that the molecular processes at the front and back of the cell are different and a cell establishes and maintains this polarity in response to extracellular stimuli. Amongst the RhoGTPases, Cdc42 is the master regulator of polarization as it is active towards the front of migrating cells(Itoh et al., 2002) and both inhibition and global activation of Cdc42 disrupts the directionality of migration(Etienne-Manneville and Hall, 2002). The phosphoinositides PtdIns(3,4,5)P$_3$(PIP$_3$) and PtdIns(3,4)P$_2$(PI(3,4)P$_2$) are also key signaling molecules that become rapidly and highly polarized in cells that are exposed to a gradient of chemottractant. Rac can stimulate the recruitment and/or activation of PI3K products at the plasma membrane(Coadwell et al., 2003). Integrin engagement also leads to Rac activation and membrane targeting(Pozo et al., 2000). One model for how migrating cells maintain polarity is based on the fact that Rho and Rac are mutually antagonistic, each suppressing the other's activity. Once a protrusion has been formed, the cell stabilizes these protrusions via the focal adhesions, majority of them through the integrin family of receptors. As integrins cluster due to ligand binding,

they initiate intracellular signals such as protein tyrosine phosphorylation, activation of RhoGTPases and changes in phopholipid biosynthesis. The adhesions formation depends on Rac and Cdc42, and then these adhesions stabilize the lamellipodium. Migrating cells need to detach and exert traction at the same time and these tractional forces derive from the interaction of myosin II activity with actin filaments that attach to these adhesion sites. Myosin II activity is regulated by myosin light chain (MLC) phosphorylation, which is either directly postively regulated by MLC kinase (MLCK) or Rho kinase(ROCK). MLCK is regulated by intracellular calcium concentration as well as by phosphorylation by a number of kinases, ROCK is regulated by binding Rho-GTP(Riento and Ridley, 2003).

The role played by the three primary RhoGTPases, Rho, Rac and Cdc42 is complex and interdependent on each other. It has been shown that Cdc42 can activate Rac1(Nobes and Hall, 1995) and Rac1 and RhoA are mutually antagonistic(Rottner et al., 1999)(Arthur and Burridge, 2001). The development of biosensors for RhoA, Rac1 and Cdc42 have helped shed light on their spatiotemporal coordination during protrusion and migration process. During one protrusion retraction cycle, RhoA activation increases and decreases in synchrony with protrusion and retraction. This activation is confined to a band of 2μm from the leading edge. Cdc42 and Rac1 on the other hand reach their peak activation with a 40s delay relative to protrusion, and their activation is limited to 1.8μm from the leading edge. The authors of this study suggested that in addition to its role in contractility, RhoA acts as an initiator of actin polymerization at the onset maybe via mDia. The same pathway may also affect Rac activation due to microtubule stabilization by RhoA-mDia and integrin clustering.

5.4.1 RhoGEFs

Besides adhesion receptors, Rho proteins are activated other cell surface receptors including the cytokine and the tyrosine kinase receptors as well as G protein coupled receptors(GPCRs)(Hall, 1999). As mentioned above, cycling between the GDP and GTP bound state is primarily controlled by guanine nucleotide exchange factrs(GEFs) and GTPase activating proteins(GAPs). The first mammalian Rho GEF was identified as a transforming gene from diffuse B-cell lymphoma cells, and was designated Dbl(Eva et al., 1988). RhoGEFs contain a DH-PH tandem domain or an unrelated domain recently identified in DOCK proteins and these multidomain proteins have domains which are protein or lipid interaction domain, indicating that they serve as localization signals and/or as scaffolds for the formation of protein complexes. GEFs accelerate the exchange reaction from GDP to GTP, from hours to less than a minute. The general mechanism of this catalytic activity is that GEFs modify the nucleotide binding site such that the nucleotide affinity is decreases and thus the nucleotide is released and subsequently replaced. The actual mechanism is quite complex and requires interaction of the GEF with 2 loops in the Rho or G protein, switch 1 and switch2. The common action is to deform the phosphate binding site resulting in reduced affinity. Almost all GEFs are regulated in a highly complex fashion. This regulation includes protein-protein or protein lipid interaction, binding of second messengers and posttranslational modification. These interactions and modifications induce either a translocation of the GEF to a specific compartment of the cell where the Rho protein is located, the release from autoinhibition by a flanking domain or region or the induction of allosteric changes in the catalytic domain(Bos et al., 2007).

In the field of cell mechanics and mechanotransduction, understanding the function and regulation of RhoGTPases is clearly very important because of their roles in integrin

signaling and other processes described above. While all three, Rho, Rac and Cdc42 are equally important and closely tied together, RhoA has been the primary focus of researchers in the field for the past decade. The most obvious reason for this is because of its direct role in regulating actomyosin contractility and actin polymerization through its two effectors, ROCK and mDia. Application of force on beads coated with an integrin ligand such as fibronectin triggers cytoskeletal rearrangements and growth of the associated adhesion complex, resulting in increased cellular stiffness(Matthews et al., 2006), also known as reinforcement(Choquet et al., 1997). RhoA has been implicated in reinforcement, but whether force applied to cells affects RhoA activity has been controversial(Rioja et al., 2009)(Katsumi et al., 2002)(Yamane et al., 2007). The aim of the study discussed in this chapter was to find out the regulation and function of RhoA in force dependent integrin signaling pathway. The project was in collaboration with the Burridge Lab and was lead by Dr. Christophe Guilluy.

5.5 Results

5.5.1 Force activates RhoA for FA reinforcement

To study how cells change their mechanical properties in response to force, we used the 3DFM to apply controlled force pulses on magnetic beads coated with fibronectin(FN). The stiffness at each was quantified as described in Chapter 2 using the Jeffrey's model. Stimulation with successive pulses of constant force triggered a local change in cellular stiffness resulting in decreased bead displacement (Figure 5.4a). We report here relative cellular stiffness by normalizing this spring constant to that observed during the first pulse.. The change in cellular stiffness was already significant between the first and the second pulse(Figure 5.4b) demonstrating that cellular adaptation to force on integrins is a rapid phenomenon as previous studies have re-

ported(Matthews et al., 2006)(Choquet et al., 1997). To explore the role of RhoA during cellular stiffening in response to force, we depleted RhoA expression by using short interfering RNA (siRNA). On depletion of RhoA expression the cells displayed decreased basal stiffness(stiffness at pulse 1,Figure 5.4c). Interestingly, the change in cellular stiffness after application of pulses of force was no longer detected in the RhoA knockdown cells (Figure 5.4d). Similar results were obtained when we treated the cells with the RhoA inhibitor C3 transferase (Figure 5.4a and Figure 5.5), indicating that RhoA activity is necessary for the cellular adaptation to force.

There are conflicting reports in the literature about the effect of force on RhoA where RhoA activity has been reported to both increase(Rioja et al., 2009) or remain unchanged(Katsumi et al., 2002)(Yamane et al., 2007) in response to force. To analyze the effect of force on RhoA activity we applied a constant force for different amounts of time on FN-coated beads by using a permanent magnet. We observed that tensional forces increased RhoA activity (Figure 5.4f-g). When cells were incubated with beads coated with RGD peptides and then subjected to tensile force, similar activation of RhoA was observed (Figure 5.5). No change in RhoA activity was induced by pulling on beads coated with non-activating anti-β1 integrin antibody (P4C10) (Figure 5.5d), indicating that integrin engagement is necessary for RhoA activation in response to force. These results are consistent with previous studies that have shown that reinforcement requires integrin ligand interaction(Matthews et al., 2006)(Choquet et al., 1997).

5.5.2 Role of RhoA-GEFs LARG and GEF-H1

Considering that application of force on integrin-based adhesions activated RhoA, we next investigated the GEFs specific for RhoA may be recruited to the AC. To test this hypothesis, we isolated ACs by separating the FN-coated beads from the
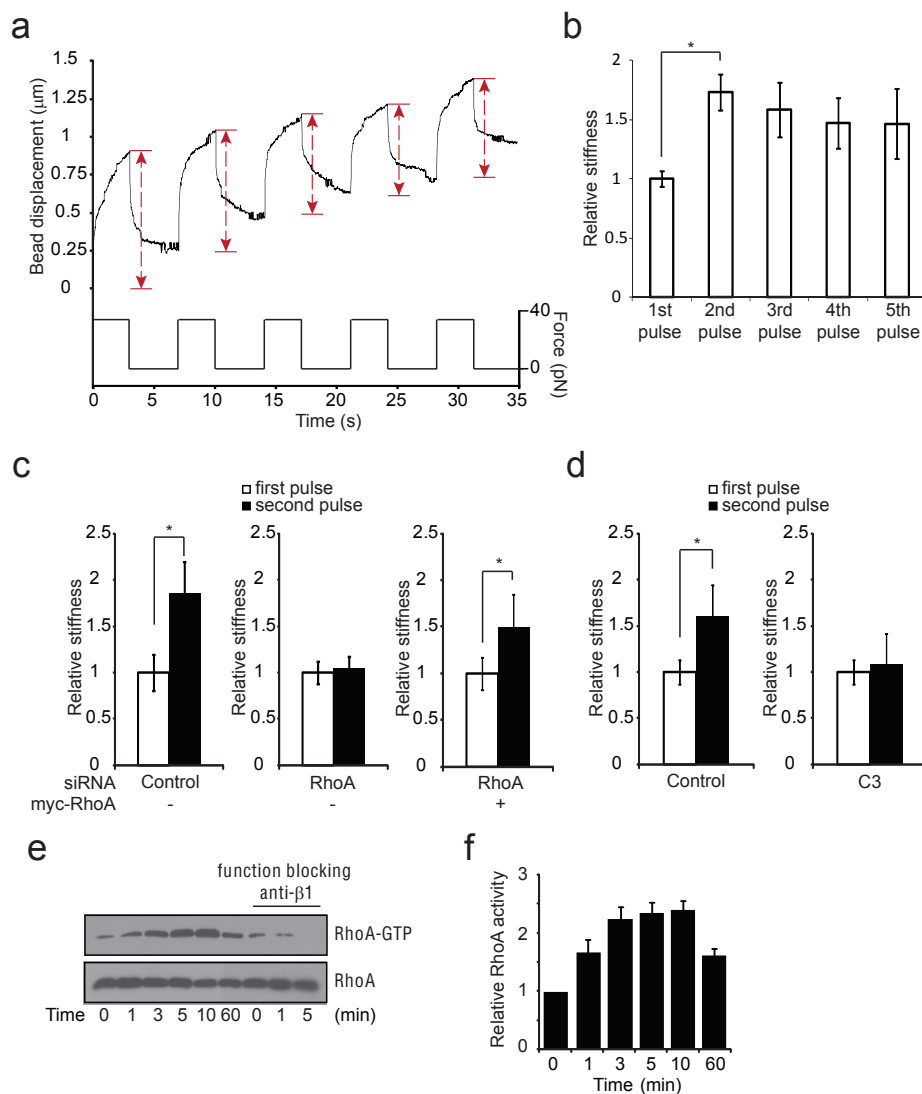
Figure 5.4: (a) Typical displacement of a FN-coated bead bound to a Ref52 fibroblast during force pulse application. (b) relative change in stiffness during application of 5 force pulses on FN-coated bead. (n=15; p<0.01).(c) change in stiffness during 2 force pulses application transfected 48 h with control siRNA or RhoA siRNA or RhoA siRNA and siRNA resistant mutant of RhoA(myc-RhoA) (n= 20; p<0.01). (d)change in stiffness during 2 force pulses application on untreated(left panel) or cells treated for 90 min with cell-permeable C3 toxin (right panel) (n=15 , p<0.01). (e,f) Ref 52 cells were incubated with the function blocking anti-β1antibody (P4C10) for 30 min and then with FN-coated beads. Active RhoA (RhoA-GTP) was isolated with GST-RBD and analyzed by western blot (e). Corresponding densitometric analysis of RhoA-GTP normalized to RhoA levels and expressed as relative to the control in the absence of stimulation by force (n=5) (f).
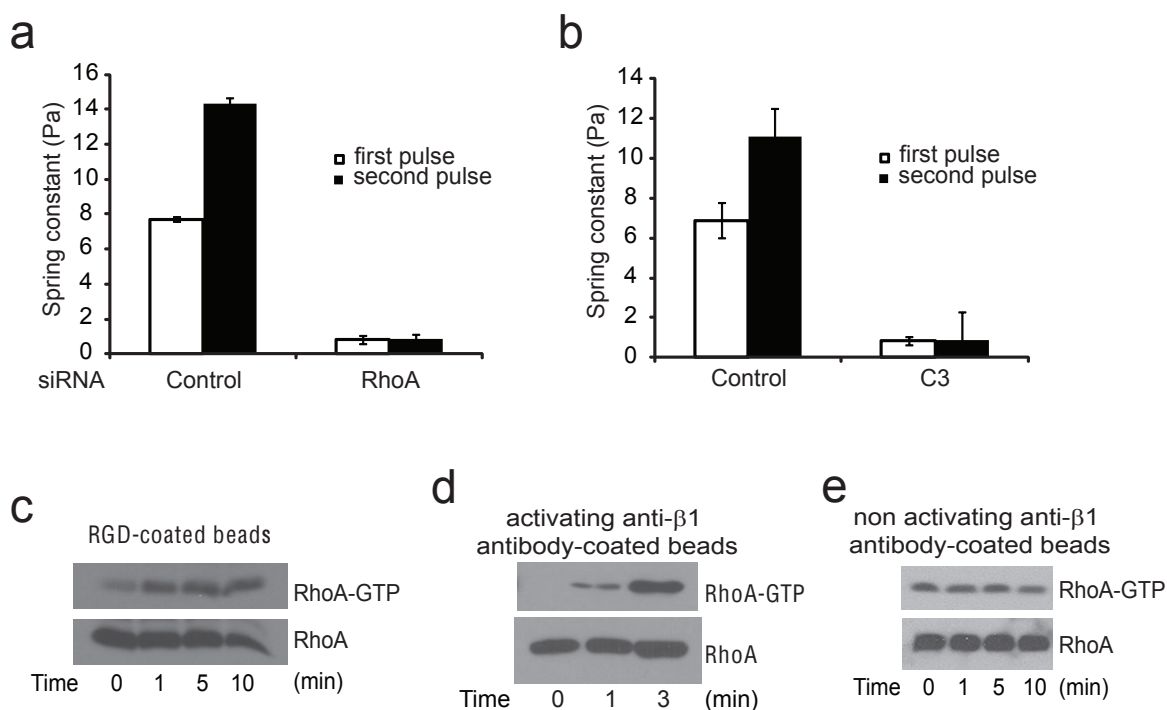
Figure 5.5: (a) Spring constant calculated for the first(white) and second (black) pulse of force applied on FN coated bead bound to Ref52 cells transfected 48h with control siRNA or RhoA siRNA(n=20). (b) Spring constant calculated for the first and second pulse of force applied to bead bound to untreated Ref52 cells(left panel) or Ref52 cells treated for 90 min with cell permeable C3 toxin $(2\mu g/ml)$(n=15). (c) Ref52 cells were incubated with RGD coated beads and stimulated with tensional forces for different amounts of time. Active RhoA(RhoAGTP) was isolated with GST RBD and analyzed by western blot. (d) MRC5 cells were incubated with beads coated with activating anti-β1 integrin antibody and stimulated with tensional forces for different amount of time. Active RhoA(RhoGTP) was isolated with GST-RBD and analyzed by western blot. (e) Ref52 cells were incubated with non-activating anti-β1 integrin antibody and stimulated with tensional forces for different amount of time. Active RhoA(RhoA-GTP) was isolated with GST-RBD and analyzed by western blot.

lysates of cells stimulated with constant force for different amounts of time. To test the quality of the adhesion complex isolation, we probed for known focal adhesion proteins in both fractions. As expected we found vinculin and Focal Adhesion Kinase (FAK) but not tubulin in the fraction(Figure 5.7). Similar to previous studies(Sawada and Sheetz, 2002)(Rericha et al., 2010), we found that force induced recruitment of vinculin to the adhesion complex (Figure 5.7a). When we looked for the presence of RhoA GEFs, we found that p115, Gef-H1 and LARG were present in the adhesion complex (Figure 5.6b). Interestingly, application of force induced the recruitment of LARG and GEF-H1 to the AC, whereas p115 localization at the adhesion complex was unaffected by tension. LARG and p115 have already been described being activated by adhesion and co-localizing with adhesion proteins(Dubash et al., 2007). However, finding the microtubule associated GEF, GEF-H1 present in integrin-based ACs was unexpected.

We next wanted to know if the activity of these GEFs was affected by mechanical force. To look for activation of RhoA GEFs, we performed affinity pulldown assays with a nucleotide-free RhoA mutant, RhoA(17A), as described earlier(García-Mata et al., 2006). This revealed that force applied to FN-coated beads increased LARG and GEF-H1 activities, but had no effect on the activities of several other RhoA GEFs such as Ect2, p115 or Net1(Figure 5.6a). In the adhesion complex fraction we found that the pool of active LARG and GEF-H1 increased after stimulation with force (Figure 5.6b), indicating that the GEFs recruited to the adhesion complex in response to force were mainly active. To determine if these GEFs are responsible for RhoA activation in response to force, we depleted their expression using siRNA. Depletion of LARG or GEF-H1 significantly decreased RhoA activation in response to force, whereas knockdown of p115 did not affect the force-induced RhoA activation (Figure 5.8a). Double knock-

a

lysate
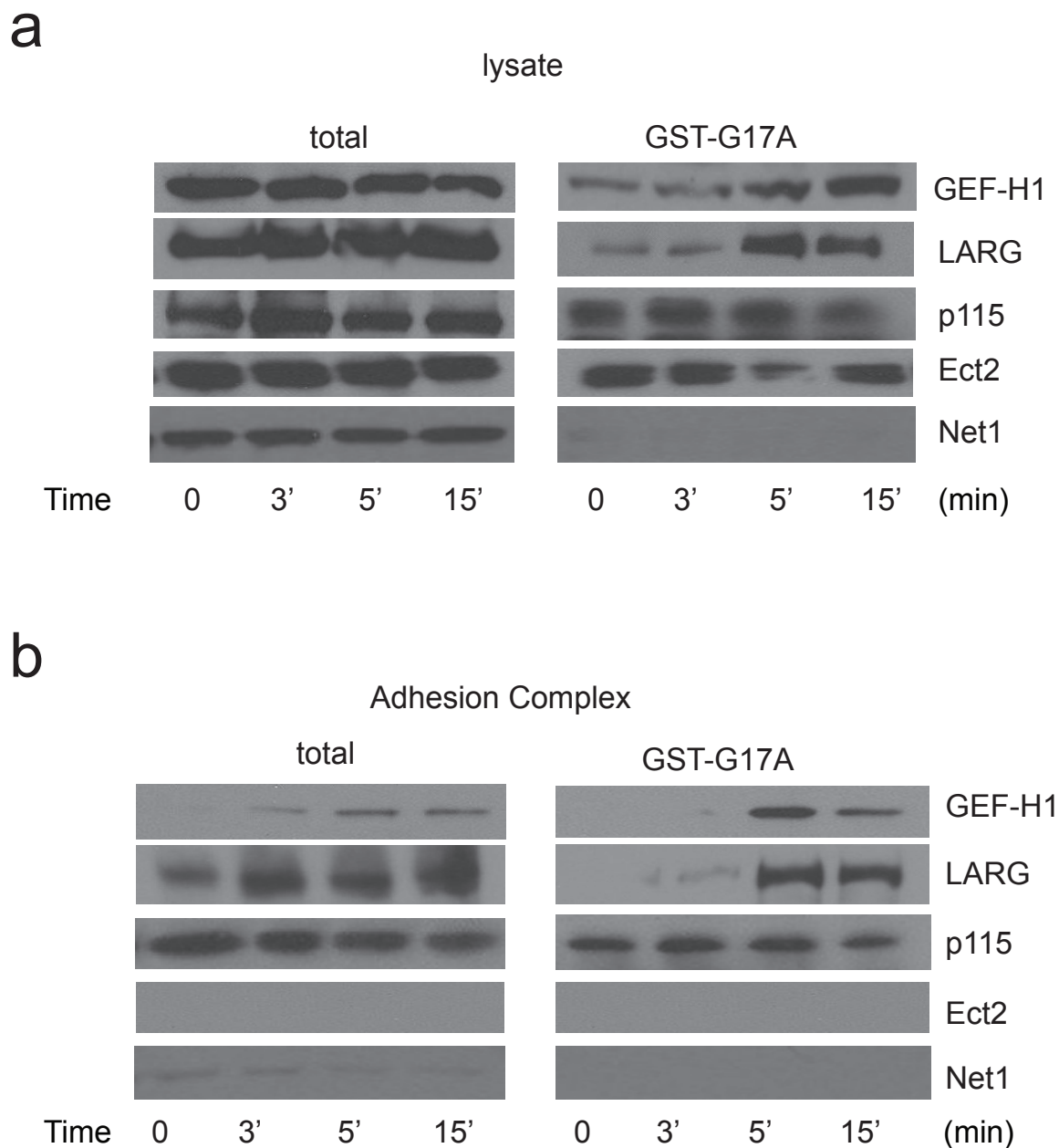
Figure 5.6: Ref 52 cells were incubated 30 min with FN-coated beads and stimulated with tensional force by using a permanent magnet for different amount of time. After magnetic separation of the adhesion complex fraction, active GEFs were isolated by performing GST-RhoAG17A pulldown with the lysate (a) or with the adhesion complex fraction (b) and analyzed by western blot. All results are representative of at least three independent experiments.

down of LARG and GEF-H1 totally abrogated RhoA activation. Integrin-mediated signaling to RhoA is required for rearrangements of the actin cytoskeleton during adhesion. Early adhesion is associated with transient RhoA inhibition and Rac activation allowing actin protrusion whereas mature adhesions are associated with the development of RhoA-mediated tension(DeMali et al., 2003). Previous studies have shown that the transient depression in RhoA activity following integrin engagement involves p190RhoGAP(Arthur et al., 2000)(Ren et al., 2000) while subsequent activation of RhoA involves p115 RhoGEF, LARG and p190 RhoGef (Lim et al., 2008). We show here that application of force on integrins stimulates the RhoA pathway through an overlapping set of regulators. To examine the role of these Rho GEFs during reinforcement we depleted their expression and used the 3DFM to monitor the change in cellular stiffness during pulses of force application. We found that knockdown of either p115, LARG, GEF-H1 or Ect2 decreased the basal rigidity of the cells (Figure 5.7a). However depletion of p115 or Ect2 did not alter force-dependent cellular stiffening (Figure 5.8c), but cells depleted for LARG or GEF-H1 lost this stiffening response following force application. Our results demonstrate that LARG and GEF-H1 are both necessary for cells to adjust their mechanical properties in response to force applied to integrins. Previous work from the Burridge lab has shown that LARG and p115 mediate the activation of RhoA downstream from adhesion to FN and participate in the formation of focal adhesions and stress fibers during spreading on fibronectin matrices. Although we observed here that LARG mediates RhoA activation and contributes to reinforcement in response to mechanical stress, we were surprised to find that p115 is not involved in this process. One possibility that we can envision is that p115 is regulated by adhesion complex formation in a tension-independent way and contributes to adhesion maturation. This could explain the significant decrease in basal rigidity observed when the cells are depleted of p115.This hypothesis is supported by the fact that active p115 was

found in the isolated ACs(Figure 5.6b) and that tensional force did not increase this pool of active p115. The increase in p115 activity during adhesion reported previously could reflect the increasing numbers of adhesions formed during cell spreading.

5.5.3   The Fyn-LARG force pathway

Next, we wanted to find the mechanism of activation of the two force sensitive GEFs, LARG and GEFH1. One of the candidate kinases was the Src family kinase (SFK), which has been shown to be activated in response to force and to contribute to cellular stiffening in response to force(Matthews et al., 2006). To test if SFKs were involved in LARG and GEF-H1 activation by force, we used the SFK inhibitor SU6656. Pharmacological inhibition of SFKs completely prevented LARG activation in response to force(Figure 5.9a), but had no effect on GEF-H1 activation, suggesting that GEF-H1 and LARG are activated through two independent mechanisms. Consistent with this, inhibition of SFKs by SU6656 partially prevented RhoA activation in response to force (Figure 5.9b). To identify which member of the SFK was responsible for LARG activation by force, we used the SYF cells (deficient in Src/Yes/Fyn tyrosine kinases). Applying force on FN-coated beads adhering to SYF-/- cells did not increase LARG activity (Figure 5.9c). Surprisingly, expression of Src in the SYF-/- cells did not rescue activation of LARG. However, re-expression of Fyn in SYF-/- cells did restore LARG activation in response to force. Consistent with this observation, analysis of the mechanical properties of SYF cells revealed that only SYF-/- cells re-expressing Fyn but not Src showed a significant increase in stiffness following application of tension on FN-coated beads (Figure 5.9d). We next looked if differences in activity between Fyn and Src in the SYF cells could explain these results but found that both, Src and Fyn were activated by forces (Figure 5.7). These observations demonstrate the existence of a Fyn/LARG pathway leading to RhoA activation and cellular stiffening
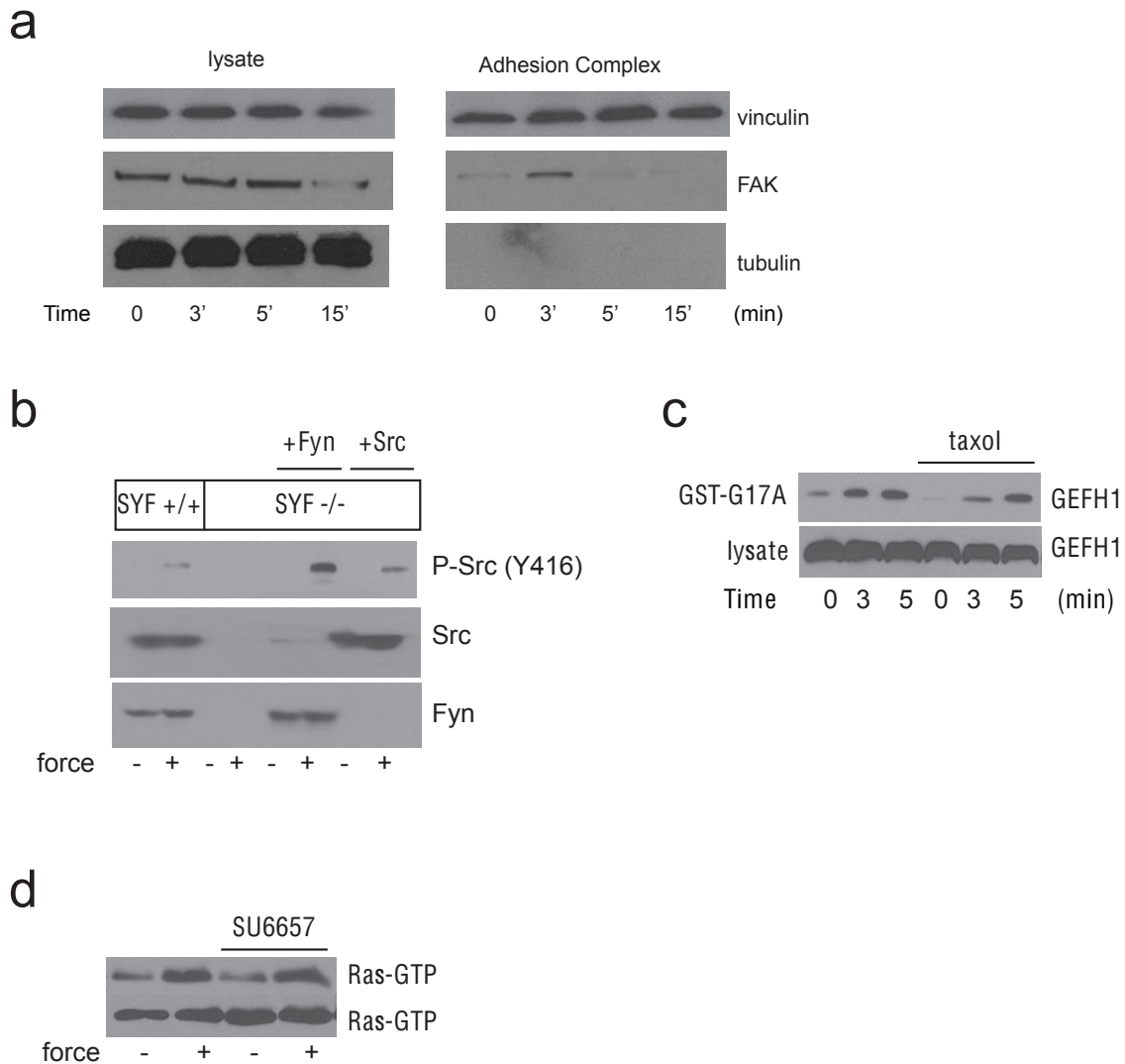
Figure 5.7: (a) Ref52 cells were incubated 30 min with FN coated beads and stimulated with tensional force by using a permanent magnet for different amount of time. After magnetic seperation of the adhesion complex fraction, the lysate and the adhesion complex fraction were analyzed by western blot. All results ere representative of atleast three independent experiments. (b) SYF cells an SYF cells re-expressing Src/Yes/Fyn (SYF(+/+)) or re-expressing Src or Fyn were incubated with FN coated beads and stimulated with force for 3 min. Src and Fyn expression and activity were analyzed by western blot. (c) Ref52 cells untreated or treated with taxol(10μM for 30 min) were incubated with the FN coated beads and stimulated by forces for different amount of time. Active GEF-H1 was sedimented with GST-RhoAG17A and analyzed by western blot. (d) Ref52 cells untreated or treated with SU6657 (2.5μM for 30 min) were incubated with FN-coated beads and stimulated with tensional forces for 3 min. Active Ras(Ras-GTP) was sedimented with GST-Raf1 and analyzed by western blot.

in response to force. Fyn has been shown to colocalize at ACs and to play a role in ECM rigidity sensing(Kostic and Sheetz, 2006). Cells on rigid substrates displayed more stress fibers (Pelham and Wang, 1997) and applied more tension on their ECM through the FAs. This suggests that the Fyn/LARG pathway can be stimulated by both cell-generated tension as well as by externally applied force, in both cases contributing to increased cellular stiffness. Interestingly Chiu and colleagues recently showed that Fyn is activated by forces at cell/cell junctions in endothelial cells(Chiu et al., 2008), suggesting a role for the Fyn/LARG pathway in mechanotransduction in this system too.

5.5.4   The FAK-Ras-ERK1/2-GEFH1 Pathway

Our observation that GEF-H1 is necessary during reinforcement was unexpected. GEF-H1 has been shown to be regulated by microtubule binding29, coupling microtubule depolymerization with RhoA activation in multiple cellular processes such as endothelial barrier permeability, migration and dendritic spine morphology(Birkenfeld et al., 2008). To test if GEF-H1 activation could result from microtubule depolymerization we pretreated cells with taxol and analyzed GEF-H1 activity using the nucleotide free RhoA pulldown assay after application of force. We found that taxol did not affect GEF-H1 activation by force (Figure 5.7b). This result suggests that GEF-H1 is activated independently of microtubule dissociation and is consistent with previous work that showed that treatment with taxol does not affect RhoA-dependent stress fibers formation in response to stretch(Rioja et al., 2009). Recent work has shown that the mitogen-activated protein kinase (MAPK) ERK1/2 can phosphorylate and activate GEF-H1. To test if ERK1/2 is necessary for GEF-H1 activation in response to force we used the MEK1/2 inhibitor U0126. MEK1/2 inhibition prevented GEF-H1 activation by tensional force (Figure 5.10a) but had no effect on LARG activation, confirming that
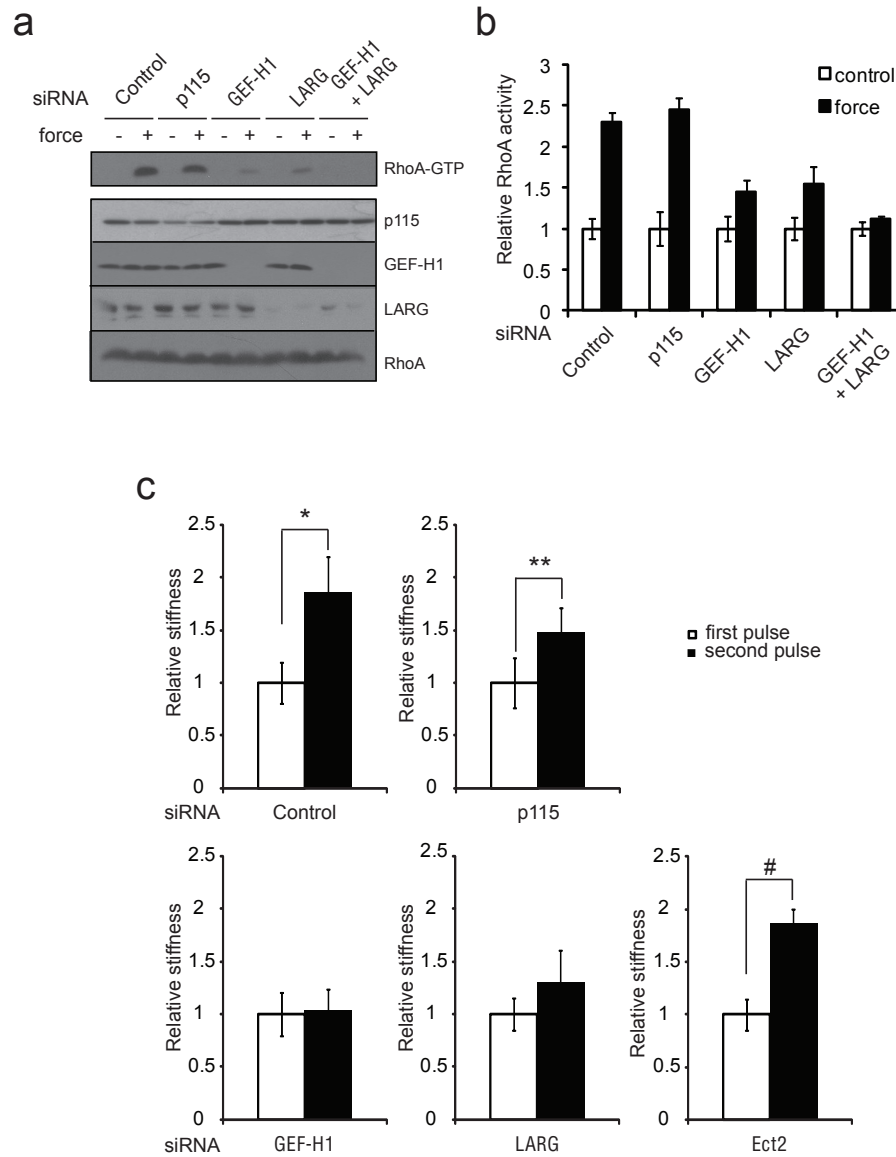
Figure 5.8: (a, b) Ref 52 cells were transfected 48 h with control siRNA or siRNA targeting p115, Gef-H1 , LARG or both Gef-H1 and LARG and incubated 30 min with FN-coated beads. After stimulation with tensional force for 5 min cells were lysed and active RhoA (RhoA-GTP) was isolated with GST-RBD and analyzed by western blot (a). b, corresponding densitometric analysis. RhoA-GTP is normalized to RhoA levels and expressed as relative to the control (n=4). (c) Change in stiffness during 2 force pulses application on FN-coated beads bound to Ref52 cells transfected 48 h with control siRNA or siRNA targeting p115, Gef-H1, LARG, Ect2 or both LARG and GEF-H1 (n=20 , p<0.01, p<0.05, # p= 0.005).

Figure 5.9: a, Ref52 cells untreated or treated with SU6656 (2.5 M for 30 min) were incubated with FN-coated beads and stimulated with tensional forces for different amounts of time. Active LARG and GEF-H1 were sedimented with GST-RhoAG17A and analyzed by western blot. b, Ref52 cells untreated or treated with SU6656 (2.5 M for 30 min) were incubated with FN-coated beads. After stimulation with tensional force for different amounts of time, cells were lysed and active RhoA (RhoA-GTP) was isolated with GST-RBD and analyzed by western blot. c, SYF cells and SYF cells re-expressing Src/Yes/Fyn (SYF (+/+)) or re-expressing Src or Fyn were incubated with FN-coated beads and stimulated with tensional forces for 3 min. Active LARG and GEF-H1 were pulled down with GST-RhoAG17A and analyzed by western blot. d, change in stiffness during 2 force pulses applied on FN-coated beads bound to SYF cells and SYF cells reexpressing Src/Yes/Fyn (SYF (+/+)) or re-expressing Src or Fyn (p=0.01; n=20).

137

two distinct pathways turn on these two GEFs. We next tested if force on integrins activates ERK1/2 and its canonical upstream regulator Ras. We observed that ERK1/2 and Ras are rapidly activated in response to tensional forces (Figure 5.10b). It has been shown that integrin-mediated cell adhesion causes activation of the Ras/MAPK pathway, but this activation has been reported to be both dependent or independent of FAK(Schlaepfer et al., 1994)(Lin et al., 1997). We found that FAK inhibition completely abolished ERK1/2 and Ras activation by force(Figure 5.10b). When we looked at GEF-H1 and LARG activation in response to force we found, as expected, that FAK inhibition prevented GEF-H1 activation and had no effect on LARG activity. This result demonstrates that force on integrins activates GEF-H1 through a signaling cascade that includes FAK, Ras and ERK1/2. It has been described that complete activation of FAK during integrin-mediated adhesion requires phosphorylation on Tyr576/577 by Src(Frame et al., 2010). Surprisingly we found that SFKs inhibition did not affect GEF-H1 activation by force (Figure 5.9a). Moreover we observed that SFKs inhibition did not prevent Ras activation in response to force (Figure 5.7d), suggesting that FAK activation by force does not require Src. Analysis of the mechanical properties of cells pretreated with the U0126 revealed that MEK1/2 inhibition prevented the significant increase in stiffness following application of tension on FN-coated beads (Figure 5.10d).

5.6   Discussion

Cells shape tissues by pulling on neighboring cells and the ECM and are finely attuned to these forces of pull and push. A cell probing its environment initiates matrix matrix adhesion through actin dependent protrusions that brings integrins to the leading edge in contact with the matrix where they can bind. Integrin binding to the ECM is followed by integrin binding to the actin cytoskeleton, which is typically moving inwards from the site of assembly at the leading edge towards the cell center. Thus
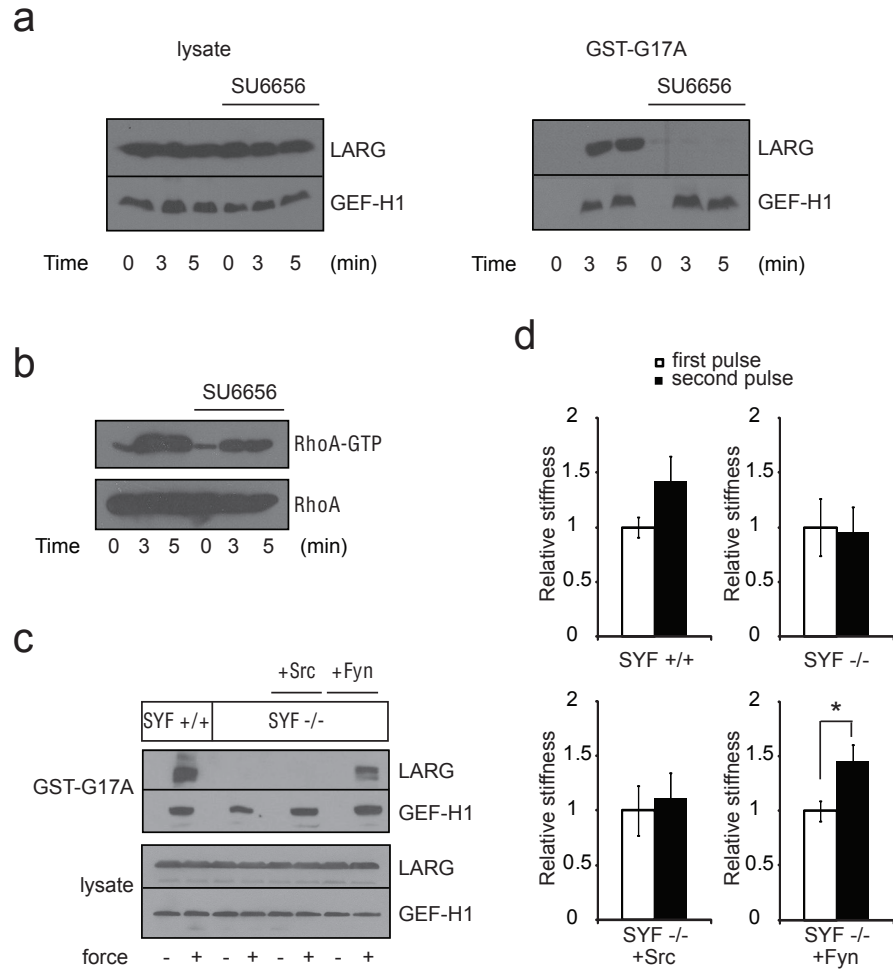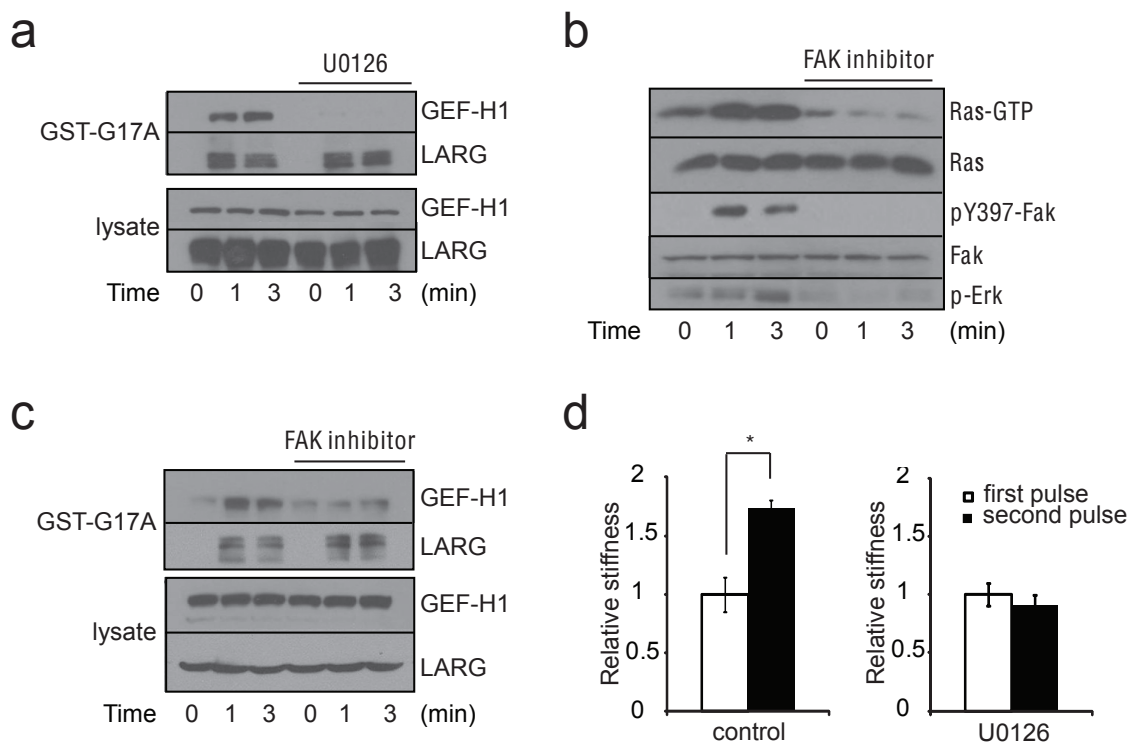
Figure 5.10: (a) Ref52 cells untreated or treated with U0126 (5 μM for 30 min) were incubated with FN-coated beads and stimulated with tensional forces for different amounts of time. Active LARG and GEF-H1 were sedimented with GST-RhoAG17A and analyzed by western blot. (b) Ref52 cells untreated or treated with the FAK inhibitor 14 (5 μM for 30 min) were incubated with FN-coated beads and stimulated with tensional forces for different amounts of time. Active Ras (Ras-GTP) was sedimented with Raf1-GST. Phosphorylated FAK(Tyr397), phosphorylated ERK1/2 (Thr202/Tyr204), total FAK were analyzed analyzed by western blot. (c) Ref52 cells untreated or treated with the FAK inhibitor 14 (5 μM for 30 min) were incubated with FN-coated beads and stimulated with tensional forces for different amounts of time. Active LARG and GEF-H1 were sedimented with GST-RhoAG17A and analyzed by western blot.(d) change in stiffness during 2 force pulses applied on FN-coated beads bound to Ref52 cells treated or not with U0126 (5 μM for 30 min) (p<0.01; n=20).
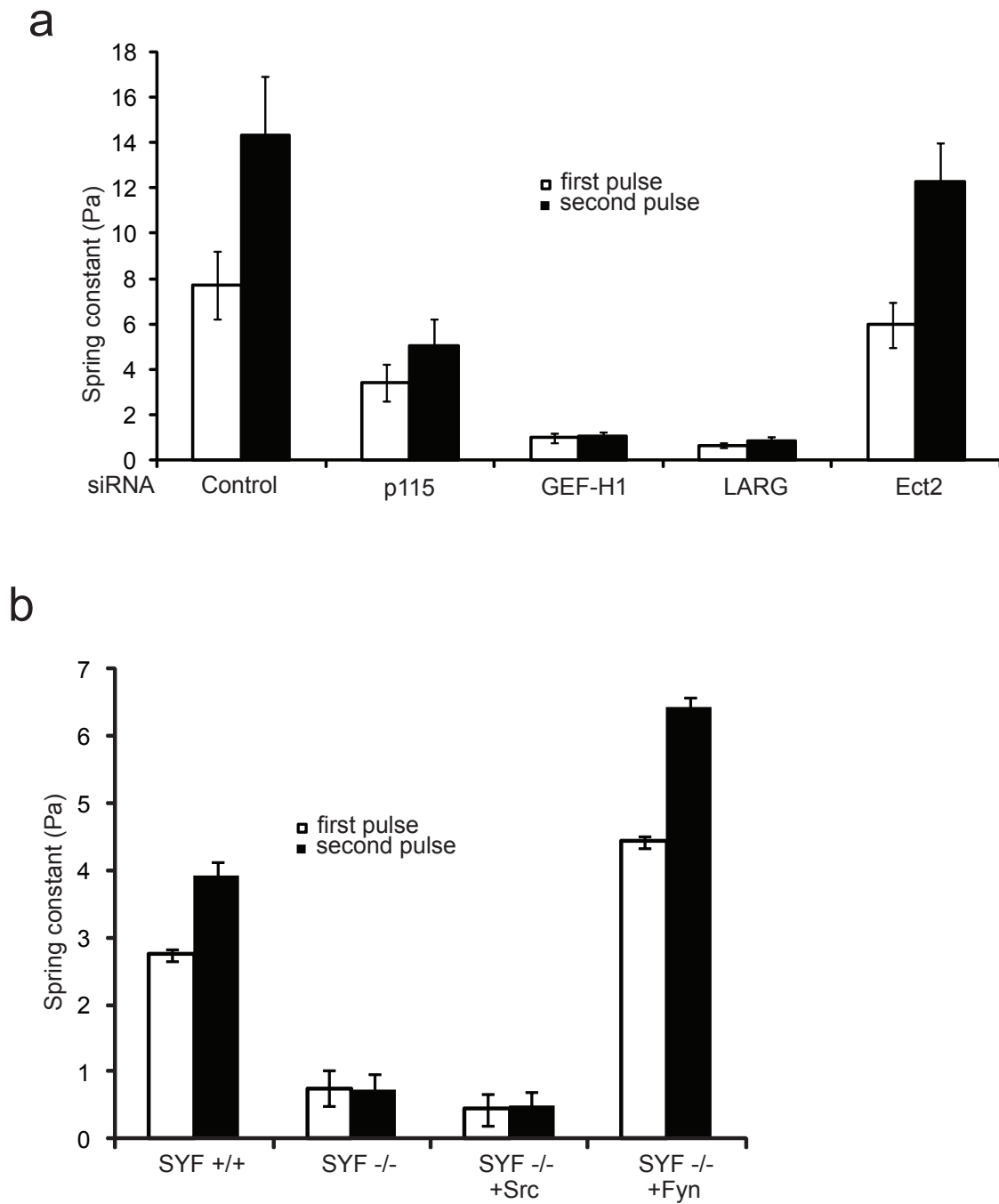
Figure 5.11: (a) Spring constant calculated for the first(white) and second(black) pulse of force applied on FN coated bead transfected 48h with control siRNA or siRNA targetting p115, LARG, Ect2 or both, LARG and GEFH1. (b) Spring constant of SYF cells and SYF cells re-expressing Src/Yes/Fyn (SYF(+/+)) or re-expressing Src or Fyn.

a force is generated across the integrin linkage which at this point are nascent focal complexes. Within seconds, these initial sites of Integrin linkage begin to strengthen as additional components are recruited. When the forces are sufficiently high enough, adhesions undergo further maturation, extending anisotropically several microns as additional proteins are recruited. These sites are focal adhesions, and it is important to state here that, long stable focal adhesions indicate force sensing and recruitment of multiple proteins. These events lead to force dependent strengthening of adhesion sites and multiple explanations exist for this phenomena.

How can force generated externally be sensed by the cell? The 5 basic mechanisms that have been suggested for mechanosensing via integrins: (1) Catch bond formation, (2) Channel opening, (3) enzyme regulation, (4) exposure of phosphorylation sites, (5) exposure of binding sites.

Lifetime of a bond generally shortens with applied force, a phenomena often called slip. However, under certain force regimes, some interactions strengthen or catch. Recent work has shown that in response to force, $\alpha_5\beta_1$ integrin switches between relaxed and tensioned states(Friedland et al., 2009) and this switch results in an increased bond strength. These catch bonds can function as molecular clutch that are engaged under tension and released when the tension is released. Another catch bond exists between myosinII and actin, though this interaction has not been well characterized.

As mentioned in the opening chapter, ion channels convert mechanical force into electrical and chemical signals (Zuvela-Jelaska et al., 2001). In endothelial cells, mechanical stress on integrin bound beads causes calcium entry into cells (Matthews et al., 2006), though these don't seem to be involved in initial strengthening of the integrin ECM link, but in later stages of cell repositioning.

A number of enzymes change their kinetics in response to mechanical stimulation, including kinases, phosphotases and GTPases. The strongest case for an enzyme reg-

ulated by force is FAK. FAK and integrin share a interesting relationship. Integrin clustering results in FAK activation, but this FAK activation can enhance the pool of activated integrins. FAK does not directly bind to integrin, thus force on integrin may activate FAK through an indirect mechanism. SFK have been shown to get activated by force indirectly via the receptor-like protein tyrosine phosphatase-α (RPTPα). Fyn has also been shown to localize near the leading edge when force is applied on fibronectin beads (Kostic and Sheetz, 2006) whereas Src gets activated by vitronectin (Choquet et al., 1997).

Mechanical stimulus has been shown to increased tyrosine phosphorylation(Pelham and Wang, 1997). To date, only the Cas protein family has been proposed to undergo conformation changes that expose phosphorylation sites (Sawada and Sheetz, 2002). When incubated with active Src kinase, increased tyrosine phosphorylation of the substrate domain of p130Cas is observed upon stretch by Fyn (Kostic and Sheetz, 2006). Interestingly, upon phosphorylation the substrate domain of Cas becomes a docking site for a variety of proteins including Crk and Ship2 that can activate GEFs.

The final mechanism for mechanotransduction is the exposure of protein protein binding site due to stretch. Talin is one the proteins where this phenomena has been reported (del Rio et al., 2009). Talin upon stretching has 11 potential binding sites for vinculin, as well as binding sites for actin filaments though interestingly, myosin II contractility is not required for recruitment of talin(Moore et al., 2011).

Ultimately, a combination of events described above regulate the cytoskeleton either via the RhoGTPases or in some cases directly via interactions involving αactinin. Our results provide some insight into the former via the RhoGEFs LARG and GefH1. Force induced RhoA activation seems to require both these GEFs even though they follow different paths of recruitment and activation. Whether LARG activation requires the SFK-FAK complex or direct activation of Fyn by RPTPα needs to be determined. It

may be. that p130Cas may have a critical role in LARG activation by providing a docking site for LARG when phosphorylated by Fyn. This would mean that p130Cas is an important mechanosensor for this part of RhoA activation. If LARG were to be activated by the SFK-FAK complex, this would point to either Talin being the mechanosensor element, or to FAK itself. The SFK-FAK complex can act as a single signaling module or as separate modules of FAK and SFK. It is the separate module of FAK which seems to activate GefH1 via ERK1/2 pathway. Again, the role of Talin and the complex kinase needs to be investigated to identify the mechanosensor element in the pathway.

Our results show that in many of our experiments, knockdowns that abrogate adhesion strengthening are accompanied by abrogation of cell pre-stress/basal stiffness. This seems to indicate that another important mechanosensing element is the tensed cytoskeleton itself. Cytoskeleton prestress is an important variable in multiple adhesion site mechanical models. A simple schematic of a model is shown in Figure 5.12. Loss of mechanosensing have implications on many diseases. To unravel this mechanism may result in discovering mechanisms of altered migration, invasion and other hallmarks of diseases like cancer. The results in Chapter 4 indicate that cells that invade more are softer than cells with low metastatic potential. If cell pre-stress is an important module for "normal" mechanotranduction, then this would mean that maybe a pathway of RhoA regulation may be altered in cancer. 3DFM experiments in combination with protein pulldowns, siRNA libraries and invasion/migration assays can give us a protocol to investigate these pathway. This is the basis for the study described in Chapter 6.
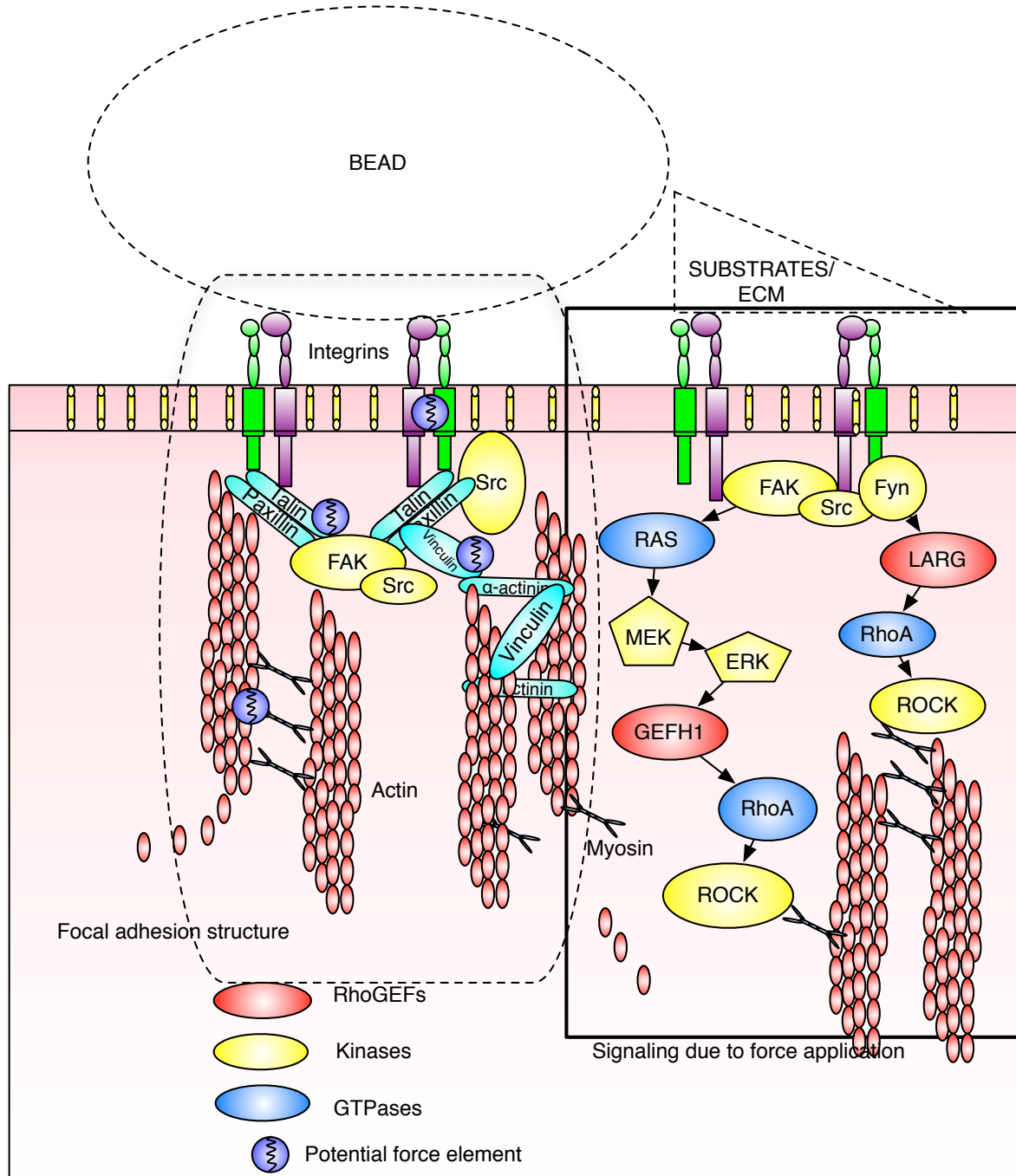
Figure 5.12: A summary of the results discussed in this chapter. The focal adhesion structure reiterates the structural elements involved when a bead attached to integrin is pulled at. The solid rectangle shows the RhoA signaling responsible for adhesion strengthening due to force or other mechanical stimuli like substrates of different stiffness.

Chapter 6

Force signaling pathways in Cancer

Thirty-five years after 'war on cancer' was declared, the discovery of anticancer targets and drugs still remains a highly challenging endeavor. Oncology has one of the poorest records for investigational drugs in clinical development with success rates that are more than three times lower than cardiovascular disease(Kamb et al., 2006). Part of the problem is the fact that the pharmaceutical industry has focussed on development of drugs that target single molecular components encoded or regulated by genes and agents that block essential functions and kill dividing cells- the traditional cytotoxics. It is now clear, however, that cell behaviors are not regulated by linear series of commands , but rather by networks of molecular interactions that involve positive and negative reinforcement as well as high levels of cross talk integrated at the whole system level. In this type of dynamic network, switching between different stable states or phenotypes requires the activities of signaling molecules in multiple pathway change in concert. This signaling dependent functioning is ubiquitous in biology. For example, adult fibroblasts can be induced to revert to pluripotent embryonic stem cells by simultaneous co-expressing a handful of different transcription factors that in turn, activate multiple downstream genes(Meissner et al., 2007)(Wernig et al., 2007)(Takahashi and Yamanaka, 2006). It is for this reason that conventional strategies for the development of anticancer therapeutics have been suboptimal, and why many active single target

drugs(e.g. Glivec) are later discovered to influence multiple signaling pathways simultaneously(Drucker et al., 2004). Another problem restricting forward progress is that cancer is often defined as a disease of cell proliferation. But deregulated growth is not sufficient to make a tissue cancerous. What makes a growing cancer malignant is its ability to metastasize. It is a disease of development as it results from loss of the normal controls that direct cells to assemble into tissues. This has lead to appreciation of the importance of cancer stem cells(Reya et al., 2001), epithelial to mesenchymal transitions(Ingber, 2003) and angiogenesis(Carmeliet, 2005) for tumor formation and metastatic progression.

I concluded Chapter 4, by saying that cell stiffness may not only be an excellent predictor of invasive potential, but that treatments that affect stiffness, independent of mechanism maybe a good cancer target. The first question thus is, what is the mechanism for this stiffness correlation? The effect seen by treating the cells with blebbistatin and increasing invasion seems to indicate that it is a mechanism that regulates actomyosin contractility. This immediately points to the RhoGTPase, RhoA.

Thus, a key obstacle for future progress in the cancer therapeutic field is to develop strategies that take into account the structural complexity and system level architecture of cellular regulation(Ingber, 2006)(Ingber, 2003)(Ingber, 2006)

6.1 RhoGTPases in cancer

The role of RhoGTPases in cancer has been controversial and conflicting over the years. Ironically, the first member of the Rho family of small GTPases were discovered some 20 years ago based on their homology with the Ras oncogene. Because of their sequence similarity to Ras, many of the earlier studies focussed on whether RhoGTPases could also act as oncogenes and whether they were required for Ras induced transformation. As mentioned earlier, Rho proteins regulate cell morphology and the

cytoskeleton and regulate cell migration in a highly complicated manner involving all 3 of the primary members of the family, RhoA, Rac and Cdc42. Detection of active RhoA at the front as well as the rear of migrating cells indicates that RhoA does different things in different locations(Hodgson et al., 2006). Given the role of Rho proteins in the regulations of cell motility in normal cells, it is likely that they are involved in the invasive phenotypes of tumor cells. Another hallmarks of tumor progression is loss of tissue architecture, which is associated with alterations in cell-cell adhesion, loss of polarity and aberrant cell proliferation. Using simple assays, Rho and Rac were first shown to play an important role in adheren junction assembly and since then these two GTPases together with Cdc42 have been shown to play important roles in many additional aspects of epithelial morphogenesis(Braga et al., 1997)(Etienne-Manneville and Hall, 2002). It is now clear that they also effect gene expression, cell proliferation and survival. The literature on Rho proteins and tumor progression is confusing as different studies have indicated contradictory roles for Rho proteins. These roles could be reconciled if Rho proteins have different functions at different stages of tumor development.

Rho proteins are clearly involved in the process of tumorigenesis, but could interfering with their function have useful antitumor effects? Some studies have already provided insight into the effects of targeting Rho proteins in tumor models. Drugs that were initially designed to target the Ras oncoproteins by interfering with their lipid modification also affect the function of Rho proteins(Du and Prendergast, 1999). Rho proteins are also involved in the loss of epithelial polarity that is evident even in benign tumors, and are also thought to be important in EMT observed in more aggressive tumors. Elevated levels of RND3/RhoE, which antagonizes RhoA function can promote loss of polarity and multilayering of epithelial cell(Hansen et al., 2000). Furthermore, down-regulation of Rac1 activity in Ras-transformed or MDCK cells leads to loss of epithelial

cell junctions and a more mesenchymal motile phenotype(Zondag et al., 2000). These studies show that the downregulation of certain Rho protein functions might be crucial in tumor cells. The literature of Rho proteins and tumor progression is confusing, as different studies have indicated contradictory roles for Rho proteins. These roles could be reconciled if Rho proteins have different functions at different stages of tumor development. In fact these roles could also be reconciled if Rho proteins have different functions due to different modes of activation. For example, it may be so that RhoA when activated due to external force either due to neighboring cells or the ECM helps maintain cellular integrity by stabilizing and lengthening focal adhesions accompanied with increased stiffness and contractility to prevent motility. Loss of this activation cascade may result in increased invasion and proliferation.

6.1.1 RhoGEFs in cancer

Perhaps, the difference in regulation of Rho proteins at different stages of cancer or due to different activating stimuli is related to which RhoGEF or RhoGAP gets activated due to the stimuli. Again, alternation between the active GTP bound state and inactive GDP bound states of the small GTPase is controlled by guanine nucleotide exchange factors (GEFs), which simulate the exchange of GDP for GTP, and by GTPase activating proteins(GAPs) which terminate the active state by stimulating GTP hydrolysis. Interestingly, the GTPases possess intrinsic guanine nucleotide exchange and GTP hydrolysis activities. However, these activities are too weak to allow efficient and rapid cycling between their active and inactive state. Members of the different Rho protein family are regulated by GEFs and GAPs with structurally distinct catalytic domains. For the 20 human Rho GTPases there are 83 GEFs and 67 GAPs, and a subset of RhoGTPases are not likely to be regulated by GEFs and GAPs (like RND3). The involvement of GEFs in cancer was first suggested by isolation of RhoGEFs as

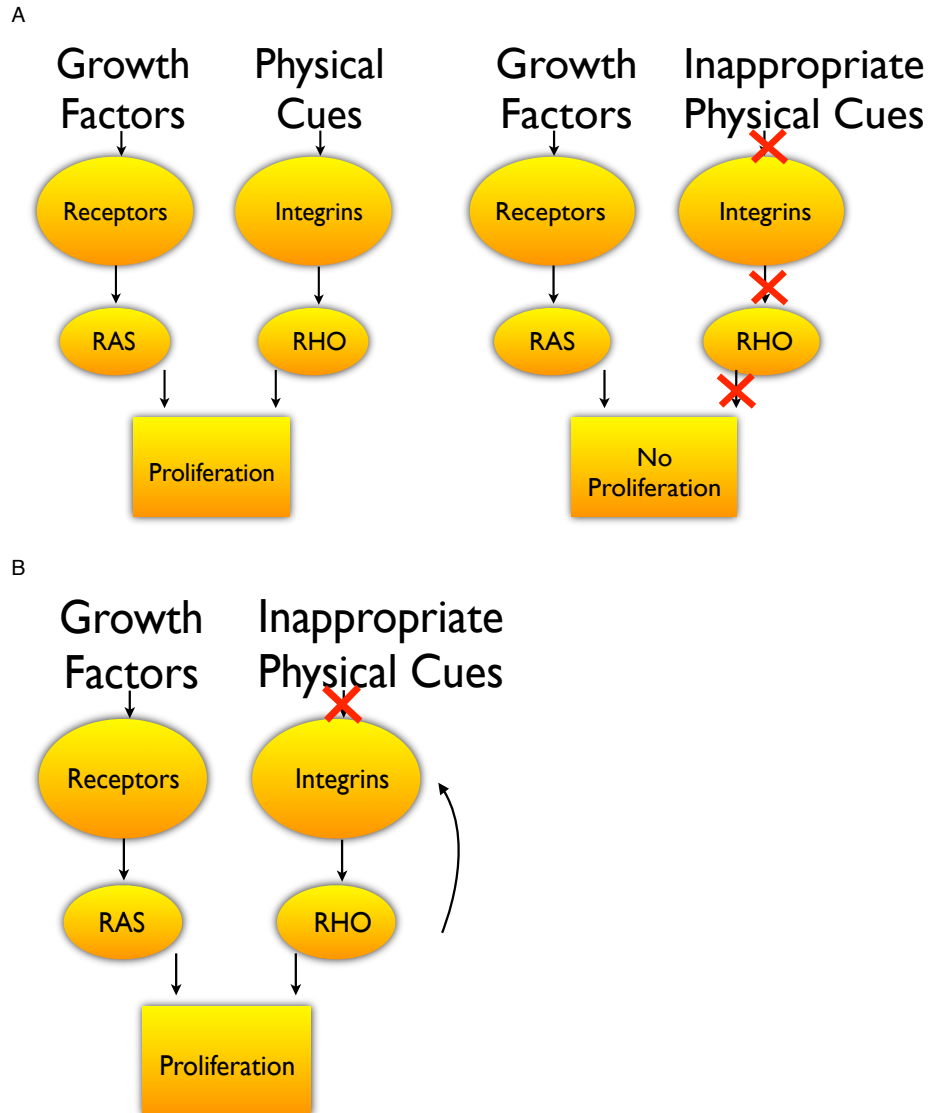Figure 6.1: Normal cells use growth factor mediated signaling and physical cues to proliferate. In cancer, the deregulation of Rho protein activity might lead to aberrant signaling in the presence or absence of the correct physical cues. This would promote deregulated growth inspite of the growth factor cues. For simplicity, the role of growth factors is depicted as RAS activation, and Rho refers generically to Rho protein.

transforming proteins in expression library functional screens using genomic DNA or mRNA derived from human cancer cells(Srivastava et al., 1986) (Miki et al., 1993). As GEF activation is the most common mechanism for signal mediated GTPase activation, the theme that has emerged is that aberrant signaling from growth factor receptors, in particular transmembrane receptor tyrosine kinases(RTKs) and GPCRs leads to aberrant GEF regulation, which contributes to mis-regulated GTPase activation in cancer. Another common mechanism of aberrant GEF activation is upregulated gene expression, and to a lesser degree missense mutations and the consequent expression of catalytically altered GEFs.

Three different RhoGEFs are structurally mutated in human cancers by chromosome rearrangement and the formation of chimeric fusion proteins. One of them, introduced in the previous chapter is the RhoA specific GEF ARHGEF12 or LARG, which was initially identified in tumor cells from patient with acute myelogenous leukemia. The rearrangement encodes a mixed-lineage leukemia(MLL)-ARHGEF12 fusion protein that retains the DH and the PH domain though whether the fusion protein is a constitutively activated variant has not yet been determined.

6.2 Cancer, a disease of mechanotransduction

In the past decade, sudden changes in ECM mechanics, ECM remodeling and the resultant disturbance in cytoskeletal tension have emerged as important factors that can promote malignant transformation, tumorigenesis and metastasis(Huang and Ingber, 2005)(Suresh, 2007a). Furthermore, several studies have shown that cytoskeletal tension in tumors is mediated by ECM stiffness(Paszek et al., 2005). Changes in tissue stiffness, tumor growth due to proliferating cells and/or elevated interstitial pressure all combine to affect the physical environment of cancerous cells inside the tumor and the

adjacent normal cells. This altered physical environment can modulate the fate of these cells through mechanotransduction. Paszek and co-workers found that matrix stiffness and cytoskeletal tension functionally cooperate in a 'mechano-circuit' that modulates phenotypic transformation in tumors by coupling the mechanosensing role of integrins in relaying external physical cues to Rho and ERK signaling pathways(Paszek et al., 2005).

Thus, overall the picture that is emerging is that, in cancer, there is alteration in the force balance between the inside of the cell and the outside of the cell. This loss of balance is a closed loop circuit, where it causes loss of external physical cue related response from the cell. The normal response of the cell would be to alter itself to retain this mechano-balance. This concept is central to idea that cancer cells lose their ability to sense touch. While the RhoGTPases have been implicated in this response, there is very little known about the mechanism and proteins responsible for this loss.

This is good point to recap the results already presented in this document. I have shown that cancer cells are softer than their lesser invasive or metastatic phenotype. The overall signature is dependent on the architecture of the actin cytoskeleton and actomyosin regulation. I have also shown that cell respond to external cues like force probing via the integrin mediated Rho pathway via the RhoGEFs, GEF-H1 and LARG. The question then is, whether loss of mechanotransduction occurs in our ovarian system? If yes, then is the mechanism conserved across different systems and mediated via RhoA and GEF-H1 and LARG? Can we alter the metastatic phenotype by altering the regulation of these GEFs? Are studies such as those described here pointing to a new tool for discovering new novel molecular cancer therapeutic targets?

6.3 Results and Discussion

6.3.1 Highly invasive cells don't respond to forces

We took the IGROV cells as our less invasive phenotypes and the Skov3 cells as the metastatic or more invasive phenotype. The first indication of difference in ability to respond to change in mechanical environment was observed when the 2 cell lines were plated on a matrigel coated coverslip. It has been reported that cells match the stiffness of the matrix on which they are plated(Tee et al., 2009). On loading this sample on the 3DFM and following the protocol described in Chapter 4, we found that the stiffness values of IGROV cells changed to a much lower significant value whereas the Skov3 cells didnt show any change in their stiffness(Figure 6.2A). This seemed to indicate that Skov3's did not interact with the environment and regulate cytoskeletal stiffness whereas the IGROVs did. To study this effect and force response, we then used the same protocol as described in Chapter 5 and observed the stiffness changes in the 2 cell lines as a function of force pulse. The result of this experiment is shown in Figure 6.2B. As predicted, the less invasive IGROV's responded to external force within the 1st 2 pulses where as this response was lost in the Skov3 cell lines. The Skov3 ovarian cancer cell lines show higher invasion potential and migratory potential than the IGROV as reported in Chapter 4 and shown in Figure 6.4.

6.3.2 Role of RhoGEFs in cancer

We next looked at the RhoA expression levels and activity for the two cell lines. As expected from the stiffness levels, IGROVs, while there was no significant difference in basal RhoA expression levels, on force application we found that the RhoA activity went up for IGROVs where as there was little or no change in the activity levels of RhoA in Skov3's(Figure 6.2C). Further, on looking at RhoAGEF levels, we

found that IGROV cells had a higher expression level of GEFH1 compared to Skov3. This is consistent with our previous finding that GEFH1 is a key RhoGEF for force sensing(Chapter 5). We did not find any difference in LARG expression levels for the two cell types.
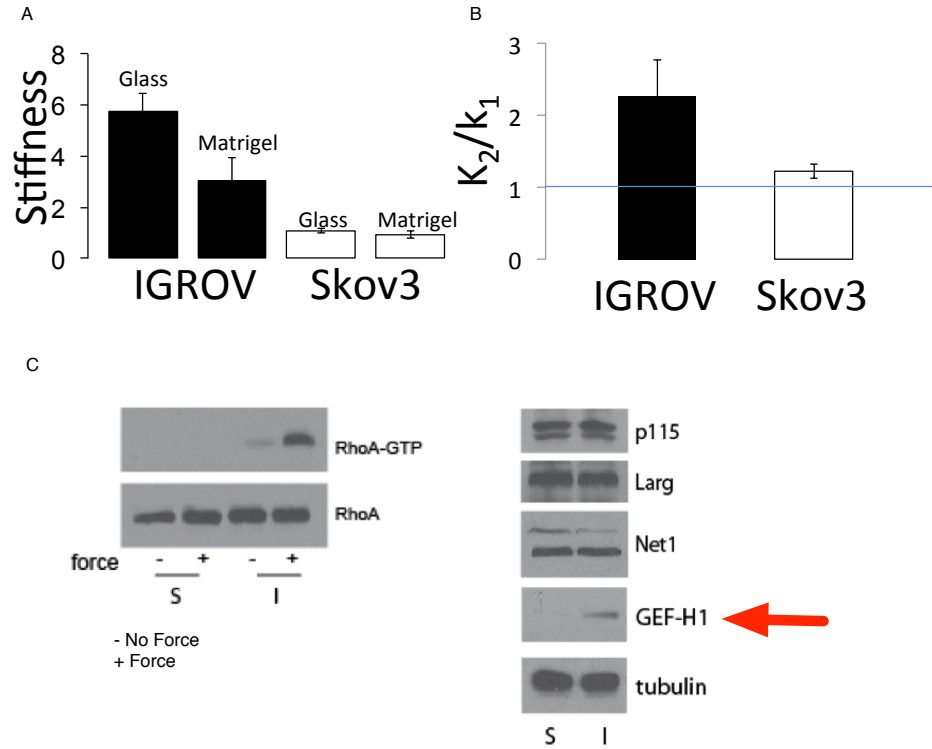
Figure 6.2: A) IGROV cells show different basal stiffness when plated on a softer substrate, whereas Skov3 cells do not. B) IGROV' s show a 2 fold increase in their stiffness when probed by a 3 second force pulse. Skov3's show no significant change in stiffness. C) IGROV(I) show increased activation of Rho due to force application. C) Skov3's have little or no GEFH1 expression compared to IGROVs (red arrow).

As mentioned earlier, FAs are mechanosensitive organelles that recruit cytoplasmic proteins to grow and change composition in response to mechanical tension(Chrzanowska-Wodnicka and Burridge, 1996) in a process known as FA maturation. Tension driving FA maturation can be supplied either by Myosin II (internally) or by forces from the ECM(externally). Activation of the integrin signaling cascade through processes de-

scribed in the previous chapter leads to tyrosine phosphorylation of early FA proteins, including FAK, paxillin and p130cas(Ballestrem et al., 2006) which then act as scaffolds phosphotyrosine (PY)-binding SH2 domain containing proteins. Since the goal of this study is to determine FA size changes due to internal 'mechanical state' of a cell type and correlate it to its metastatic state, we will not classify different sized structures as FA, focal complexes or fibrillar adhesions, but will refer to all membrane plaques marked by PY or another FA protein as adhesions. In the previous chapter, I reported that the 2 cell types had distinct differences in their actin structure which is again shown in Figure 6.3. The IGROVs have a highly cortical actin structure whereas the Skov3 cells have a much more diffused and distributed structure with distinct lamellipodia. As expected from their migrational characteristics, we observed highly elongated and large focal adhesions for the IGROV cells and small and dispersed FAs for Skov3. These are consistent with observations recently reported regarding highly migratory cells having small FAs(Rericha et al., 2010).

6.3.3   GEFH1 alters cell mechanics and metastatic potential

Next, we wanted to investigate the role of GEFH1 on invasion having already studied its effect on stiffness and mechanoresponse in the previous chapter. We depleted GEFH1 levels in both the cell types using siRNA and measured the stiffness and force response for the IGROV cells. As expected, we found that depletion of GEFH1 resulted in loss of basal stiffness and abrogation of force response in IGROVs(Figure 6.4). This observation further validates the role of GEFH1 as a key mediator of force response through integrin signaling which is conserved in different cell types. To validate the role of stiffness and force response in metastasis, we did invasion and migration assays on GEFH1 knockdown cells and found that the less invasive IGROVs became highly metastatic with a 3 fold increase in the invasive potential(Figure 6.4C). GEFH1
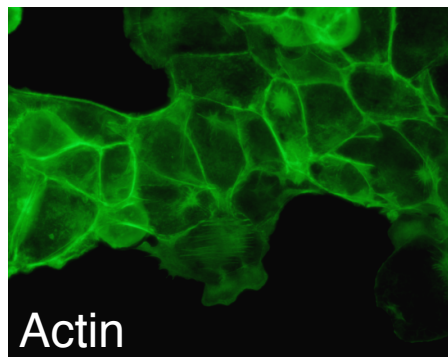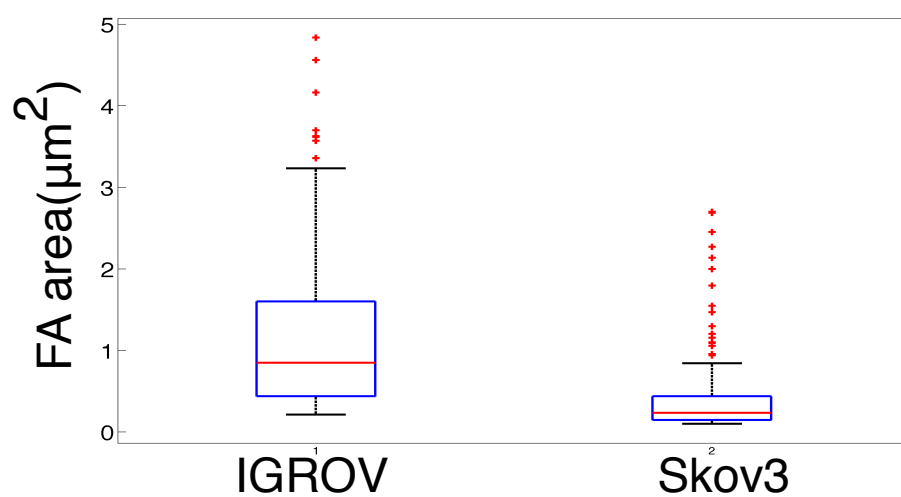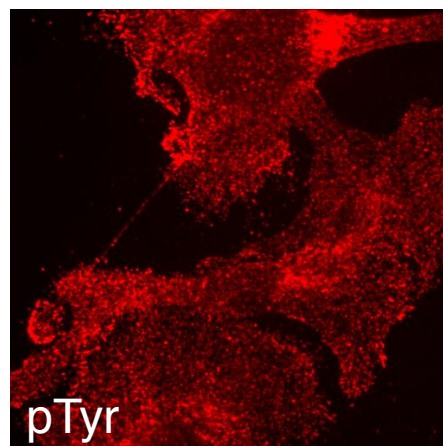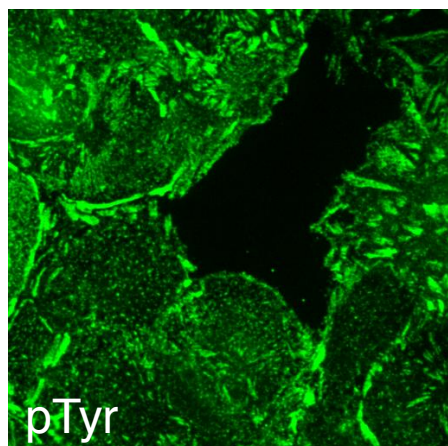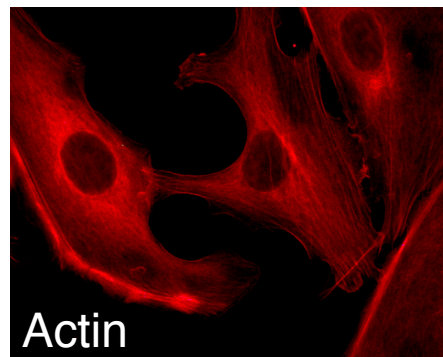
Figure 6.3: Morphological differences between IGROV and Skov3 cells. IGROVs show high levels of cortical actin(quantified earlier) and longer focal adhesion. Focal adhesion area quantified in the bottom panel.

knockdown also decreased adhesion size compared to control and changed the overall morphology of the cell with very little to no cortical actin, more diffused actin and increased spreading and lamellipodia structures(Figure 6.5). Preliminary observations also point to thinner actin filaments, though more quantitative analysis will be required for this observation. The decrease in adhesion size and change in morphology is consistent with what we would expect having looked at Skov3 cells earlier. Thus, GEFH1 is a key player in loss of mechanotransduction in cancer cells and affects the force sensing apparatus through FA and the actin cytoskeleton.
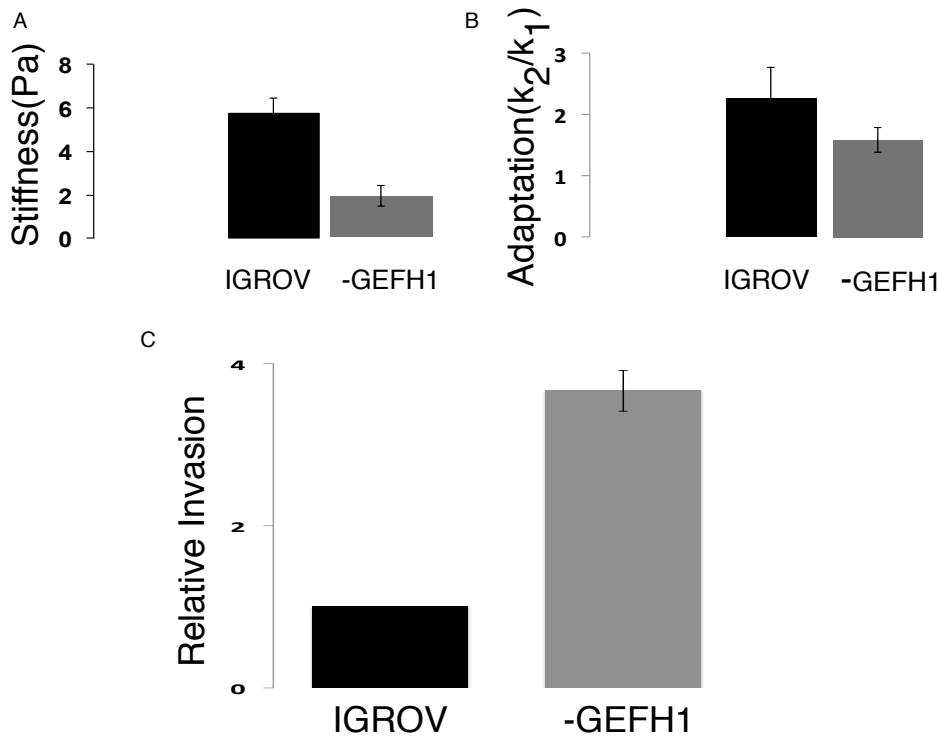
Figure 6.4: Effect of GEFH1 knockdown on IGROV cells. A) Knockdown of GEFH1 results in 3 fold decrease in the basal stiffness of IGROV cells. B) GEFH1 knockdown also results in decrease in mechanoresponse when compared to control (black). C) Knocking down GEFH1 results in a 4 fold increase in invasion in ovarian cancer cells.

RhoA can be activated by a vast number of GEFs, each of which have their own specificity in terms of activation. TO test whether the phenomena we were observing
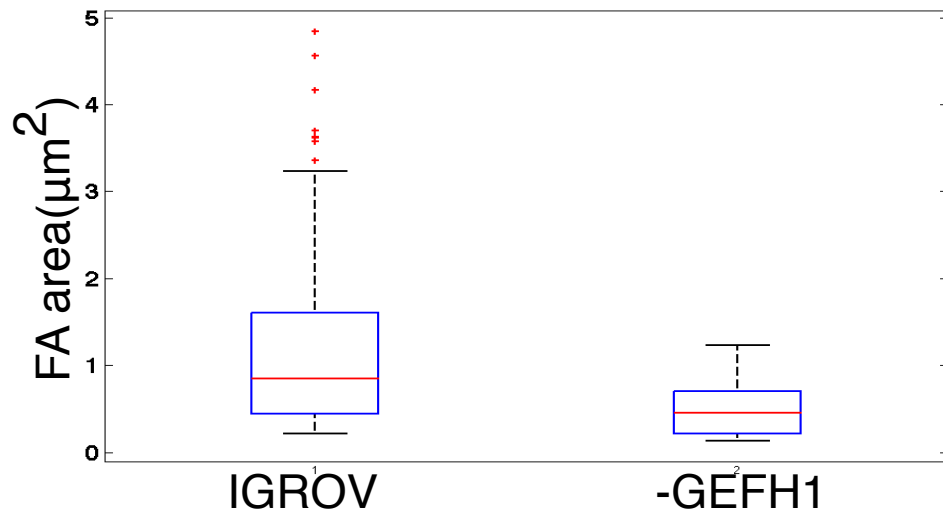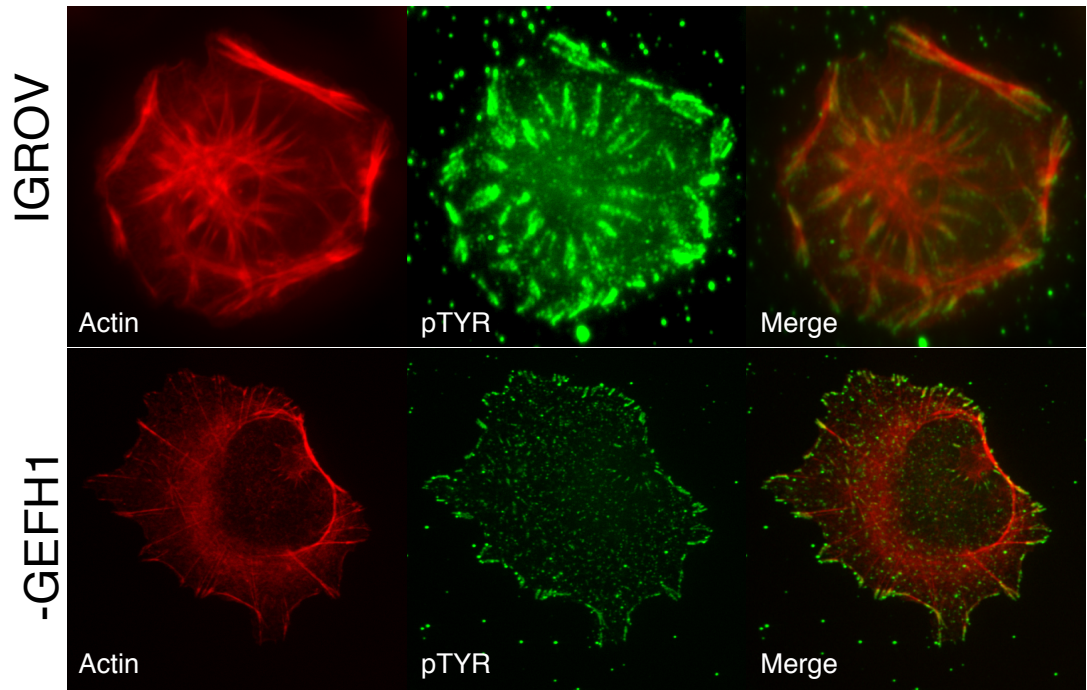
Figure 6.5: Effect of GEFH1 on cell morphology. Fluorescence images of cell morphology, actin on top and PY epitopes(P-Tyr) bottom to visualize adhesions. The merged image is shown in the third panel. (Bottom) Area of individual adhesions with PY-immunolabeed cells.

was driven by force activation of RhoA or was independent of force, we over expressed Net1 an GEFH1 in the Skov3 cells. Neuroepithelioma transforming gene 1(NET1) is a RhoA specific GEF that was originally identified in a genetic screen for novel oncogenes. At steady state, NET1 localizes to the nucleus and the deletion of the N terminal redistributes NET1 to the cytosol and promotes the formation of actin stress fibers, which is a consequence of RhoA activation. If RhoA activation was what was controlling our stiffness dependent phenotypes, then we would see the same effect on stiffness by over expressing NET1 as we would by over expressing GEFH1. However, we found that over expression of NET1 had no effect on the stiffness of Skov3 cells or the ability to respond to forces(Figure 6.6A). GEFH1 overexpression on the other hand resulted in a 3 fold increase in stiffness and a statistically significant change in stiffness over the 2 force pulses, an indication of mechanoresponse. As expected, this overexpression of GEFH1 resulted in a 50% drop in the invasive potential of Skov3 cells which indicates that the mechanotransduction pathway in this system is purely dependent on expression levels of GEFH1 and not on any other RhoA GEF(Figure 6.6B).

6.4   Conclusions

One of the most exciting and challenging developments in cncer biology over the past decade is the recognition that tumor growth, invasion and metastasis are all intricately tied to the constituent cells ability to sense, process and adapt to mechanical forces in their environment. The challenge has been how dramatic changes in cell shape, motility and actuation of mechanical cues are linked to genomic disruptions and instabilities, altered sensitivity to soluble signals that facilitate matrix remodeling and angiogenesis. Currently very little is known about this interaction, which portions of each are necessary and sufficient for tumor progression and under what circumstances elements of one can offset or potentiate elements of the other. It was recently shown that ERK and
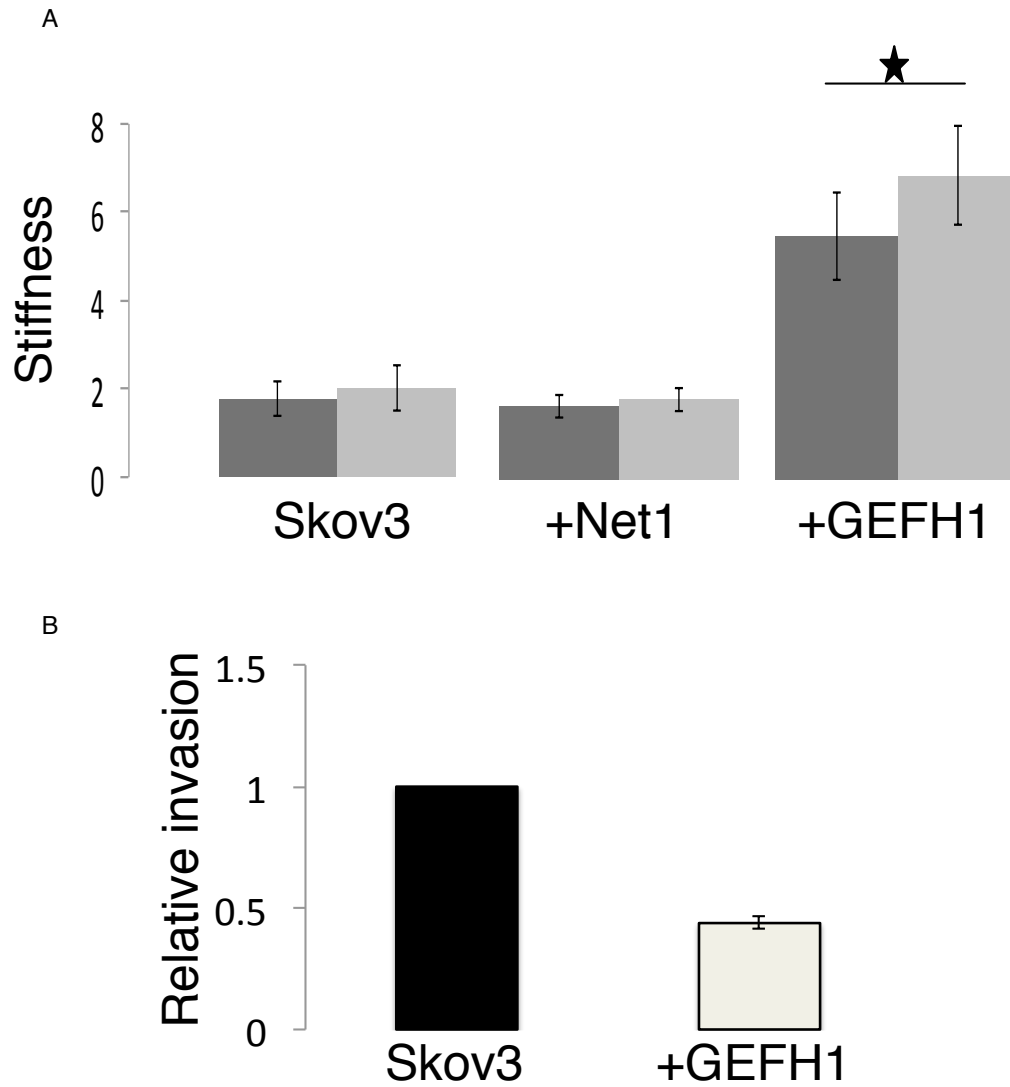
Figure 6.6: GEFH1 specifically alters stiffness dependent invasion. A) Overexpressing Net1 in Skov3s has no effect on stiffness or mechanoresponse, whereas overexpressing GEFH1 increases basal stiffness and force response. B) GEFH1 overexpression also decreases invasive potential in Skov3 cells making them less malignant.

Rho appear to be part of an integral mechanoregulatory circuit that functions to link physical cues from stromal ECM through integral adhesions to molecular pathways that control cell growth and tissue phenotype(Paszek et al., 2005). These results pointed to intertwining between the mitogenic EGFR/Erk and the Rho/ROCK pathway.

GEFH1 may be one such link between the 2 signaling cascades. We have shown that force dependent activation of GEFH1 is via the MAPK signaling pathway. Further, GEFH1 activates RhoA resulting in control of the internal stiffness and force response in cells. We have shown here that the more invasive cell line loses its expression of GEFH1 which results in loss of force dependent activation of RhoA and this phenotype can be partially rescued by over expression of the GEF which results in increase in basal stiffness and mechanoresponse and reduction its invasive potential. Conversely, the less invasive cells show elevated levels of GEFH1 expression and knocking down this GEF results in increase in invasion and loss of focal adhesion stability and change in actin morphology. These results point to the role of GEFH1 in EMT, where the IGROVs show epithelial like morphology and Skov3's show more mesenchymal like characteristics. Infact, IGROVs express higher levels of Vimentin, an Epithelial biomarker(private communication with Dr. K Mythreye).

Thus, potentially GEFH1 expression and activation may be deregulated during EMT resulting in loss of basal stiffness and the ability of the cells to respond to cues and subsequent increasing invasive and metastatic potential. Combined with the results shown in Chapter 4 with the TβRIII receptor seems to indicate that loss of stiffness is necessary for increases invasion/migration and a result of some genetic alteration. The loss of stiffness in most cases seems to be accompanied by loss of mechanoresponse which would further result in cells ignoring physical cues from ECM and more proliferation.

These studies show that stiffness/mechanoresponse assays like magnetic tweezers have

great potential to investigate molecular pathways because of this ubiquitous loss of stiffness due to deregulation. Current work in our lab with collaborators interested in different pathways has already taken this route. The development of the MHTS will further aid in this remarkable and new path of discovery in cancer therapeutics.

Chapter 7

Future Work

Most diseases present as a complex genetic profile with multiple changes in molecular expressions. Nonetheless, a patient goes to the doctor's office often because of a mechanical defect in a tissue or organ: a new swelling or lump, pain due to nerve compression, stiffness that limits movements, edema caused by leak of tissue bodily fluids or obstructed airflow that restricts breathing. Cures and remedies are often judged successfully by the patient only when such mechanical defects are remedied. In order to understand health related and disease related aspects of living systems-all of which work and move as multi-molecular collectives, we must first be able to explain how physical forces and mechanical structures contribute to the 'active' material properties of living cells and tissues, as well as how these forces impact information processing and cellular decision making.

Looking ahead, there are still a number of challenges that lie ahead to this exciting field of cell mechanics. We still struggle with the question of what determines stiffness and other constitutive physical properties of the cell. There are 2 approaches to this questions. One is the bottom up reductionist approach which is rooted in the traditional viscoelastic paradigm(Bausch and Kroy, 2006)(Pollard, 2003). At the level of fundamental constituents and their use in reconstituted systems *in vitro*, cell derived materials and molecules are rich because, among other things, they are well defined,

they can have motors and crosslinkers that provide contraction and change on/off rates, and they can be manipulated precisely(Chaudhuri et al., 2007)(Choy et al., 2007)(Shaevitz and Fletcher, 2007). Like living cells these materials can get around limits set by thermal forces and the fluctuation dissipation theorem(Mizuno et al., 2007). In certain limiting cases, or if the networks are prestressed, physical properties comparable to those observed in living cells can be approximated, but the mechanism remains unclear(Deng et al., 2006)(Gardel et al., 2006). From a top down perspective, by contrast, there has emerged a striking analogy between the dynamics of intact living cell and that of the universal but relatively featureless pattern of inert soft glassy materials such as foams, pastes and colloids(Fabry et al., 2001)(Trepat et al., 2007). Glassy dynamics cannot predict what will happen to matrix dynamics if a particular protein is mutated, but suggest that dynamics of cytoskeletal proteins generically, and transitions between fluid-like vs. solid-like behavior in particular, are governed by free energy barriers incorporated into a rough energy landscape(Frauenfelder et al., 1991). Integration of the competing paradigms of viscoelasticity vs. glassy dynamics along with central role of cytoskeletal prestress into a single unified framework has become a major challenge in cell biophysics.

Cancer screening has become one of the most powerful tools in reducing tumor mortality, as exemplified by the cervical Pap smear test. Current assays of cell metastases involve the observation of the lateral mobility of cells in a "scratch assay", or through porous membranes in an invasion assay. These assays usually take several hours to days of cell tracking. We have proposed to replace the migration assay with one that measures the cell stiffness and cell mechanical response. These measurements as discussed in this document take seconds and if combined with the developing high throughput system would elucidate the time course of the biochemical pathways at the heart of the

mechanical and hence, metastatic propensity. As mentioned earlier, we have a proto-type multi-well assay system and our next steps are to move from a 16 well to a 96 well assay and validate the system on cell lines and ex-vivo tumor cells. The bead methodology offers great flexibility in attaching the force probe(bead) to specific receptors through ligand functionalized beads. Once attached, two complimentary experiments can be performed: passive diffusion and active pulling on the bead. The active pulling can not only measure the cell stiffness but also provoke a stress response. e mechanics of the cell is remarkably affected by the stiffness of the supporting substrate. We plan to use polyacrylamide substrates of tunable stiffness in the 96 well plate to be able to do these measurements under different mechanical conditions. I have shown preliminary data here that shows that the stiffness of cells vary with substrate stiffness, more so in normal cells than in their cancer phenotypes. Overall, the results in Chapter 4, shows that cell stiffness is a reliable marker for malignancy, and has great potential to be used as a clinical assay, in combination with a traditional test. The stiffness test would allow for quick grading and simple readouts which require very little interpretation.

Our results also show that stiffness could be an important therapeutic target. We have zeroed in on the Rho signaling pathway as a candidate pathway, but our TGF-β results indicate that this may be path independent. Even though cancer is not just one disease, but many pathologic conditions including uncontrolled growth, invasion and metastasis, all three pathomechanisms of malignancy require changes in active and passive biomechanics of the tumor cell and stroma. Stiffness is thus a potential target for malignancy, independent of the peculiar molecular manifestation in individual cancer. From a medical perspective, insights into the biomechanical changes that occur during tumor progression may lead to novel selective treatments by altering tumor cells biomechanical properties. Such drugs would probably not cure by killing cancer cells,

but may effectively hinder the propagation of the neoplasm. These possible treatments would cause only mild side effects and may be an option for older and frail patients who can no longer tolerate radical surgery and cytostatic drugs(Fritsch et al., 2010).
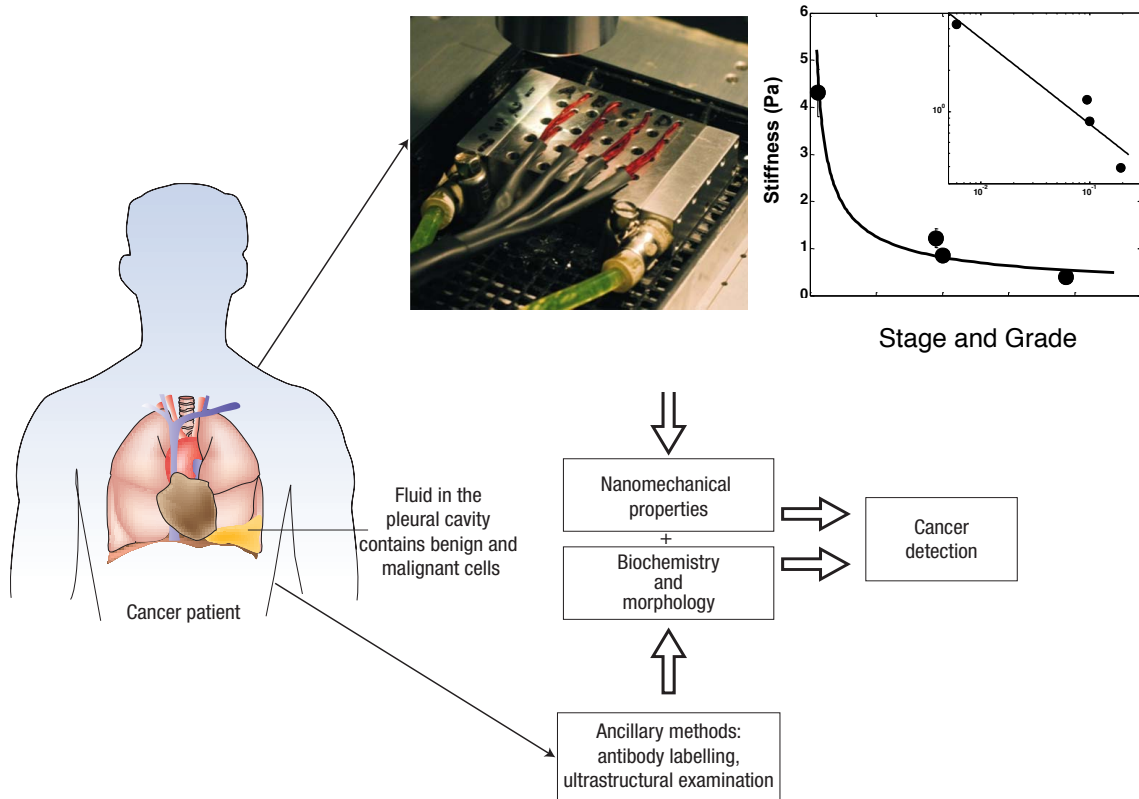
Figure 7.1: Adapted from (Suresh, 2007b)Techniques like the 3DFM and MHTS can be used in a clinical setting in combination with tradition assays to grade tumors from patients.

It is clear now that cells can sense and transduce a broad range of mechanical forces into distinct sets of biochemical signals that ultimately regulate cellular processes, including adhesion, proliferation, differentiation and apoptosis. There is also accumulating evidence that in diseases like cancer, there is deregulation of this transduction. Thus, deciphering at the nanoscale the design principles by which sensory elements

are integrated into structural proteins motifs whose conformations can be switched mechanically is crucial to understand mechanotransduction. Central to this, is identification of the force sensing proteins in the cells and understanding their function. Single molecule studies have revealed an unexpected richness of mechanosensory motifs, including force regulated conformational changes of loop exposed molecular recognition sites, intermediate states in the unraveling pathway that might either expose cryptic binding or phosphorylation sites, or regions that display enzymatic activity only when unmasked by force. Discovery of these motifs will require using high resolution single molecule techniques like FRET and TIRF in conjunction with the 3DFM, a process that has already started in our lab.

The results and techniques discussed are not restricted to one disease or one signaling pathway. Because of the central role of the cytoskeleton in cell structure and intracellular organization, perturbations in the architecture of any of the three main cytoskeletal networks can result in marked pathologies. For example, mutations in the gene encoding intermediate filament proteins are associated with many diseases in humans, including predisposition to liver disease in the case of some keratins, amyotrophic lateral sclerosis (also known as Lou Gehrig's disease) in the case of neuronal class of intermediate filaments called neurofilaments and progeria in the case of improperly assembled nuclear lamins.

In a 1960 lecture, cell and developmental biologist Paul A. Weiss stated, " Life is a dynamic process. Logically, the elements of the a process can be only elementary processes, and not elementary particles or any other static units. Cel life, accordingly can never be defined in terms of a static inventory of compounds, however detailed, but only in terms of their interactions". The cytoskeleton is result of all those interactions

and its mechanical property is its most significant identity.

Appendix A

Appendices

A.1 Bead preparation

A.1.1 Spot labeling

Magnetic beads with 2.8 micron diameter were purchased from Dynal (Invitrogen). The beads were suspended in ethanol and delivered to a cover slip (Corning) then dispersed by scraping the cover slip with a razor blade. The cover slips were then placed into a sputtering system with a gold sputtering target set to a pressure of 60milliTorr and a current of 15 milliAmperes for between 180 and 300 seconds. The sputtered substrates were submerged in 0.5 micromolar M-PEG-SH solution to minimize any nonspecific binding inter- actions. The cover slips were then placed into tubes with approximately 30 milliliters of DI water and then sonicated for thirty minutes to dislodge the beads from the substrate. The cover slips were then taken out of the tubes and the beads allowed to settle overnight. The beads were held at the bottom of the tube with a magnet while the supernatant was removed by pipette. The remaining suspension was then collected and dispersed by vortex. The beads were then diluted in a PBS buffer solution.

A.1.2 Fibronectin bead coating

1. Fn-coated beads were prepared by diluting 2.8μ tosyl-activated Dynabeads (Dynal, Invitrogen Corp) into 0.1 mg/mL fibronectin solution(Invitrogen Corp or a

gift from the Burridge lab).

2. Commercial Fibronectin was first dialyzed overnight into PBS, with at least 2 changes of buffer.

3. $10\mu L$ of the stock bead solution per 0.5 mL Fn solution was rotated overnight at 4 degrees, then spun down at 1000 RPM for 1 min.

4. The beads were resuspended in 1 M Tris buffer, pH 7.4, and rotated again overnight and then washed with 2 changes of PBS.

A.2 Fitting Jeffrey's model to cell pulling data

In Chapter 4, Chapter 5 and Chapter 6, magnetic beads are pulled on for 10 seconds and 3 seconds and 3 seconds respectively. The obtained data is tracked and then fit using the Jeffrey's model. The fitting is carried out for the time of force application only and as previously mentioned, the stiffness values are only compared for beads which have been pulled for the same amount of time. For e.g.. in Chapter 4, all the cell data are from beads which were pulled for 10 seconds to which the model is fit and stiffness is obtained using a least squares method. In Chapter 5 and Chapter ??, all data being compared are pulled for 3 seconds and allowed to relax for 4 seconds. The fitting is shown in the figure below.

A.3 Methods used in Chapter 4

A.3.1 Cell culture

Seven human ovarian cancer cell lines, OVCA429, IGROV, SKOV3, HEY, DOV13, OV2008, Ovca420 were cultured in RPMI 1680 (Life Technologies Invitrogen), with 10%
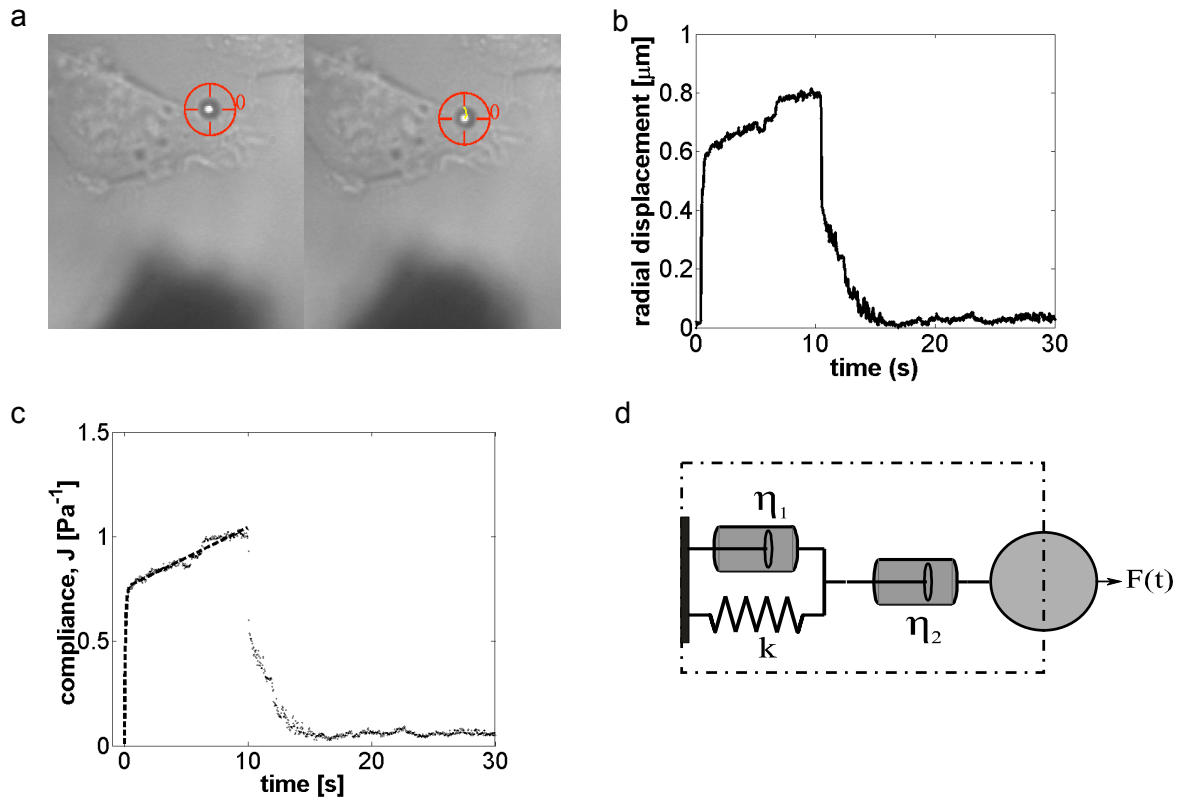
Figure A.1: Magnetic tweezer set up and spring constant calculation. a) Experimental setup showing a 2.8 micron fibronectin coated magnetic bead on a cell being pulled by the pole tip. The tracker generated by video spot tracker is used to track bead displacement. b) Tracked radial displacement shown for the bead pulled by an applied 10 second force. c) The tracked displacement in (b) is converted to compliance as described in the text and then fitted using a least squares method to a Kelvin Voigt model shown by the dotted line. d) A Jeffreys model is shown. All stiffness values reported are the value of the spring constant of the spring k.

FBS at 37°C in a humidified incubator. Ovarian cancer stable cells lines, Ovca429Neo, Ovca429 TβRIII were derived and characterized previously(26). Antibody to pMLC was obtained from Cell signaling technologies (Cat.No. 3671) and Pan-cytokeratin antibody was obtained from Santa Cruz (Cat.No. 81714).

Primary short term epithelial ovarian cancer cell cultures were established from the ascites of patients with Stage III/IV epithelial ovarian cancer as described previously(43). Briefly, ascitic fluid was centrifuged at 4°C for 10 min at 2000 rpm and hemolysis of erythrocytes was done by resuspending cells in 0.17M NH_4Cl for 10 min on ice. Cells were then washed three times in Hanks Balanced Salt Solution (HBSS) and finally resuspended in 30mL RPMI media per 1cm pellet. Cell suspensions were layered over 10mL Ficoll and centrifuged for 25 min at 25°C at 2500 rpm. Cells were seeded on 10mg/mL fibronectin coated culture dishes in RPMI media containing 20% FBS and 1% penicillin/streptomycin solution at 37°C in 5% CO_2. Adhered cells were subject to limited dispase digestion for the first passage to remove fibroblasts and stained with a pan-cytokeratin antibody to confirm epithelial origin.

A.3.2   Immunofluorescence

Cells were fixed in 4% paraformaldehyde and permeabilized with 0.1% Triton X for 5 minutes. Blocking was performed with 1% bovine serum albumin and then cells were incubated either with a 1:50 dilution of Phalloidin conjugated to either Texas Red (Molecular Probes) or Alexa 488 for 20 min to visualize actin or stained for pMLC or cytokeratin using primary antibody from either Cell signaling or Santa Cruz technologies at (1:200) or santa cruz followed by secondary fluorescent conjugated antibody obtained from Invitrogen. Immunofluorescence images were obtained using a Nikon inverted microscope.

A.4 Methods used in Chapter 5

A.4.1 Cell culture

REF52, SYF MEFs and MRC5 cells were grown in Dulbeccos modified Eagles medium (DMEM; Invitrogen) supplemented with 10% fetal bovine serum (Sigma) and antibiotic-antimycotic solution (Sigma). Taxol and SU6656 and U0126 were purchased from Calbiochem. FAK inhibitor 14 was purchased from Tocris. Cell-permeable C3 transferase was from Cytoskeleton.

A.4.2 GST-RBD, GST-Raf1 and GST-RhoAG17A pulldowns

1. Ref52 cells were lysed in 50 mM Tris (pH 7.6), 500 mM NaCl, 1% Triton X-100, 0.1% SDS, 0.5% deoxycholate, 10 mM $MgCl_2$, 200 μM orthovanadate and protease inhibitors.

2. Lysates were clarified by centrifugation, equalized for total volume and protein concentration, and rotated for 30 minutes with 30 μg of purified GST-RBD bound to glutathionesepharose beads.

3. The bead pellets were washed in 50 mM Tris (pH 7.6), 150 mM NaCl, 1% Triton X-100, 10 mM $MgCl_2$, 200 μM orthovanadate, with protease inhibitors, and subsequently processed for SDS-PAGE.

4. For active Ras pulldown experiments, cells were lysed in 25 mM Tris (pH 7.6), 150 mM NaCl, 5 mM $MgCl_2$, $1\% NP_4O$, 5% glycerol and protease inhibitors.

5. For affinity precipitation of exchange factors with the nucleotide-free RhoA mutant (G17A), cells were lysed in 20 mM HEPES (pH 7.6), 150 mM NaCl, 1% Triton X-100, 5 mM $MgCl_2$, 200μM orthovanadate plus protease inhibitors.

6. Equalized and clarified lysates were incubated with 20 μg of purified RhoA(17A) bound to glutathione-sepharose beads for 45 minutes at 4°C. Samples were then washed in lysis buffer and processed for SDS-PAGE.

A.4.3   Isolation of adhesion complex

Fibronectin-coated beads were incubated with cells for 40 min and the bound adhesion complexes were isolated in ice-cold lysis buffer (20 mM Tris pH 7.6 NaCl 150 mM, 1% NP-40 2 mM $MgCl_2$ 20μg/ml aprotinin, 1 μg/ml leupeptin, 1 μg/ml pepstatin). Beads were isolated from the lysate using a magnetic separation stand and re-suspended in ice cold pulldown lysis buffer or denatured and reduced in Laemmli buffer.

A.4.4   Purification of recombinant proteins

Construction of the pGEX4T-1 prokaryotic expression constructs containing RhoA(G17A) and the Rho-binding domain (RBD) of Rhotekin have been described previously44. Plasmid containing the Raf1-GST construct is a kind gift from Dr Der (University of North Carolina at Chapel Hill). Briefly, expression of the fusion proteins in Escherichia coli was induced with 100 μ M IPTG for 12-16 hours at room temperature. Bacterial cells were lysed in buffer containing 50 mM Tris pH 7.6 (for GST-RBD) or 20 mM HEPES pH 7.6 [for GST-RhoA(17A)], 150 mM NaCl, 5 mM $MgCl_2$, 1 mM DTT, 10 μg/ml each of aprotinin and leupeptin, and 1 mM phenylmethylsulfonyl fluoride, and the proteins purified by incubation with glutathione-sepharose 4B beads (GE Healthcare) at 4°C.

A.4.5   Antibodies

The anti-RhoA antibody (26C4), anti-Lsc (M-19) and anti-Ect2 (C-20) were from Santa Cruz Biotechnology. The antibodies against LARG was a kind gift of Kozo

Kaibuchi (Nagoya University, Japan). Anti-net1 was purchased from Abcam, anti tubulin was purchased from SIGMA. Anti-phospho Src (Tyr416) and anti-GefH1 were purchased from Cell Signaling. Anti Pan Ras antibody (OP40) was from EMB Chemicals.Anti Fyn (610163) was from BD Transduction laboratories. Blocking function anti $\beta 1$ integrin (P4C10) was from Millipore.

A.4.6 RNA interference

siRNAs were purchased from the UNC Nucleic Acid Core Facility/Sigma-Genosys (Sigma-Aldrich). The following siRNAs were used in this study: negative control 5-UCACUCGUGCCGCAUUUCCTT-3 ; RhoA targeted sequence: 5-GACATGCTTGCTCATAGTCTT 3; LARG/Arhgef12 first duplex targeted sequence: 5- GGACGGAGCTGTAATTGCA-3 ; LARG/Arhgef12 second duplex targeted sequence: 5-TGAAAGAACCTCGAAACTT-3 ; p115/Arhgef1 targeted sequence: 5GGGCTGAGCAGTATCCTAG-3 ; Gef-H1/Arhgef2 (first duplex) targeted sequence: 5-CACGTTTCCTTAGTCAGCT-3 ; Gef-H1/Arhgef2 (second duplex) targeted sequence: 5-CACCAAGGCCTTAAAGCTC-3 ; Ect2 targeted sequence: 5-TGCTGAGAATCTTATGTAC-3. SiRNAs were transfected with Lipofectamine2000 (Invitrogen).

Bibliography

Afzelius, B. (2004). Cilia-related diseases. *Journal of Pathology*, 204(4):470–477.

Ahmed, F., Wyckoff, J., Lin, E., Wang, W., Wang, Y., Condeelis, J. S., and Seagall, J. E. (2002). Gfp expression in the mammary gland for imaging of mammary tumor cells in transgenic mice. *Cancer research*.

Alberts, B. (2008). Molecular biology of the cell: Reference edition. page 1601.

Alto, N., Soderling, J., and Scott, J. D. (2002). Rab32 is an a-kinase anchoring protein and participates in mitochondrial dynamics. *The Journal of Cell Biology*.

Andrade, Y., Fernandes, J., Vazquez, E., Fernandez-Fernandez, J., Arniges, M., Sanchez, T., Villalon, M., and Valverde, M. (2005). Trpv4 channel is involved in the coupling of fluid viscosity changes to epithelial ciliary activity. *Journal of Cell Biology*, 168(6):869–874.

Arthur, W. and Burridge, K. (2001). Rhoa inactivation by p190rhogap regulates cell spreading and migration by promoting membrane protrusion and polarity. *Molecular Biology of the Cell*.

Arthur, W., Petch, L., and Burridge, K. (2000). Integrin engagement suppresses rhoa activity via a c-src-dependent mechanism. *Current Biology*.

Ashkin, A. and Dziedzic, J. M. (1989). Internal cell manipulation using infrared laser traps. *Proceedings of the National Academy of Sciences of the United States of America*.

Baconnais, S., Tirouvanziam, R., Zahm, J., and Puchelle, E. (1999). Ion composition and rheology of airway liquid from cystic fibrosis fetal tracheal xenografts. *American Journal of Respiratory Cell and Molecular Biology*.

Balland, M., Desprat, N., Icard, D., Fereol, S., Henon, S., and Gallet, F. (2006). Power laws in microrheology experiments on living cells: Comparative analysis and modeling. *Physical Review E*.

Ballestrem, C., Erez, N., Kirchner, J., Kam, Z., Bershadsky, A., and Geiger, B. (2006). Molecular mapping of tyrosine-phosphorylated proteins in focal adhesions using fluorescence resonance energy transfer. *Journal of Cell Science*.

Banes, A. (2000). Flexible bottom culture plate for applying mechanical load to cell cultures. *US Patent 6,048,723*.

Bausch, A. and Kroy, K. (2006). A bottom-up approach to cell mechanics. *Nature Physics*.

Bausch, A., Möller, W., and Sackmann, E. (1999). Measurement of local viscoelasticity and forces in living cells by magnetic tweezers. *Biophysical journal*.

Becker, M., Sauer, M., Muhlebach, M., Hirsh, A. J., and Randell, S. H. (2003). Cytokine secretion by cystic fibrosis airway epithelial cells. *American journal of respiratory and critical care medicine*.

Beningo, K., Dembo, M., Kaverina, I., Small, J. V., and li Wang, Y. (2001). Nascent focal adhesions are responsible for the generation of strong propulsive forces in migrating fibroblasts. *The Journal of Cell Biology*.

Beningo, K., Hamao, K., Dembo, M., Wang, Y., and Hosoya, H. (2006). Traction forces of fibroblasts are regulated by the rho-dependent kinase but not by the myosin light chain kinase. *Archives of biochemistry and Biophysics*.

Birkenfeld, J., Nalbant, P., Yoon, S., and Bokoch, G. (2008). Cellular functions of gef-h1, a microtubule-regulated rho-gef: is altered gef-h1 activity a crucial determinant of disease pathogenesis? *Trends in cell biology*.

Block, S., Goldstein, L., and Schnapp, B. J. (1990). Bead movement by single kinesin molecules studied with optical tweezers. *Nature*.

Bos, J., Rehmann, H., and Wittinghofer, A. (2007). Gefs and gaps: critical elements in the control of small g proteins. *Cell*.

Boucher, R. (2007). Cystic fibrosis: a disease of vulnerability to airway surface dehydration. *Trends in molecular medicine*.

Braga, P., Allegra, L., Dall'Oglio, G., Angelini, M., and Mocchi, A. (1992). A new rheometer with special features designed for bronchial mucus analysis in clinical practice. *Biorheology*.

Braga, V., Machesky, L., Hall, A., and Hotchin, N. A. (1997). The small gtpases rho and rac are required for the establishment of cadherin-dependent cell–cell contacts. *The Journal of Cell Biology*.

Brokaw, C. (1971). Bend propagation by a sliding filament model for flagella. *The Journal of experimental biology*.

Brokaw, C. (2001). Simulating the effects of fluid viscosity on the behaviour of sperm flagella. *Mathematical Methods in the Applied Sciences*, 24(17-18):1351–1365.

Brokaw, C. (2002). Computer simulation of flagellar movement viii: coordination of dynein by local curvature control can generate helical bending waves. *Cell motility and the cytoskeleton*.

Brokaw, C. (2005). Computer simulation of flagellar movement ix. oscillation and symmetry breaking in a model for short flagella and nodal cilia. *Cell motility and the cytoskeleton.*

Burridge, K. and Chrzanowska-Wodnicka, M. (1996). Focal adhesions, contractility, and signaling. *Annual review of cell and developmental biology.*

Bursac, P., Lenormand, G., Fabry, B., Oliver, M., Weitz, D. A., Viasnoff, V., Butler, J. P., and Fredberg, J. J. (2005). Cytoskeletal remodelling and slow dynamics in the living cell. *Nature Materials*, 4(7):557–61.

Cai, Y., Biais, N., Giannone, G., Tanase, M., Jiang, G., Hofman, J. M., Ladoux, B., and Sheetz, M. P. (2006). Nonmuscle myosin iia-dependent force inhibits cell spreading and drives f-actin flow. *Biophysical journal.*

Camalet, S. and Julicher, F. (2000). Generic aspects of axonemal beating. *New Journal of Physics*, 2:1–23.

Carmeliet, P. (2005). Angiogenesis in life, disease and medicine. *Nature.*

Carpenter, W. (1850). On the mutual relations of the vital and physical forces. *Philosophical Transactions of the Royal Society of London.*

Cassimeris, L., Gard, D., Tran, P., and Erickson, H. (2001). Xmap215 is a long thin molecule that does not increase microtubule stiffness. *Journal of Cell Science*, 114(16):3025–3033.

Chaudhuri, O., Parekh, S., and Fletcher, D. A. (2007). Reversible stress softening of actin networks. *Nature.*

Chauvière, A., Preziosi, L., and Verdiere, C. (2010). Cell mechanics: from single scale-based models to multiscale modeling.

Chen, C., Mrksich, M., Huang, S., Whitesides, G., and Ingber, D. (1997). Geometric control of cell life and death. *Science*, 276(5317):1425–8.

Cheng, C., Tempel, D., van Haperen, R., and de Crom, R. (2006). Atherosclerotic lesion size and vulnerability are determined by patterns of fluid shear stress. *Circulation.*

Chilvers, M. and O'Callaghan, C. (2000). Analysis of ciliary beat pattern and beat frequency using digital high speed imaging: comparison with the photomultiplier and photodiode methods. *Thorax*, 55(4):314–317.

Chiu, Y., McBeath, E., and Fujiwara, K. (2008). Mechanotransduction in an extracted cell model: Fyn drives stretch-and flow-elicited pecam-1 phosphorylation. *The Journal of Cell Biology.*

Choquet, D., Felsenfeld, D., and Sheetz, M. (1997). Extracellular matrix rigidity causes strengthening of integrin-cytoskeleton linkages. *Cell*, 88(1):39–48.

Choy, J., Parekh, S., Chaudhuri, O., Liu, A., Theriot, J. A., and Fletcher, D. A. (2007). Differential force microscope for long time-scale biophysical measurements. *Review of Scientific Instruments*.

Chrzanowska-Wodnicka, M. and Burridge, K. (1996). Rho-stimulated contractility drives the formation of stress fibers and focal adhesions. *The Journal of Cell Biology*.

Chu, S. (1991). Laser manipulation of atoms and particles. *Science*.

Coadwell, W., Stephens, L., and Hawkins, P. (2003). Phosphoinositide 3-kinase-dependent activation of rac. *FEBS letters*.

Coughlin, M. and Schmid-Schonbein, D. S. G. W. (2008). Recoil and stiffening by adherent leukocytes in response to fluid shear. *Biophysical journal*.

Cribb, J. (2010). *Driven and Thermal Microparticle Rheology of Complex Biopolymer Systems*. PhD thesis, University of North Carolina at Chapel Hill.

Cross, S., Jin, Y., Rao, J., and Gimzewski, J. (2007). Nanomechanical analysis of cells from cancer patients. *Nature Nanotechnology*.

Cui, W., Bryant, M., Sweet, P., and McDonnell, P. J. (2004). Changes in gene expression in response to mechanical strain in human scleral fibroblasts. *Experimental eye research*.

Davidson, M., Hess, H., and Waterman, C. (2010). Nanoscale architecture of integrin-based cell adhesions. *Nature*.

Davis, C. and Sears, P. (2009). Empirical model of ciliary dynamics for human airway epithelium. *Proc. Biophys. Soc. Meeting*.

Davis, P. (2006). Cystic fibrosis since 1938. *American journal of respiratory and critical care medicine*.

del Rio, A., Perez-Jimenez, R., Liu, R., Roca-Cusachs, P., Fernandez, J., and Sheetz, M. (2009). Stretching single talin rod molecules activates vinculin binding. *Science*, 323(5914):638.

DeMali, K., Wennerberg, K., and Burridge, K. (2003). Integrin signaling to the actin cytoskeleton. *Current opinion in cell biology*.

Deng, L., Trepat, X., Butler, J., Millet, E., Morgan, K., Weitz, D., and Fredberg, J. (2006). Fast and slow dynamics of the cytoskeleton. *Nature Materials*, 5(8):636–640.

Desprat, N., Richert, A., Simeon, J., and Asnacios, A. (2008). Creep function of a single living cell. *Biophysical journal*, 88(3):2224–2233.

Dillon, R., Fauci, L., and Omoto, C. (2003). Mathematical modeling of axoneme mechanics and fluid dynamics in ciliary and sperm motility. *Dynamics of Continuous Discrete and Impulsive Systems-Series a-Mathematical Analysis*, 10(5):745–757.

Dirksen, E. (1982). Ciliary basal body morphogenesis - the early events. *Symposia of the Society for Experimental Biology*, (35):439–463.

Dong, M., How, T., Kirkbride, K., Gordon, K., Lee, J., Hempel, N., Kelly, P., Moeller, B., Marks, J., and Blobe, G. (2007). The type iii tgf-beta receptor suppresses breast cancer progression. *J Clin Invest*, 117(1):206–17.

Doyle, A. and Yamada, K. (2010). Cell biology: Sensing tension. *Nature*.

Drucker, L., Afensiev, F., Radnay, J., Shapira, H., and Michael, L. (2004). Co-administration of simvastatin and cytotoxic drugs is advantageous in myeloma cell lines. *Anti-Cancer Drugs*.

Du, W. and Prendergast, G. C. (1999). Geranylgeranylated rhob mediates suppression of human tumor cell growth by farnesyltransferase inhibitors. *Cancer research*.

Dubash, A. D., Wennerberg, K., Garcia-Mata, R., Menold, M., Menold, M., Arthur, W., and Burridge, K. (2007). A novel role for lsc/p115 rhogef and larg in regulating rhoa activity downstream of adhesion to fibronectin. *Journal of Cell Science*.

Einstein, A. (1906). On the theory of the brownian movement. *Annalen der Physik*.

Elbaum, M., Fygenson, D., and Libchaber, A. (1996). Buckling microtubules in vesicles. *Physical Review Letters*, 76(21):4078–4081.

Etienne-Manneville, S. and Hall, A. (2002). Rho gtpases in cell biology. *Nature*.

Eva, A., Vecchio, G., Rao, C., and Aaronson, S. A. (1988). The predicted dbl oncogene product defines a distinct class of transforming proteins. *Proceedings of the National Academy of Sciences of the United States of America*.

Even-Ram, S., Doyle, A., Conti, M., Matsumoto, K., Adelstein, R., and Yamada, K. (2007). Myosin iia regulates cell motility and actomyosin–microtubule crosstalk. *Nature cell biology*, 9(3):299–309.

Fabry, B., Butler, J., Glogauer, M., Navajas, D., and Fredberg, J. (2001). Scaling the microrheology of living cells. *Physical Review Letters*.

Fisher, J., Cribb, J., Desai, K., Vicci, L., Wilde, B., and Superfine, R. (2006). Thin-foil magnetic force system for high-numerical-aperture microscopy. *Review of Scientific Instruments*.

Fisher, J., Cummings, J., Desai, K., Vicci, L., Wilde, B., Keller, K., Weigle, C., Bishop, G., Taylor, R., Davis, C., Boucher, R., O'Brien, E., and Superfine, R. (2005). Three-dimensional force microscope: A nanometric optical tracking and magnetic manipulation system for the biomedical sciences. *Review of Scientific Instruments*, 76(5).

Fletcher, D. A. and Mullins, R. D. (2010). Cell mechanics and the cytoskeleton. *Nature*, 463(7280):485–492.

Frame, M., Patel, H., Serrels, B., Lietha, D., and Eck, M. J. (2010). The ferm domain: organizing the structure and function of fak. *Nature Reviews Molecular Cell Biology*.

Frauenfelder, H., Sligar, S., and Wolynes, P. G. (1991). The energy landscapes and motions of proteins. *Science*.

Frey, E. and Omoto, C. B. C. K. (1997). Reactivation at low atp distinguishes among classes of paralyzed flagella mutants. *Cell Motility and the Cytoskeleton*.

Friedl, P. (2004). Prespecification and plasticity: shifting mechanisms of cell migration. *Current opinion in cell biology*.

Friedl, P., Borgmann, S., and Brocker, E. (2001). Amoeboid leukocyte crawling through extracellular matrix: lessons from the dictyostelium paradigm of cell movement. *Journal of Leukocyte Biology*.

Friedl, P. and Wolf, K. (2003). Tumour-cell invasion and migration: diversity and escape mechanisms. *Nature Reviews Cancer*.

Friedl, P. and Wolf, K. (2010). Plasticity of cell migration: a multiscale tuning model. *The Journal of Cell Biology*, 188(1):11–19.

Friedland, J., Lee, M., and Boettiger, D. (2009). Mechanically activated integrin switch controls alpha 5 beta 1 function. *Science*.

Fritsch, A., Höckel, M., Kiessling, T., Nnetu, K. D., Wetzel, F., Zink, M., and Käs, J. A. (2010). Are biomechanical changes necessary for tumour progression? *Nature Publishing Group*, 6(10):730–732.

Galbraith, C., Yamada, K., and Sheetz, M. (2002). The relationship between force and focal complex development. *Journal of Cell Biology*. hdhdohd.

García-Cardeña, G., Comander, J., and Anderson, K. R. (2001). Biomechanical activation of vascular endothelium as a determinant of its functional phenotype. *Proceedings of the National Academy of Sciences of the United States of America*.

García-Mata, R., Wennerberg, K., Arthur, W., and Burridge, K. (2006). Analysis of activated gaps and gefs in cell lysates. *Methods in Enzymology*.

Gardel, M., Nakamura, F., Hartwig, J. H., and Weitz, D. A. (2006). Prestressed f-actin networks cross-linked by hinged filamins replicate mechanical properties of cells. *Proceedings of the National Academy of Sciences of the United States of America*.

Gatza, C., Oh, S., and Blobe, G. Roles for the type iii tgf-beta receptor in human cancer. *Cell Signal*.

Gheber, L., Korngreen, A., and Priel, Z. (1998). Effect of viscosity on metachrony in mucus propelling cilia. *Cell Motility and the Cytoskeleton*, 39(1):9–20.

Gittes, F., Mickey, B., Nettleton, J., and Howard, J. (1993). Flexural rigidity of microtubules and actin-filaments measured from thermal fluctuations in shape. *Journal of Cell Biology*, 120(4):923–934.

Gordon, K. J. and Blobe, G. (2008). Role of transforming growth factor-[beta] superfamily signaling pathways in human disease. *Biochimica et Biophysica Acta (BBA)*.

Grashoff, C., Hoffman, B., Brenner, M., Zhou, R., Parsons, M., Yang, M., McLean, M., Sligar, S., Chen, C., Ha, T., and Schwartz, M. A. (2010). Measuring mechanical tension across vinculin reveals regulation of focal adhesion dynamics. *Nature*, 466(7303):263–266.

Gray, J. (1930). Photographic and stroboscopic analysis of ciliary movement. *Proc. Roy. Soc. B,*, 107:313–32.

Guck, J., Schinkinger, S., Lincoln, B., Wottawah, F., Ebert, S., Romeyke, M., Lenz, D., Erickson, H. M., Ananthakrishnan, R., Mitchell, D., Käs, J., Ulvick, S., and Bilby, C. (2005). Optical deformability as an inherent cell marker for testing malignant transformation and metastatic competence. *Biophysical journal*, 88(5):3689–98.

Hall, A. (1999). Signaling to rho gtpases. *Experimental cell research*.

Hanahan, D. and Weinberg, R. (2000). The hallmarks of cancer. *Cell*, 100(1):57–70.

Hansen, S., Zegers, M., Woodrow, M., Chardin, P., Mostov, K. E., and McMahon, M. (2000). Induced expression of rnd3 is associated with transformation of polarized epithelial cells by the raf-mek-extracellular signal-regulated kinase pathway. *Molecular and Cellular Biology*.

Hastie, A., Marcheseragona, S., Johnson, K., and Wall, J. (1988a). Structure and mass of mammalian respiratory ciliary outer arm 19s dynein. *Cell Motility and the Cytoskeleton*, 11(3):157–166.

Hastie, A., MarcheseRagona, S., Johnson, K. A., and Wall, J. S. (1988b). Structure and mass of mammalian respiratory ciliary outer arm 19s dynein. *Cell Motility and the Cytoskeleton*.

Heilbrunn, L. (1926). The physical structure of the protoplasm of sea-urchin eggs. *American Naturalist.*

Heilbrunn, L. (1927). The viscosity of protoplasm. *Quarterly Review of Biology.*

Hill, D., Swaminathan, V., Estes, A., Cribb, J., Brien, E. O., and Superfine, R. (2010). Force generation and dynamics of individual cilia under external loading. *Biophysical journal.*

Hines, M. and Blum, J. (1979). Bend propagation in flagella. ii. incorporation of dynein cross-bridge kinetics into the equations of motion. *Biophysical journal.*

Hodgson, L., Klemke, R., and Hahn, K. (2006). Spatiotemporal dynamics of rhoa activity in migrating cells. *Nature.*

Hohng, S., Zhou, R., Nahas, M., Yu, J., Schulten, K., Lilley, D., and Ha, T. (2007). Fluorescence-force spectroscopy maps two-dimensional reaction landscape of the holliday junction. *Science*, 318(5848):279.

Hove, J., Köster, R., Forouhar, A., Fraser, S. E., and Gharib, M. (2003). Intracardiac fluid forces are an essential epigenetic factor for embryonic cardiogenesis. *Nature.*

Howard, J. (2001). Mechanics of motor proteins and the cytoskeleton. *Pub.- Sinauer Associates, Inc.*

Huang, S. and Ingber, D. (2005). Cell tension, matrix mechanics, and cancer development. *Cancer Cell.*

Hughes, A. (1950). The physical properties of cytoplasm:: A study by means of the magnetic particle method part i. experimental. *Experimental Cell Research.*

Hussain, N., Jenna, S., Glogauer, M., Quinn, C., and McPherson, P. S. (2001). Endocytic protein intersectin-l regulates actin assembly via cdc42 and n-wasp. *Nature cell biology.*

Icard-Arcizet, D., Cardoso, O., Richert, A., and Henon, S. (2008). Cell stiffening in response to external stress is correlated to actin recruitment. *Biophysical journal.*

Ichimura, H., Parthasarathi, K., Quadri, S., and Bhattacharya, J. (2003). Mechanooxidative coupling by mitochondria induces proinflammatory responses in lung venular capillaries. *Journal of Clinical Investigation.*

Ingber, D. (2003). Tensegrity ii. how structural networks influence cellular information processing networks. *Journal of Cell Science.*

Ingber, D. (2006). Cellular mechanotransduction: putting all the pieces together again. *The FASEB journal.*

Itoh, R., Kurokawa, K., and Matsuda, M. (2002). Activation of rac and cdc42 video imaged by fluorescent resonance energy transfer-based single-molecule probes in the membrane of living cells. *Molecular and Cellular Biology*.

Jacques-Fricke, B., Seow, Y., Sachs, F., and Gomez, T. M. (2006). Ca2+ influx through mechanosensitive channels inhibits neurite outgrowth in opposition to other influx pathways and release from intracellular stores. *Journal of Neuroscience*.

Jaffe, A. and Hall, A. (2005). Rho gtpases: biochemistry and biology. *Annual Reviews*.

Jakowlew, S. (2006). Transforming growth factor- in cancer and metastasis. *Cancer and Metastasis Reviews*.

Ji, J., Jing, H., and Diamond, S. L. (2008). Hemodynamic regulation of inflammation at the endothelial–neutrophil interface. *Annals of Biomedical Engineering*.

Johnson, N., Villalon, M., Royce, F., Hard, R., and Verdugo, P. (1991). Autoregulation of beat frequency in respiratory ciliated cells - demonstration by viscous loading. *American Review of Respiratory Disease*, 144(5):1091–1094.

Johnstone, M. (2004). The aqueous outflow system as a mechanical pump: evidence from examination of tissue and aqueous movement in human and non-human primates. *Journal of glaucoma*.

Kamb, A., Wee, S., and Lengauer, C. (2006). Why is cancer drug discovery so difficult? *Nature Reviews Drug Discovery*, 6(2):115–120.

Katsumi, A., Milanini, J., Kiosses, W., Chien, S., Hahn, K. M., and Schwartz, M. (2002). Effects of cell tension on the small gtpase rac. *The Journal of Cell Biology*.

Katz, E., Skorecki, K., and Tzukerman, M. (2009). Niche-dependent tumorigenic capacity of malignant ovarian ascites-derived cancer cell subpopulations. *Clin Cancer Res*, 15(1):70–80.

Klein-Nulend, J., Bacabac, R., Veldhuijzen, J., and Loon, J. J. W. A. V. (2003). Microgravity and bone cell mechanosensitivity. *Advances in Space Research*.

Kojima, H., Kikumoto, M., Sakakibara, H., and Oiwa, K. (2002). Mechanical properties of a single-headed processive motor, inner-arm dynein subspecies-c of chlamydomonasstudied at the single molecule level. *Journal of Biological Physics*.

Kostic, A. and Sheetz, M. (2006). Fibronectin rigidity response through fyn and p130cas recruitment to the leading edge. *Molecular Biology of the Cell*.

Kotani, N., Sakakibara, H., Burgess, S., Kojima, H., and Oiwa, K. (2007). Mechanical properties of inner-arm dynein-f (dynein i1) studied with in vitro motility assays. *Biophysical journal*, 93(3):886–894.

Krieg, M., Arboleda-Estudillo, Y., Puech, P., Kafer, J., and Heisenberg, C. P. (2008). Tensile forces govern germ-layer organization in zebrafish. *Nature cell biology*.

Lecuit, T. and Lenne, P.-F. (2007). Cell surface mechanics and the control of cell shape, tissue patterns and morphogenesis. *Nature Reviews Molecular Cell Biology*.

Lefkowitz, R. and Shenoy, S. (2005). Transduction of receptor signals by beta-arrestins. *Science*, 308(5721):512–7.

Levine, A. and Lubensky, T. C. (2000). One-and two-particle microrheology. *Physical Review Letters*.

Li, Y., Haga, J., and Chien, S. (2005). Molecular basis of the effects of shear stress on vascular endothelial cells. *Journal of biomechanics*.

Lim, Y., Lim, S., Tomar, A., Gardel, M., Uryu, S. A., Waterman, C., and Schlaepfer, D. D. (2008). Pyk2 and fak connections to p190rho guanine nucleotide exchange factor regulate rhoa activity, focal adhesion formation, and cell motility. *The Journal of Cell Biology*.

Lin, T., Aplin, A., Shen, Y., Aukhil, Q. C. I., and Juliano, R. (1997). Integrin-mediated activation of map kinase is independent of fak: evidence for dual integrin signaling pathways in fibroblasts. *The Journal of Cell Biology*.

Lindemann, C. (1994a). A" geometric clutch" hypothesis to explain oscillations of the axoneme of cilia and flagella. *Journal of Theoretical Biology*.

Lindemann, C. (1994b). A model of flagellar and ciliary functioning which uses the forces transverse to the axoneme as the regulator of dynein activation. *Cell motility and the cytoskeleton*.

Lindemann, C. (2007). The geometric clutch as a working hypothesis for future research on cilia and flagella. *Reproductive Biomechanics*, 1101:477–493.

Machemer, H. (1972). Ciliary activity and the origin of metachrony in paramecium: effects of increased viscosity. *Journal of Experimental Biology*.

Machin, K. (1958). Wave propagation along flagella. *J. exp. Biol.*

Maret, G. and Wolf, P. E. (1987). Multiple light scattering from disordered media. the effect of brownian motion of scatterers. *Zeitschrift für Physik B Condensed Matter*.

Marshall, W. and Nonaka, S. (2006). Cilia: tuning in to the cell's antenna. *Current Biology*.

Mason, T., Ganesan, K., Zanten, J. V., Wirtz, D., and Kuo, S. (1997). Particle tracking microrheology of complex fluids. *Physical Review Letters*, 79(17):3282–3285.

Mason, T. and Weitz, D. A. (1995). Optical measurements of frequency-dependent linear viscoelastic moduli of complex fluids. *Physical Review Letters*.

Massagué, J. (2008). Tgf [beta] in cancer. *Cell*.

Matsui, H., Wagner, V., Hill, D., Schwab, U., Rogers, T., Button, B., Taylor, R., Superfine, R., Rubinstein, M., Iglewski, B., and Boucher, R. (2006). A physical linkage between cystic fibrosis airway surface dehydration and pseudomonas aeruginosa biofilms. *Proceedings of the National Academy of Sciences of the United States of America*, 103(48):18131–18136.

Matthews, Overby, D., Mannix, R., and Ingber, D. (2006). Cellular adaptation to mechanical stress: role of integrins, rho, cytoskeletal tension and mechanosensitive ion channels. *Journal of cell science*.

McGrath, J., Somlo, S., Makova, S., Tian, X., and Bruekner, M. (2003). Two populations of node monocilia initiate left-right asymmetry in the mouse. *Cell*.

Meissner, A., Wernig, M., and Jaenisch, R. (2007). Direct reprogramming of genetically unmodified fibroblasts into pluripotent stem cells. *Nature biotechnology*.

Mierke, C., Kollmannsberger, P., Zitterbart, D. P., Smith, J., Fabry, B., and Goldmann, W. (2008). Mechano-coupling and regulation of contractility by the vinculin tail domain. *Biophysical journal*, 94(2):661–670.

Miki, T., Smith, C., Long, J., Eva, A., and Fleming, T. P. (1993). Oncogene ect2 is related to regulators of small gtp-binding proteins. *Nature*.

Mitran, S. (2007). Metachronal wave formation in a model of pulmonary cilia. *Computers and Structures*, 85(11-14):763–774.

Mizuno, D., Tardin, C., Schmidt, C., and MacKintosh, F. (2007). Nonequilibrium mechanics of active cytoskeletal networks. *Science*, 315(5810):370.

Moore, S. W., Roca-Cusachs, P., and Sheetz, M. P. (2011). Stretchy proteins on stretchy substrates: The important elements of integrin-mediated rigidity sensing. *Developmental Cell*, 19(2):194–206.

Nabeshima, K., Inoue, T., Shimao, Y., and Sameshima, T. (2002). Matrix metalloproteinases in tumor invasion: role for cell migration. *Pathology International*.

Navajas, D., Butler, J., and Fredberg, J. (1999). Novel rheology of the human airway smooth muscle cell. *Proceedings of the First Joint BMES/EMBS Conference*.

Nedelec, F. (2002). Computer simulations reveal motor properties generating stable antiparallel microtubule interactions. *Journal of Cell Biology*, 158(6):1005–1015.

Nicastro, D., Schwartz, C., Pierson, J., Gaudette, R., Porter, M., and McIntosh, J. (2006). The molecular architecture of axonemes revealed by cryoelectron tomography. *Science*, 313(5789):944–948.

Nobes, C. and Hall, A. (1995). Rho, rac, and cdc42 gtpases regulate the assembly of multimolecular focal complexes associated with actin stress fibers, lamellipodia, and filopodia. *Cell*.

Nonaka, S., Tanaka, Y., Okada, Y., Takeda, S., and Hirokawa, N. (1998). Randomization of left-right asymmetry due to loss of nodal cilia generating leftward flow of extraembryonic fluid in mice lacking kif3b motor protein. *Cell*.

O'Brien, E. T., Cribb, J., Marshburn, D., Taylor, R., and Superfine, R. (2008). Chapter 16: Magnetic manipulation for force measurements in cell biology. *Methods Cell Biology*, 89:433–50.

Ohmuro, J. and Ishijima, S. (2006). Hyperactivation is the mode conversion from constant-curvature beating to constant-frequency beating under a constant rate of microtubule sliding. *Molecular Reproduction and Development*, 73(11):1412–1421.

Okuno, M. and Hiramoto, Y. (1979). Direct measurements of the stiffness of echinoderm sperm flagella. *Journal of Experimental Biology*, 79(Apr):235–243.

Olofsson, B. (1999). Rho guanine dissociation inhibitors: Pivotal molecules in cellular signalling. *Cellular signalling*.

Osterhout, W. (1914). The chemical dynamics of living protoplasm. *Science*.

Paszek, M., Zahir, N., Johnson, K., Lakins, J., Reinhart-King, C. A., Dembo, M., Boettiger, D., and Weaver, V. (2005). Tensional homeostasis and the malignant phenotype. *Cancer Cell*.

Pazour, G., Dickert, B., Vucica, Y., and Cole, D. G. (2000). Chlamydomonas ift88 and its mouse homologue, polycystic kidney disease gene tg737, are required for assembly of cilia and flagella. *The Journal of Cell Biology*.

Pelham, R. and Wang, Y. (1997). Cell locomotion and focal adhesions are regulated by substrate flexibility. *Proceedings of the National Academy of Sciences of the United States of America*.

Pollard, T. (2003). The cytoskeleton, cellular motility and the reductionist agenda. *Nature*.

Ponti, A., Machacek, M., Gupton, S., Waterman, C., and Danuser, G. (2004). Two distinct actin networks drive the protrusion of migrating cells. *Science*.

Porter, M. and Sale, W. S. (2000). The 9+ 2 axoneme anchors multiple inner arm dyneins and a network of kinases and phosphatases that control motility. *The Journal of Cell Biology*.

Pozo, M. D., Price, L., Alderson, N., and Schwartz, M. (2000). Adhesion to the extracellular matrix regulates the coupling of the small gtpase rac to its effector pak. *The EMBO Journal*.

Praetorius, H. and Spring, K. R. (2001). Bending the mdck cell primary cilium increases intracellular calcium. *Journal of Membrane Biology*.

Praetorius, H. and Spring, K. R. (2003). Removal of the mdck cell primary cilium abolishes flow sensing. *Journal of Membrane Biology*.

Puchelle, E., Zahm, J., and Aug, F. (1981). Viscoelasticity, protein content and ciliary transport rate of sputum in patients with recurrent and chronic bronchitis. *Biorheology*.

Purcell, E. (1977). Life at low reynolds number. *Am. J. Phys.*

Radmacher, M. (2002). Measuring the elastic properties of living cells by the atomic force microscope. *Methods in Cell Biology*.

Rahimi, R. and Leof, E. B. (2007). Tgf signaling: A tale of two responses. *Journal of cellular biochemistry*.

Ren, X., Kiosses, W., Sieg, D., and Otey, C. (2000). Focal adhesion kinase suppresses rho activity to promote focal adhesion turnover. *Journal of Cell Science*.

Rericha, E., Schlaepfer, D., and Waterman, C. (2010). Myosin ii activity regulates vinculin recruitment to focal adhesions through fak-mediated paxillin phosphorylation. *The Journal of Cell Biology*.

Resnick, A. and Hopfer, U. (2007). Force-response considerations in ciliary mechanosensation. *Biophysical journal*.

Reya, T., Morrison, S., Clarke, M., and Weissman, I. L. (2001). Stem cells, cancer, and cancer stem cells. *Nature*.

Ridley, A. and Cory, G. (2002). Braking waves. *Nature*.

Riedel-Kruse, I., Hilfinger, A., Howard, J., and Jülicher, F. (2007). How molecular motors shape the flagellar beat. *HFSP Journal*.

Riento, K. and Ridley, A. J. (2003). Rocks: multifunctional kinases in cell behaviour. *Nature Reviews Molecular Cell Biology*.

Rikmenspoel, R. (1976). Contractile events in cilia of paramecium, opalina, mytilus, and phragmatopoma. *Biophysical journal*, 16(5):445–470. 0006-3495.

Rioja, Spatz, J., Ballestrem, C., and Kemkemer, R. (2009). Force-induced cell polarisation is linked to rhoa-driven microtubule-independent focal-adhesion sliding. *Journal of Cell Science.*

Riordan, J., Rommens, J., Kerem, B., Alon, N., Lok, S., Plavsik, N., and Chou, J. L. (1989). Identification of the cystic fibrosis gene: cloning and characterization of complementary dna. *Science.*

Riveline, D., Zamir, E., Balaban, N., and Bershadsky, A. D. (2001). Focal contacts as mechanosensors. *The Journal of Cell Biology.*

Rotsch, C. and Radmacher, M. (2000). Drug-induced changes of cytoskeletal structure and mechanics in fibroblasts: an atomic force microscopy study. *Biophys J,* 78(1):520–35.

Rottner, K., Hall, A., and Small, J. V. (1999). Interplay between rac and rho in the control of substrate contact dynamics. *Current Biology.*

Salathe, M. (2007). Regulation of mammalian ciliary beating. *Annual Review of Physiology,* 69:401–422.

Sanderson, M. and Dirksen, E. (1986). Regulatory mechanisms of mammalian respiratory-tract cilia - mechanosensitivity mediated by calcium. *Cell Motility and the Cytoskeleton,* 6(2):244–244.

Sanderson, M. and Sleigh, M. (1981). Ciliary activity of cultured rabbit tracheal epithelium - beat pattern and metachrony. *Journal of Cell Science,* 47(Feb):331–347.

Satir, P. and Christensen, S. (2007). Overview of structure and function of mammalian cilia. *Annu Rev Physiol,* 69:377–400.

Satir, P. and Matsuoka, T. (1989). Splitting the ciliary axoneme - implications for a switch-point model of dynein arm activity in ciliary motion. *Cell Motility and the Cytoskeleton,* 14(3):345–358. Ay285 Times Cited:33 Cited References Count:28.

Satir, P. and Sleigh, M. A. (1990). The physiology of cilia and mucociliary interactions. *Annual review of physiology.*

Sawada, Y. and Sheetz, M. (2002). Force transduction by triton cytoskeletons. *The Journal of Cell Biology.*

Sawamoto, K., Wichterle, H., and Gonzalez-Perez, O. (2006). New neurons follow the flow of cerebrospinal fluid in the adult brain. *Science.*

Schlaepfer, D. D., Hanks, S. K., Hunter, T., and van der Geer, P. (1994). Integrin-mediated signal transduction linked to ras pathway by grb2 binding to focal adhesion kinase. *Nature.*

Schmitz, K., Holcomb-Wygle, D., Oberski, D., and Lindemann, C. (2000). Measurement of the force produced by an intact bull sperm flagellum in isometric arrest and estimation of the dynein stall force. *Biophysical journal*, 79(1):468–478.

Schwartz, M. A. (2010). Integrins and extracellular matrix in mechanotransduction. *Cold Spring Harbor perspectives in biology*.

Seifriz, W. (1939). A materialistic interpretation of life. *Philosophy of Science*.

Shaevitz, J. and Fletcher, D. A. (2007). Load fluctuations drive actin network growth. *Proceedings of the National Academy of Sciences of the United States of America*.

Shingyoji, C., Higuchi, H., Yoshimura, M., Katayama, E., and Yanagida, T. (1998). Dynein arms are oscillating force generators. *Nature*, 393(6686):711–714.

Sleep, J., Wilson, D., Simmons, R., and Gratzer, W. (1999). Elasticity of the red cell membrane and its relation to hemolytic disorders: an optical tweezers study. *Biophysical Journal*.

Spero, R. C. (2010). *Small Particle Transport in Fibrin Gels and High Throughput Clot Characterization*. PhD thesis, University of North Carolina at Chapel Hill.

Spero, R. C., Vicci, L., Cribb, J., Bober, D., Swaminathan, V., and Superfine, R. (2008). High throughput system for magnetic manipulation of cells, polymers, and biomaterials. *Review of Scientific Instruments*.

Srivastava, S., Wheelock, R., Aaronson, S. A., and Eva, A. (1986). Identification of the protein encoded by the human diffuse b-cell lymphoma (dbl) oncogene. *Proceedings of the National Academy of Sciences of the United States of America*.

Suresh, S. (2007a). Biomechanics and biophysics of cancer cells. *Acta Materialia*.

Suresh, S. (2007b). Nanomedicine: Elastic clues in cancer detection. *Nature Nanotechnology*.

Tadir, Y., Wright, W., Vafa, O., Ord, T., and Berns, M. W. (1990). Force generated by human sperm correlated to velocity and determined using a laser generated optical trap. *Fertility and Sterility*.

Takahashi, K. and Yamanaka, S. (2006). Induction of pluripotent stem cells from mouse embryonic and adult fibroblast cultures by defined factors. *Cell*.

Tan, J., Tien, J., Pirone, D., Gray, D. S., Bhadriraju, K., and Chen, C. S. (2003). Cells lying on a bed of microneedles: an approach to isolate mechanical force. *Proceedings of the National Academy of Sciences of the United States of America*.

Taylor, H., Satir, P., and Holwill, M. E. J. (1999). Assessment of inner dynein arm structure and possible function in ciliary and flagellar axonemes. *Cell Motility and the Cytoskeleton*.

Tee, S. Y., Bausch, A. R., and Janmey, P. A. (2009). The mechanical cell. *Current Biology*, 19(17):R745–R748.

Teff, Z., Priel, Z., and Gheber, L. (2007). Forces applied by cilia measured on explants from mucociliary tissue. *Biophysical journal*, 92(5):1813–1823.

Trepat, X., Deng, L., An, S., Navajas, D., Butler, J. P., and Fredberg, J. J. (2007). Universal physical responses to stretch in the living cell. *Nature*.

Tseng, Y. and Wirtz, D. (2001). Mechanics and multiple-particle tracking microheterogeneity of [alpha]-actinin-cross-linked actin filament networks. *Biophysical Journal*.

Tuszynski, J., Luchko, T., Portet, S., and Dixon, J. (2005). Anisotropic elastic properties of microtubules. *European Physical Journal E*, 17(1):29–35.

Uhlig, S. (2003). Taking a peep at the upper airways. *American journal of respiratory and critical care medicine*.

Vernon, G. and Woolley, D. (2002). Microtubule displacements at the tips of living flagella. *Cell motility and the cytoskeleton*.

Vernon, G. and Woolley, D. (2004). Basal sliding and the mechanics of oscillation in a mammalian sperm flagellum. *Biophysical journal*.

Vicci, L. and Superfine, R. (2004). Methods and systems for controlling motion of and tracking a mechanically unattached probe. *US Patent App. 10/786,427*.

Vicente-Manzanares, M., Ma, X., Adelstein, R. S., and Horwitz, A. R. (2009). Non-muscle myosin ii takes centre stage in cell adhesion and migration. *Nat Rev Mol Cell Biol*, 10(11):778–790.

Vicente-Manzanares, M., Zareno, J., Choi, C. K., and Horwitz, A. F. (2007). Regulation of protrusion, adhesion dynamics, and polarity by myosins iia and iib in migrating cells. *The Journal of Cell Biology*.

Vicker, M. (2002). F-actin assembly in dictyostelium cell locomotion and shape oscillations propagates as a self-organized reaction-diffusion wave. *FEBS letters*.

Vollrath, M., Kwan, K., and Corey, D. P. (2007). The micromachinery of mechanotransduction in hair cells. *Annual review of neuroscience*.

Wang, W., Wyckoff, J., Frohlich, V., Oleynikov, Y., Bottinger, E. P., Seagall, J. E., and Condeelis, J. S. (2002). Single cell behavior in metastatic primary mammary tumors correlated with gene expression patterns revealed by molecular profiling. *Cancer research*.

Weinberg, R. A. (2007). The biology of cancer. page 796.

Welch, M. D. and Mullins, R. (2002). Cellular control of actin nucleation. *Annual review of cell and developmental biology*.

Wernig, M., Meissner, A., Foreman, R., Brambrink, T., Bernstein, B. E., and Jaenisch, R. (2007). In vitro reprogramming of fibroblasts into a pluripotent es-cell-like state. *Nature*.

Winters, S., Davis, C., and Boucher, R. (2007). Mechanosensitivity of mouse tracheal ciliary beat frequency: roles for ca2+, purinergic signaling, tonicity, and viscosity. *American Journal of Physiology-Lung Cellular and Molecular Physiology*, 292(3):L614–L624.

Wyckoff, J., Jones, J., Condeelis, J., and Segall, J. (2000). A critical step in metastasis: in vivo analysis of intravasation at the primary tumor. *Cancer research*.

Yager, J., Chen, T., and Dulfano, M. (1978). Measurement of frequency of ciliary beats of human respiratory epithelium. *Chest*, 73(5):627–633.

Yamane, M., Matsuda, T., Ito, T., Fujio, Y., and Azuma, J. (2007). Rac1 activity is required for cardiac myocyte alignment in response to mechanical stress. *Biochemical and Biophysical Research Communication*.

Zhong, C., Chrzanowska-Wodnicka, M., Brown, J., Shaub, A., and Burridge, K. (1998). Rho-mediated contractility exposes a cryptic site in fibronectin and induces fibronectin matrix assembly. *The Journal of Cell Biology*.

Zigmond, S. (2004). Formin-induced nucleation of actin filaments. *Current opinion in cell biology*.

Zondag, G., Evers, E., Klooster, J. T., Janssen, L., and Collard, J. G. (2000). Oncogenic ras downregulates rac activity, which leads to increased rho activity and epithelial–mesenchymal transition. *The Journal of Cell Biology*.

Zuvela-Jelaska, L., Woolf, C., and Corey, D. (2001). Transport and localization of the deg/enac ion channel bnac1 alpha to peripheral mechanosensory terminals of dorsal root ganglia neurons. *Journal of Neuroscience*.